COMPUTATIONAL AND EXPERIMENTAL TRANSIENT ASSESSMENT OF SUPERCRITICAL CO_2 BASED NATURAL CIRCULATION LOOPS

Thesis

Submitted in partial fulfillment of the requirements of the degree of

DOCTOR OF PHILOSOPHY

by

SRIVATHSA THIMMAIAH

(165100 ME16P03)

DEPARTMENT OF MECHANICAL ENGINEERING

NATIONAL INSTITUTE OF TECHNOLOGY KARNATAKA,

SURATHKAL, MANGALORE - 575 025

APRIL, 2024

COMPUTATIONAL AND EXPERIMENTAL TRANSIENT ASSESSMENT OF SUPERCRITICAL CO_2 BASED NATURAL CIRCULATION LOOPS

Thesis

Submitted in partial fulfillment of the requirements of the degree of

DOCTOR OF PHILOSOPHY

by

SRIVATHSA THIMMAIAH

(165100 ME16P03)

Under the guidance of

Dr. ARUN M.

DEPARTMENT OF MECHANICAL ENGINEERING

NATIONAL INSTITUTE OF TECHNOLOGY KARNATAKA,

SURATHKAL, MANGALORE - 575 025

APRIL, 2024

DECLARATION

I hereby *declare* that the Research Thesis entitled **"Computational And Experimental Transient Assessment Of Supercritical CO_2 Based Natural Circulation Loops "** which is being submitted to the **National Institute of Technology Karnataka, Surathkal** in partial fulfillment of the requirements for the award of the **Doctor of Philosophy** in **Department of Mechanical Engineering** is a *bonafide report of the research work carried out by me*. The material contained in this Research Thesis has not been submitted to any University or Institution for the award of any degree.

SRIVATHSA THIMMAIAH
165100 ME16P03
Department of Mechanical Engineering
NITK, Surathkal - 575 025
(Signature with date)

Place: NITK-Surathkal
Date:

CERTIFICATE

This is to *certify* that the Research Thesis entitled **"Computational And Experimental Transient Assessment Of Supercritical CO_2 Based Natural Circulation Loops "** submitted by Srivatsa Thimmaiah (Register Number: 165100 ME16P03) as the record of research work carried out by him, *is accepted as the Research Thesis submission* in partial fulfillment of the requirements for the award of the degree of Doctor of Philosophy.

Dr. ARUN M.
Assistant Professor
Research Supervisor
Department of Mechanical Engineering
NITK, Surathkal - 575 025
(Signature with date & Seal)

Chairman - DRPC
(Signature with date & Seal)

DEDICATED TO

MY MOTHER GAURI THIMMAIAH

AND

MY FAMILY MEMBERS

VANI SRIVATSA, THANMAI SRIVATSA GOWDA & THANAV SRIVATSA GOWDA

ACKNOWLEDGMENT

First and foremost I would like to express my sincere gratitude to my mother Gauri Thimmaiah for the encouragement she has given in pursuing doctoral course. I will never forget the enthusiasm she shown while signing my application form on the day of my admission to doctoral course. It gives me immense pleasure to acknowledge my Research Supervisor **Dr. Arun M.** for his guidance, help, support and the patience throughout my studies at NITK. I am very grateful to them for their observations and suggestion by which is greatly contributed to the quality of my research work and this thesis.

A special thanks to my mentor **Dr. Ajay Kumar Yadav** for the support and guidance he has extended during my difficult circumstances and throughout my studies at National Institute of Technology Karnataka, Surathkal.

I am thankful to **Dr. S. M. Murigendrappa**, Professor and Head, Department of Mechanical Engineering, for the support and providing facilities required to complete this research work successfully. Furthermore, I take this opportunity to acknowledge the former HODs, Mechanical engineering, **Dr. Gangadharan K.V., Dr. Narendranath S., and Dr. Shrikantha S. Rao, Dr. Satyabodh M. Kulkarni**, for their support and encouragement. I would also wish to express my gratitude to my RPAC members, **Dr. Anish** and **Dr. Keyur Raval**, their valuable suggestions during my research work assessment meet.

I gratefully acknowledge the help extended by **Dr. Tabish Wahidi** while performing the FLUENT simulations of Natural circulation loop and also in carrying out the experimental work at CFD workshop.

I would like to thank all the faculty members and students of Department of Mechanical Engineering, namely Dr. Abdul Razzak Buradi, Dr. Shankar Kodate, Dr. Madagonda Biradar, Vasista, Kishore Babu, and all others who taught me many valuable lessons and whose experience greatly broaden my engineering skills. The numerous discussions with my friends and colleagues and other, although not necessarily related to this thesis, comprised an essential part of its evolution.

Finally I wish to dedicate this thesis to my mother **Gauri Thimmaiah** who always encouraged me to push the limits of my knowledge, face the intellectual challenges and never settle on the average.

SRIVATHSA THIMMAIAH

APRIL, 2024

NITK, SURATHKAL

ABSTRACT

Natural circulation loop is a geometrically simple heat transporting device in which fluid flow establishes due to density gradient across the loop, which is induced as a result of temperature difference in a loop. It is a fundamentally passive system in which the buoyancy force launches fluid circulation by surpassing all the resistive force in the system. This distinctive competence of NCL makes its operation and maintenance highly economical and also highly reliable in terms of safety of men and machinery. Since the inception of natural circulation loops in the field of engineering applications, water and the brine solutions are the most accredited and extensively used working fluids due to its abundance and also its favorable eco-friendly properties. However, extensive research on CO_2 applications revealed that it possesses almost all the properties which are essentially required to meet the qualification criteria of heat transport system. In natural circulation loops, supercritical CO_2 is gaining more popularity due to its superior transport properties compared to all natural as well as synthetic fluids. Hence detailed analysis of heat transport capabilities and stability behaviour of CO_2 in natural circulation loops is very vital.

The loop fluid flow dynamics in NCLs for any impetuous changes in operating parameters is of critical importance and hence finding an elegant solution for these dynamics is very much essential to incorporate it in specific applications. Inability of systems to sustain themselves against small perturbations for which physical system is subjected to is considered as instability. NCL has an inherent problem of instability caused by the combined effect of buoyancy, friction and inertial forces at varying operating conditions. Further, due to non-linearity of natural convection process, NCLs are prone to several kinds of instabilities. This instability in fluid flow creates flow oscillation, chaotic non-linear dynamic behaviour and flow reversal. The primary objective of the present work is to accomplish a comparative study on the dynamic performance among various configurations of NCL.

To explore the instability phenomenon in sCO_2 based NCLs which are configured with various types of heat sources i.e., heater, heat exchanger and isothermal wall at the source with a cold heat exchanger (CHX) at sink have been studied by using 2-D as well as 3-D computational fluid dynamics (CFD) simulations. Further, experimental work has been carried out over a range of supercritical pressures (80 bar to100 bar) and heat inputs (250 W to 2000 W) at source. Transient results for mass flow rate, temperature and velocity variation for different operating pressures and temperatures. Obtained results are also validated with the published experimental and numerical data and found in good agreement.

Two-dimensional computational fluid dynamics simulation results show the higher instabilities for hot heat-exchanger loop (HHX-CHX) than an isothermal heater and heat-exchanger loop (ISO-CHX). With an increase in heat input, loops attain stability at a faster rate for a given operating pressure. At a lower heat input both the loops show bidirectional fluctuation, whereas it is unidirectional at high heat input. Nusselt number shows that the HHX-CHX loop's heat transfer capability is more compared to ISO-CHX loops.

3-D numerical analysis is conducted to get moderately accurate transient and stability behavior of sCO_2 based NCLs which are configured with three different types of heat sources i.e., heater, hot heat exchanger (HHX) and isothermal wall (ISO) at the source. Three-dimensional unsteady conservation equations (mass, momentum and energy equations) are solved to assess the transient and stability behavior of sCO_2 mass flow rate, temperature and velocity as a function of time. Effect of pressure on sCO_2 mass flow rate is also assessed to compare its stability behavior in all the configurations. Performance of the loop fluid has been studied by varying the quantum of heat inputs at source by keeping constant mass flow rate and temperature of cooling media at sink. It is observed that irrespective of the boundary condition at source, the loop experiences some initial disturbances or instabilities before reaching steady state. However, time needed for the attainment of steady state varies with the nature

of heat input employed at source. Results show a higher magnitude of instabilities in Heater-CHX loop than HHX-CHX and ISO-CHX loops, and these instabilities mitigate at a faster rate in the ISO-CHX loop at all levels of heat input and operating pressure of the loop. It is also observed that as loop fluid operating pressure increases, the instability of the system decreases and the loop fluid mass flow rate increases. Further, the Nusselt number in the case of Heater-CHX loop is more compared to other loops because of its high turbulent kinetic energy.

To assess the actual behaviour of the sCO_2 based Natural circulation, experimental setup is designed, fabricated and test is conducted at various pressures and temperatures. The practical behaviour shows that instability is inevitable at lower pressure and temperature and system approaches stable conditions at higher pressure and temperature due to stronger and dominating buoyancy forces. The simulation results also revealed the similar behaviour at lower as well as at higher operating conditions.

Key words: Natural circulation loop, Supercritical CO_2, Instability, Heat Transfer, CFD.

Table of Contents

List of Tables

List of Figures

List of Symbols

Acronyms

A	Area, (m^2)
A	Area, m^2
C_p	Specific heat at constant pressure, (J kg^{-1} K^{-1})
C_p	Specific heat at constant pressure, J/(kg.K)
d	diameter, (m)
d	diameter, m
g	accelaration due to gravity, m/s^2
h	Enthalpy, J/kg
m	mass flow rate, (kg/s
m	mass flow rate, kg/s
Nu	Nusselt number, Nu=$\frac{\bar{h}d}{\lambda}$
p	Pressure, Pa
P_{c}	Critical pressure, MPa
P_κ	Turbulent kinetic energy production term
Pr	Prandtl number, $Pr = \frac{\mu C_p}{\lambda}$
Pr	Prandtl number, $Pr = \frac{\mu C_p}{\lambda}$
Pr_{T}	Turbulent Prandtl number
Q	Heat input, W
Q	Heat input,(W)
Re	Reylonds number, Re=$\frac{\rho v d}{\mu}$
Re	Reynolds number, $Re = \frac{\rho V d}{\mu}$
sCO_2	supercrtical carbon dioxide

sCO_2NCL	supercritical carbon dioxide based NCL
T	Temperature, K
t	time, s
T_{c}	Critical temperature,$^\circ$C
u	Velocity in X- direction, m/s
u	Velocity in X- direction, m/s
v	Velocity in Y- direction, m/s
v	Velocity in Y- direction, m/s
w	Velocity in Z- direction, m/s
GWP	Global warming potential
ODP	Ozone depletion potential
X	X-axis
Y	Y-axis

Greek Symbols

$\bar{h}$	Heat transfer coefficient, W/(m^2.K)
$\bar{h}$	Heat transfer coefficient, $\bar{h} = \frac{\int_0^A hdA}{\int_0^A dA}, \quad W\ (m^{-2}K^{-1})$
β^*	Compressibilty
β	Volume expansion coefficient, (1/K)
β	Volume expansion coefficient, 1/K
κ	Turbulent Kinetic energy, m^2/s^2
λ	Thermal conductivity, W/(m.K)
μ	Viscosity, Pa.s
μ_T	Turbulent viscosity = $c_\mu \rho \frac{\kappa^2}{\varepsilon}$

ρ_r	local density along the radial direction.
ρ	Density, kg/m^3
ε	Turbulent Kinetic energy dissipation rate, m^2/s^3
G	Rate of generation of turbulent kinetic energy, kg/(m.s^3)

Subscripts

r	radial direction, (m)
r	radial direction
ss	steady state
x	axial location, (m)
x	local, value of axial location

CHAPTER 1

Introduction

The recent spate of nuclear disasters, including the Windscale fire accident (1957, United Kingdom), Three Mile Island accident (1968, USA), Chernobyl disaster (1986, Ukrainian SSR), and Fukushima Daiichi nuclear disaster (2011), has drawn the attention of numerous researchers looking for a workable solution. All of these catastrophes are caused by active cooling systems that go wrong, which pushed the researcher to look for a new, dependable passive cooling strategy to keep the system secure. The absence of moving components minimizes the possibility of a failure in the removal of heat from the source and makes it an attractive alternative for reducing such damages. This is the major reason why natural convection is preferred over forced convection in power plants where safety is paramount. This research is being conducted on a natural circulation loop to better understand the transient flow behaviour and heat transfer capabilities at different pressure, heating methods and boundary conditions.

1.1 Natural circulation loop

Natural circulation loops (NCLs), in general, possesses simple geometrical constructional feature and are essentially comprises of source, sink, riser and down comer piping. The source and sink are interconnected by riser and down comer piping to form a loop. When such a loop is filled with a working fluid and if differential temperature is maintained across source and sink then continuous circulation of fluid establishes in the loop path without any aid of external driving force. In NCLs circulation of working fluid can set-in automatically under the influence of gravity and activation of the heat source and sink, provided the heat sink is at higher elevation than the heat source. Further, to reap the maximum natural circulation flow rate of working fluid, the loop shall be installed perfectly in a vertical position. The working fluid circulation thus established in the loop is eventually expected to attain a steady circulation state, if boundary conditions are maintained constant at both the source and sink. Further, this state of circulation turns out to be perpetual, if the integrity of the closed loop is maintained. Fundamentally the flow establishes in the loop due to the thermally induced density difference between the source and sink, which is generally called as buoyancy force and is also known as thermosyphonic force. The prime purpose of NCL is to transport heat from a source to a sink without the aid of moving parts in the system. It makes the system intrinsically safe and appreciably reduces the maintenance and operating costs. In absence of any sort of mechanical moving parts in the loop, the system becomes non-energy consuming, non-vibrating and noiseless passive system. These inherent and attractive features of NCLs made it to influence several engineering applications in conventional as well as nuclear industries. The most popular among these applications are natural circulation Boilers, Internal combustion engines cooling system, transformers core cooling system, Gas turbine blades cooling (Greif 1988), Solar water heaters (Yamaguchi et al. 2010), Geothermal power extraction (Kreitlow et al. 1978), Nuclear reactor core cooling (Chatoorgoon et al. 2005) etc., Further, the most emerging field of application of NCLs is electronic components heat dissipation (Chauhan and Kandlikar 2019; Samba et al. 2013)

1.2 Natural Flow Phenomenon in Natural Circulation Loops

Figure 1.1 shows a rectangular NCL schematic comprises of source, sink, the interconnecting piping between these two and the working fluid. The circulation in the loop establishes only when the working fluid absorbs heat at source and rejects it at sink. After absorbing the heat at source the working fluid density decreases and it becomes lighter, which makes it rises in the loop. In the meantime, at sink while rejecting the heat its density increases and becomes denser, which makes it to descend in the loop, thus establishes a circulation in the loop. The most essential prerequisite which determines the fluid flow in loop is the elevation difference between the source and the sink and essentially the elevation of sink shall be higher than the source.

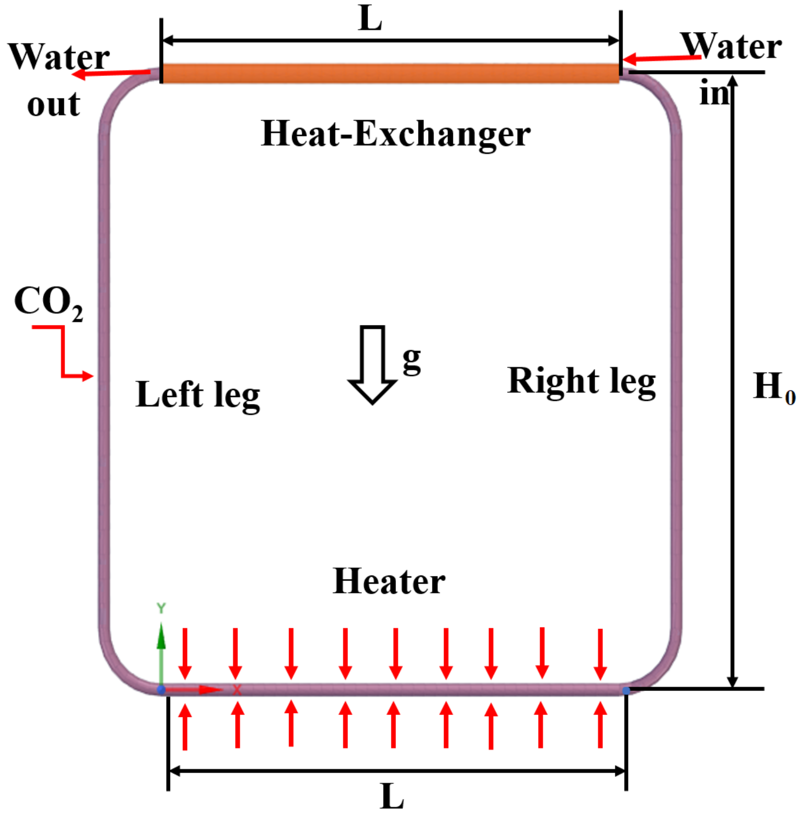

Figure 1.1: Schematic of natural circulation loop.

In NCLs the mass flow rate is directly proportional to the loop area of cross section i.e., the flow area, the differential density between source and sink, the loop average density, gravitational force, height of the loop and inversely proportional to retarding frictional forces i.e., the hydraulic resistance in the loop. In other words, the driving pressure differential induced in loop can be enhanced by increasing the loop height and which in turn increases the density difference between the two vertical legs. For a definite quantity of heat transport, the driving force in the NCLs can be increased by increasing the height and hence obviously there is practically no physical upper limit on this value except an economic limitation, as increase in height would increases the constructional cost of the loop. For a fixed loop height and specified boundary conditions, the flow rate develops in the loop is depend on the hydraulic resistance, which in function of friction factor, local loss coefficients and the ratio of L/D. Thus the desired flow rates can be obtained by reducing hydraulic resistance by increasing the diameter of loop and increasing the height. Widening of fluid flow path i.e., increase in the loop cross sectional area, decreases the hydraulic flow resistance and hence reduces the opposing frictional pressure gradient, thereby increases the flow rate. Further, the differential density between the source and the sink depends on the quantum of heat being transported and finally for a given location the value of gravity is constant.

If the quantum of heat absorption at source and the quantum of heat rejection at sink are in equilibrium, then the fluid flow is expected to achieve a steady state condition. At steady state condition, the driving pressure differential induced across the raiser and down comer by buoyancy force will get balanced by the retarding frictional pressure differential. Any imbalance in these forces will develop instability in the loop in the form of working fluid mass flow rate oscillation, flow reversals, pressure and temperature fluctuations.

For any applications, the most important requisite of NCLs is the induced flow in the loop shall be stable and unidirectional while it passes through the source and sink. If this condition is satisfies then transporting heat from the source to the sink in NCLs will be indistinguishable from pumped flow.

1.3 Various Configurations of natural circulation systems

NCLs can be generally classified based on their application in the domestic and industrial usage. These classifications often help in analyzing these NCLs in its various applications. An effort has been made in the Fig. 1.2 to elaborate some of the most significant types of NCLs based on type of working fluid, its interaction with surrounding, Physical constructional feature, inventory, number of Loops involved and body force etc.

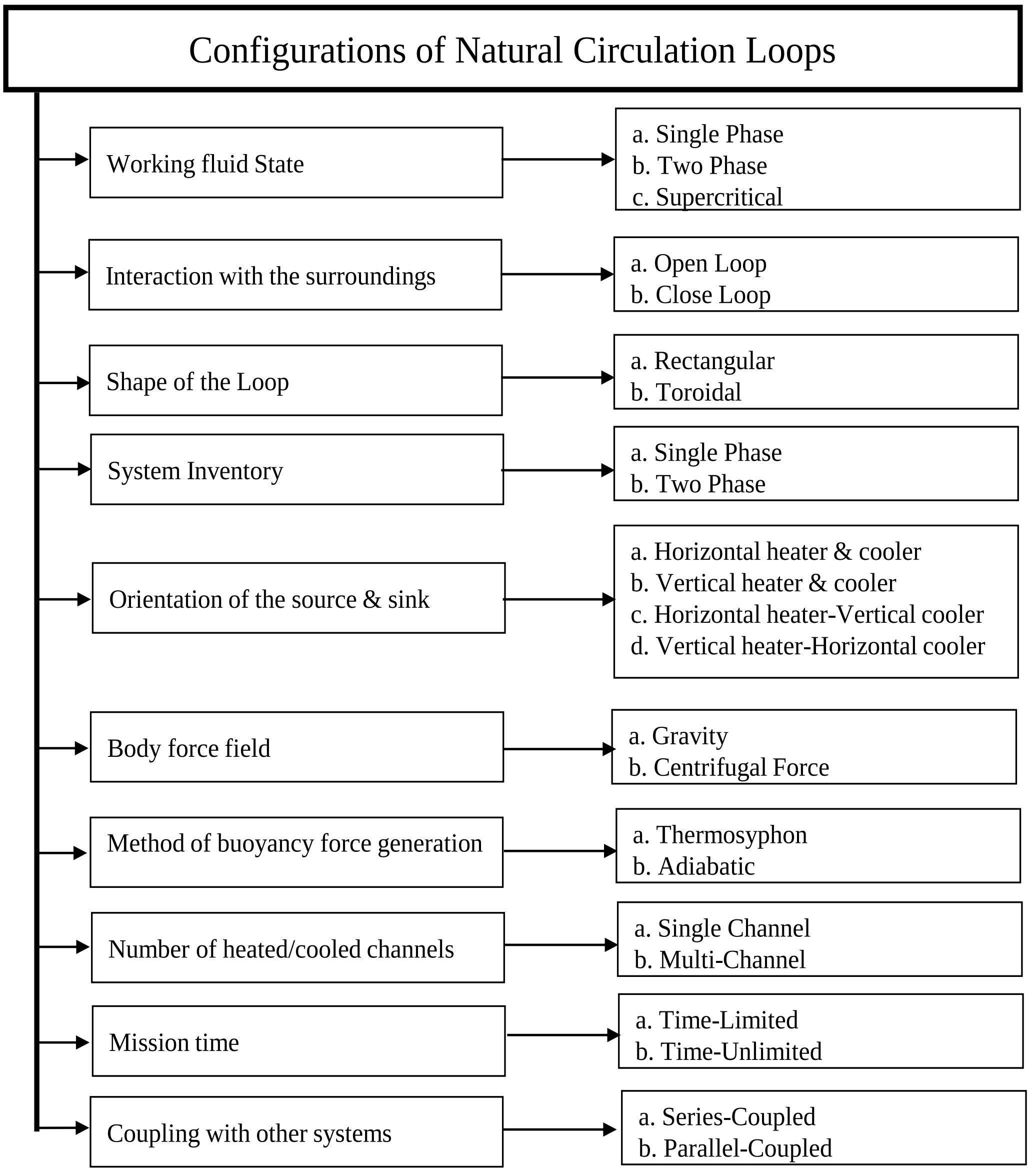

Figure 1.2: Classification of NCL (Vijayan and Nayak 2010).

1.3.1 Classification of NCLs based on thermodynamic state of working fluid

The most common classification of is based on the thermodynamic state of the working fluid NCLs can be classified as:

a Single-phase NCLs

b Two-phase NCLs

c Supercritical NCLs

a. **Single-phase natural circulation Loops**: In a single-phase NCL, the entire loop contains a working fluid in only one state i.e., it is either in a liquid state or a gaseous state. Single-phase liquid-filled NCLs are more commonly used for nuclear reactor core cooling and gas-filled NCLs are widely used in the cooling of radioactive waste.

b. **Two-phase natural circulation loop**: If any location in the loop experiences two-phase flow conditions, then it is referring to as a two-phase NCLs. Two-phase NCLs with only boiling or both boiling and condensation are relevant to cooling of certain systems.

c. **Supercritical natural circulation loop**: If loop operates above the state of thermodynamic critical point, then such NCLs are classified as supercritical natural circulation loops. The main advantage of operating NCLs at supercritical state is that the volumetric coefficient of thermal expansion above critical point is very high and hence it can generate better driving forces in the loop which in fact comparable to that of two-phase Loops. Thermodynamically, supercritical NCLs are more efficient compared to conventional loops and in fact supercritical water systems like supercritical power plant, the heat transfer characteristics are excellent and hence the higher the efficiency of system. Apart from higher efficiency, the unsafe phenomenon like Critical Heat Flux can be completely eliminated by operating NCLs at supercritical state, as there is no phase change involved in the operation. In supercritical state heat transfer deterioration occurs at high heat fluxes but it is much milder compared to the CHF. Further, the power density is significantly larger at supercritical state, which results in smaller system for a given rating. These exemplary characteristics of supercritical NCLs have gained attention from nuclear as well as fossil-fueled power plant designers.

1.3.2 Classification of NCLs based on Interface with the surroundings

Based on interaction of loop fluid with the surroundings, NCLs can be classified as:

a Closed-loop systems

b Open-loop Systems.

a. **Closed-loop natural circulation Loop**:If the loop fluid in NCLs exchanges only energy with the surroundings, then it is called as closed loop NCLs. The loops which are used in power conversion or energy transport systems are belongs to this category.

b. **Open-loop natural circulation system**: If the loop fluid in NCLs exchanges both mass and energy with the surroundings, then it is called as Open-loop NCLs. Open-loop NCLs will be constructed either with only a heat source or with only a heat sink. Ventilation systems and waste storage facilities are generally belongs to this category.

1.3.3 Classification of NCLs based on buoyancy force generation in the system

Based on the means of buoyancy force generation, NCLs can be classified as:

a Thermosyphon systems

b Adiabatic NCLs

a. **Thermosyphon systems**: In a NCL, if the driving buoyancy force is generated thermally, then it is known as thermosyphon loop. The primary purpose of thermosyphon NCLs is to transport heat energy from source to sink.

b. **Adiabatic NCLs**: If the buoyancy force generated in loop adiabatically by injecting a lighter immiscible fluid, then it is known as Adiabatic NCLs. Adiabatic NCLs can be gas liquid two-phase systems. The primary purpose of adiabatic NCLs is to generate a circulation rate.

1.3.4 Classification of NCLs based on constructional feature of the loop

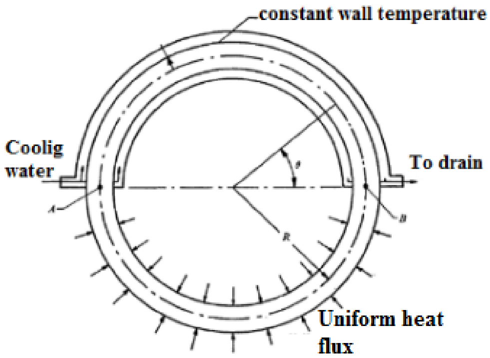

(a) Toroidal NCL (Creveling et al. 1975)

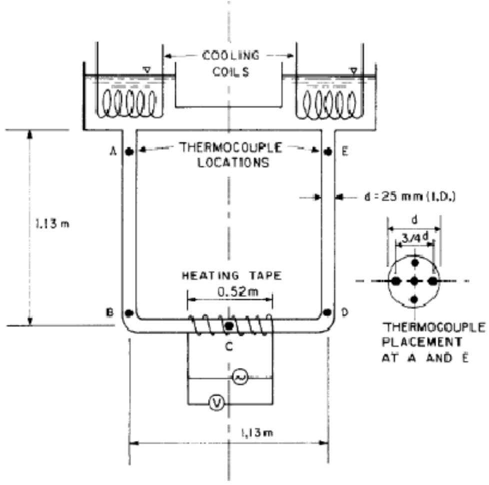

(b) Open type NCL (Bau and Torrance 1981)

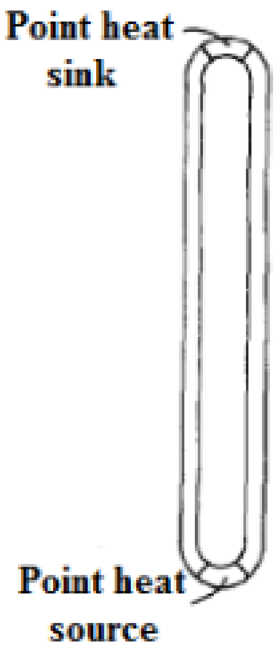

(c) Rectangular NCL (Welander 1967)

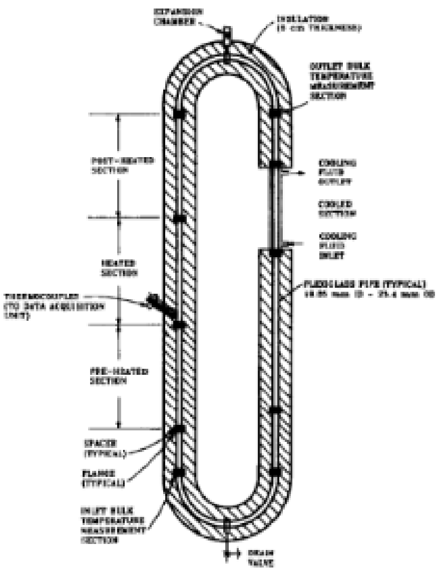

(d) Semi rectangular NCL (Bernier and Baliga 1992)

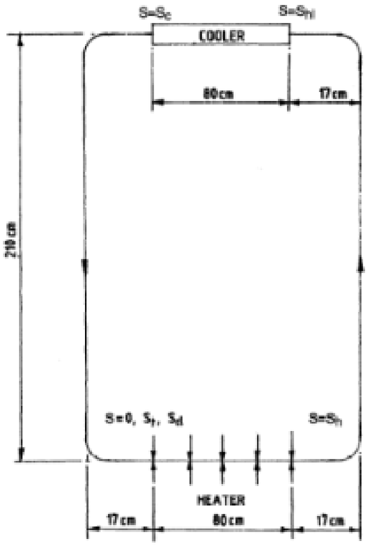

(e) Closed type NCL (Nayak et al. 1995)

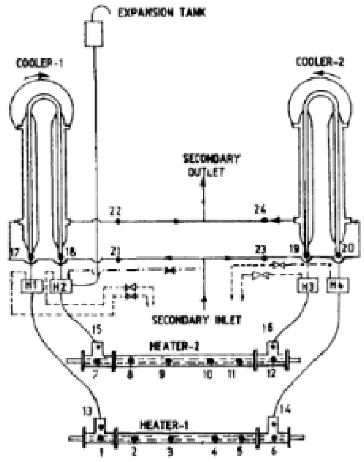

(f) Figure of eight loop(Vijayan and Date 1992)

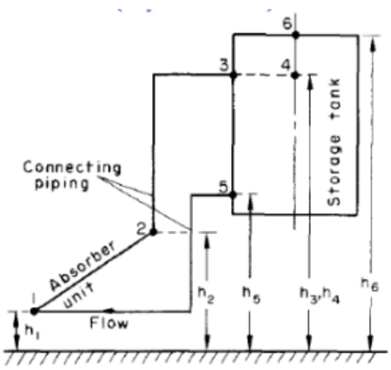

(g) Typical solar heating NCL (Ong 1974)

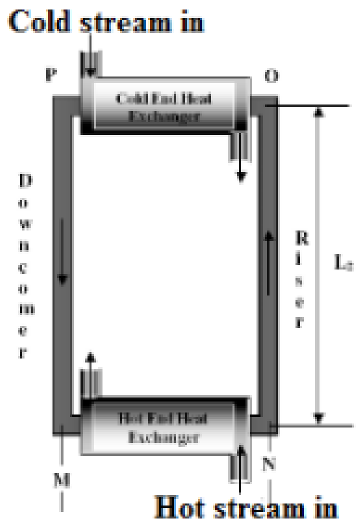

(h) Rectangular NCL with end heat-exchanger (Rao et al. 2005)

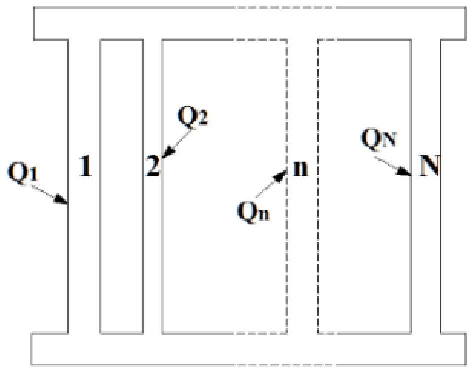

(i) Multiple path thermosyphon (Chato 1963)

Figure 1.3: Various geometrical configurations of natural circulation loop (Vijayan and Nayak 2010).

In general, NCLs are classified based on the shape of the loop, such as toroidal, rectangular, square, U-loop, figure-of-eight, etc. Figure 1.3 shows the classification of NCLs based on constructional feature of the loop. Constructional feature of industrial NCLs are very complex in nature and hence it is not easy to comprehend the phenomena of working fluid circulation inside the loop.

In view of this for a laboratory study purpose, the loops with simple shapes are found to be more useful. Further, it is very easy to construct a simplified laboratory scale loop with lesser number of instruments, which can make available huge quantum of repetitive data in a shorter duration at a lower cost. Comparatively modeling of simple loops for theoretical and computational study is far easier and less time-consuming. To understand the steady state, transient, and stability characteristics of NCLs, rectangular loops have been extensively used in the theoretical and computational studies.

1.3.5 Classification of NCLs based on system inventory

Depending on the system inventory, NCLs can be single-phase and two-phase NCLs. In Single-phase NCLs working fluid circulates in a loop without any inventory loss, whereas in Two-phase NCLs inventory levels keep on reduces in the loop.

1.3.6 Classification of NCLs based on positioning of source and sink in the loops.

The source and sink location in the loops will have a major impact on the steady state and stability behavior of NCLs. Depending on the location of the source and sink, NCLs can be classified as both Heater and Cooler orientated horizontally, both Heater and Cooler orientated vertically, horizontal Heater - vertical Cooler, and vertical Heater-horizontal Cooler.

1.3.7 Classification of NCLs based on body force or driving force in the loop

In fact, a body force field is the only driving force upon which the NCLs functions and there are two types of body force fields which are most are relevant to NCLs viz., gravity and centrifugal force fields. Most of the NCLs functions on the influence gravity force field and which are static in nature and hence these loops are referred to as stationary NCLs. Whereas, a centrifugal force field application is more or less restricted to cool rotating machineries and these loops are referred as rotating NCLs. Further, depending on the rotational speed of the machines, rotating NCLs can be designed to have acceleration values several times higher than the gravity/stationary NCLs.

1.3.8 Classification of NCLs based on Number of heated or cooled channels

NCLs can be classified as single-channel or multi-channel loops, depending on the number of heated or cooled sections. Since the working/loop fluid in the multi-channel loops are circulate in a parallel heated or cooled channels, it is often referred to as parallel-channeled systems. Majority of industrial NCLs are falls under the parallel-channeled category and typical examples are nuclear power reactor and fossil-fueled power plants.

1.3.9 Classification of NCLs based on Mission time

NCLs can be classified based on the heat sink inventory capacity i.e., limited or finite and unlimited or infinite pool inventory, wherein NCLs can perform passively for a limited time or eternally for unlimited time. Based on mission time the NCLs are classified as:

a. Mission time-limited NCLs

b. NCLs with unlimited mission time.

a. **Natural circulation Loops with Mission time-limited** : In these types of NCLs, the heat exchangers are immersed in large pools and it can be connected to either the heat source or the heat sink.

b. **Natural circulation Loops with mission time-unlimited** : If the NCLs operated with an infinite heat sink i.e., the pool with an infinite inventory, then it is possible to have natural circulation loops with mission time-unlimited. Such systems are possible only if the ultimate heat sink is the atmosphere or the ocean.

1.3.10 Classification of NCLs based on Coupling with other natural circulation systems

NCLs can be classified as standalone or coupled systems based on coupling of one NCL with the other. Further, coupled NCLs can be classified as:

a. NCLs Coupled in Series

b. NCLs Coupled in Parallel

c. Parallel-series or series-parallel coupled NCLs.

a. **NCLs Coupled in Series** : In NCLs, which coupled in series, the heat source of the succeeding loop will be the heat sink of the preceding loop. A series-coupled NCL has at least two NCLs connected in series, such that at steady state each of the loops in series transports the same amount of heat. The loops in series can operate with the same fluid or different fluids. The last loop in the series is usually an open loop rejecting heat to the ultimate heat sink.

b. **NCLs Coupled in Parallel**: In NCLs, which coupled in parallel, the same heat source is shared by several loops in the system. The advantage of the parallel-coupled NCLs is that even if one of the loops in the system fails, the system can still work at reduced heat transport capacity. On the other hand, in a series-coupled system, if any of the loops in the series fails, then the entire heat transport capability becomes zero.

c. **NCLs Coupled in Series-parallel or parallel-series**: NCLs can also be coupled or arranged in series-parallel or parallel-series. In a parallel-series coupled system one of the parallel systems is essentially a series-coupled system.

1.4 Advantages of Natural Circulation Loop

a. **Free from rotating equipment:** : The popularity of NCLs in both industrial as well as domestic application is primarily due to its near zero operational and maintenance expenses, as it is free from rotating equipment in the system. Apart from the economic advantage it addresses all safety issues in the system, which is associated with the mechanical failure of the pumps.

b. **Uniform distribution flow in the system**: Nuclear power plants, High capacity Boilers and Solar water heater are usually consisting of multiple numbers of unequal and diverse curvature parallel tubes connected between inlet and outlet headers. It is essential requirement to design the system to ensure uniform flow in all the connected tube to avoid the overheating of the tubes. It is very much required to match flow and pressure drop in these parallel tubes. By deploying the natural circulation concept in this system, the uniform distribution of pressure and hence uniform flow can be ensured in these parallel tubes to the maximum possible extent compared to pump-assisted circulation.

c. **Flow flexibility**: In a two-phase forced circulation system, as the heat input increases the flow decreases, whereas in NCLs the flow increases with increase in heat input. This is one of the important features of NCLs over assisted circulation systems, which can evade causing critical heat flux. The NCLs are capable of operating in a pressure and flow mal-distributed system without causing critical heat flux or else it can damage the tubes in a long run of the system.

d. **Inherent Safety Feature**: The solid grounds on which the operation of NCL rests is natural gravity which is never expected to fail and hence the reliability of system is assured. Whereas forced circulation system depends on the pumps or compressors, which are prone to fail due to mechanical and external power failure. Uninterrupted flow can be ensured by incorporating NCLs concept in the system and this feature has been incorporated in many applications. Further, NCLs can be designed to develop a high flow rate with a lower driving force compared to forced circulation systems and this feature can be easily achieved by increasing the diameter of tubes.

e. **Simpler Geometrical Construction**: The NCLs can be designed with minimum pressure losses to ensure maximum flow rates. Due to its simpler piping layout, number of pipe fittings like U-bends, elbows, valves, loop seals, etc., will naturally reduce and which in turn minimizes piping frictional losses. Reduced frictional losses in the piping obviously enhance the working fluid flow rate in the loop. Further, due to its simpler geometrical constructional feature, NCLs can be factory-fabricated which considerably increases the quality of workmanship.

1.5 Drawbacks of Natural Circulation Loops

a. **Less flexibility to change driving force**: Revamping / Capacity enhancement of NCL is not as easy as in case of pump-assisted circulation system. In forced circulation, it can be accomplished by replacing the pump with another one of a different capacity without affecting the rest of the loop. However, in case of NCLs the driving force in the system can be increased only by increasing the loop height and hence it demands for significant modification in the existing system, which may eventually become uneconomical.

b. **System shall design for low pressure losses**: NCLs are generally operates with significantly lower driving force compared to the forced circulation systems and hence sheer care shall be taken to design the system for lower pressure losses. The factors which dictate the terms on design aspect to achieve low system pressure losses are pipe diameter, piping layout, minimizing or elimination of components in the system. The drawbacks of implementing these strategies in the design will have a major impact on the cost of the project. For a given system capacity, increase in diameter of pipe diameter will increase cost of foundation, supporting structures and pipe. Further, increase in pipe diameter increases the volume of working fluid in the system which is highly unsafe due to availability of large high-enthalpy fluid. Piping layout shall be as compact as possible or else it will increase the cost. Elimination of piping components like isolation valves, control valves and measuring instruments in the loops is highly unacceptable considering the safety of the system.

c. **Lower mass flux concerns**: Usage of larger diameter pipes in NCL will leads to lower mass flux compared to forced circulation systems. The critical quality is comparatively very high if the mass flux is low and it can lead to a larger loop fluid volume compared to a pumped. Large volumes can result in zonal control problems and instability.

d. **Stability concerns**: Instability is an inherent phenomenon in both NCLs and forced circulation system, however NCLs are more susceptible to instability in the form of oscillation of flow, pressure and temperature and flow reversals. This is attributable to imbalance between the driving force and resistive force in the system. The driving force in NCLs is very weak as it is fundamentally influenced by natural factors like gravity and physical property of the loop fluid. Flow can be established in the system only when the driving force dominates all the resistive forces in the loop. Any change in the driving force will affects the flow, which may lead to a persistent oscillatory behavior for certain operating conditions. These kinds of instabilities are more pronounced in two-phase NCLs compared to single-phase or supercritical NCLs. In forced circulation system, driving force can be designed as per the system requirements and also it can be easily controlled by various means. Stabilizing techniques in NCLs is very limited due to its influence on the flow rate and its flexibility to enhance the flow rate is evidently depending on increase in the height of the loop.

d. **Apprehensions of Low-pressure and low-flow in the loop:** Power and system pressure will play a prominent role on the flow rate of NCLs and the flow is normally stagnant during the initial startup and hence stage-wise power and pressure rising is mandatory in the NCLs. This low pressure and flow during start-up scenarios causes system to operate anywhere between low-pressure stagnant condition and full-pressure nominal flow condition.

e. **Thermal and stability margins:** The geometrical structure and operating parameters of a system limits the Critical Heat flux, which is the basis for the thermal margin and hence the maximum power. The instability in the system does not usually occur during normal operation, but it occurs usually while operational transient like variation in the power input to the system, failure of any equipment in the system etc,. NCLs are more prone to get into instability mode of operation even for a slightest variation in the normal operating condition due to its weak driving force. The effects of instability and CHF on thermal margin in forced circulation system will be very marginal compared to NCLs and hence instability and CHF conditions should be avoided during NCLs normal operation.

e. **Development of system specific stable start-up procedure:** Instabilities at low pressure and low power is very common in the NCLs and in many instances it occurs right from startup to inception of boiling process. During pressure and power raising process, normally the system enters into unstable zone and it shall be avoided as instability can cause power oscillations and premature CHF occurrence. To avoid the instability, in such circumference, it is essential to designer shall develop and specify a startup procedure for all types of system.

1.6 Qualifying Criteria for a fluid to become working fluids in natural circulation loops

The most essential requirements for a fluid to get qualify as a working fluid in natural circulation loops are:

- Working Fluid shall be abundantly available and shall be cost effective.
- Shall be Nontoxic and Environmentally benign.

- Fluid shall possess Low viscosity, which ensures very little friction to flow.
- Higher the volumetric heat capacity of a working fluid; which ensures lower pumping velocity required for a given enthalpy flux and temperature difference, and therefore the pumping losses will be lower.
- High specific heat: Higher specific heat capacity of fluid ensures that the temperature of fluid does not change simultaneously, which gives benefits of heated or cooled working fluid for a long time by restraining its temperature.
- High thermal conductivity: Working fluid with a higher thermal conductivity are good conductors of thermal energy.
- High density: volumetric heat capacity of a fluid is product of its density and specific heat capacity, higher the density higher will be the volumetric heat capacity.
- Noncorrosive, chemically stable nature, negligible ozone depletionnature, low global warming potential etc.

Carbon dioxide fulfills all the qualification criteria mentioned above and hence it is the most qualified prospective working fluid for natural circulation loops. CO_2 is a very few naturally available non-toxic and non-flammable working fluids that do not contribute to ozone depletion, if it leaks to the atmosphere. It has very low global warming potential ($\sim$ 1) compared to synthetic refrigerants (GWP$\sim$ 1000). Hence CO_2 can easily and safely supersede all conventional working fluids like CFCs, HCFCs, hydrocarbons and ammonia in several fields of application. These environmentally benevolent nature and splendid thermo-physical properties of CO_2 made it to gain more popularity as a primary and as well as secondary working fluid in both natural and forced circulation systems. Yadav et al. (2012a) carried out comparative analysis between CO_2 and other working fluids for using it in forced circulation-type secondary loops and concluded that it possesses an exceptional secondary fluid characteristic, which are very much required for refrigeration and air conditioning applications. For low temperature refrigeration and air-conditioning applications, CO_2 based NCLs are very compact compared to other widespread conventional working fluids. Compared to other fluids, CO_2 offers very low viscosity and a very high thermal expansion coefficient, as shown in Table 1.1. The phase diagram of CO_2 is shown in Fig. 1.4 on the P-T plane.

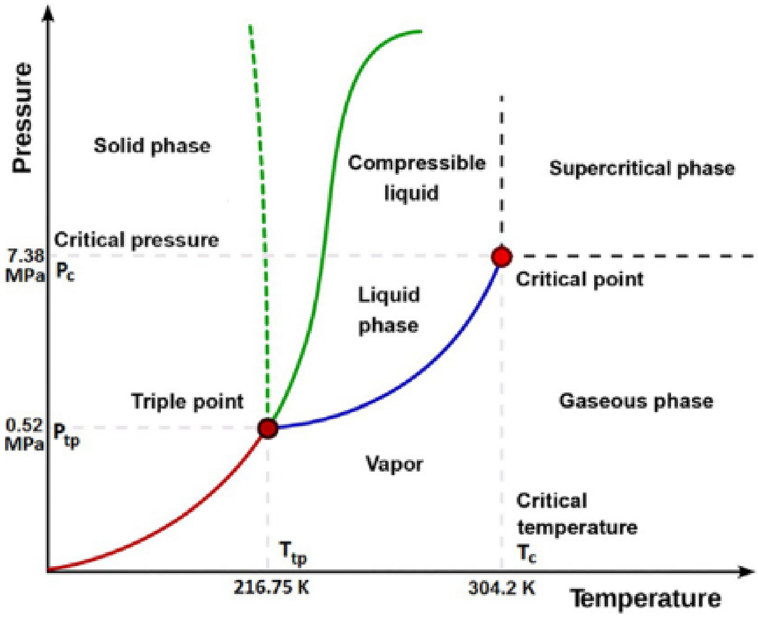

Figure 1.4: Phase diagram (NIST 2018).

Table 1.1: Comparison of properties for different secondary fluids.

REFRIGRENTS	**R12 (CFC)**	**R22 (HCFC)**	**R134a (HFC)**	**R717 (Natural)**	**R744 (Natural)**
Molecular formula (g/mol)	CCl_2F_2	$CHClF_2$	CH_2FCF_3	NH_3	CO_2
ODP	0.82	0.055	0.0	0.0	0.0
GWP	8100	1700	1300	0.0	1
Flammability	No	No	No	Yes	No
Toxicity	No	No	No	Yes	No

REFRIGRENTS	R12 (CFC)	R22 (HCFC)	R134a (HFC)	R717 (Natural)	R744 (Natural)
Molecular weight	120.9	86.5	102.03	17.03	44.01
Normal Boiling Point (0°C)	-29.8	-40.8	-26.2	-33.3	-78.4
Critical pressure (bar)	41.1	49.7	40.7	114.27	73.8
Critical temperature (0°C)	112.0	96.0	101.1	133.0	31.2
Sat. pressure at 0°C (bar)	3.09	4.98	2.93	4.29	34.8
Volumetric refrigeration capacity at 0°C (kJ/m^3)	2740	4344	2860	4360	22545
Viscosity at 0°C (mPa.s)	248.7 (L) 10.74 (V)	218.2 (L) 11.50 (V)	271.1 (L) 10.73 (V)	170.1 (L) 9.06 (V)	99.4 (L) 14.79 (V)
Density at 0°C, (kg/m^3)	1396.1(L) 17.87 (V)	1281.5 (L) 21.23 (V)	1294.8 (L) 14.42 (V)	638.6 (L) 3.45 (V)	927.4 (L) 97.65 (V)
Thermal conductivity 0°C (mW/mK)	75.9 (L) 8.84 (V)	94.8 (L) 9.42 (V)	92.0 (L) 11.51 (V)	559.2 (L) 23.37 (V)	110.4 (L) 19.67 (V)

CO_2 attains a supercritical fluid state when it operates above temperature of 304.25 K and pressure of 7.37 MPa. CO_2 system offers certain unique advantages when it is operated near or above critical state in comparison to other fluids Variation of specific heat of CO_2 with temperature and pressure is shown in Fig.1.5 on the specific heat and Temperature plane.

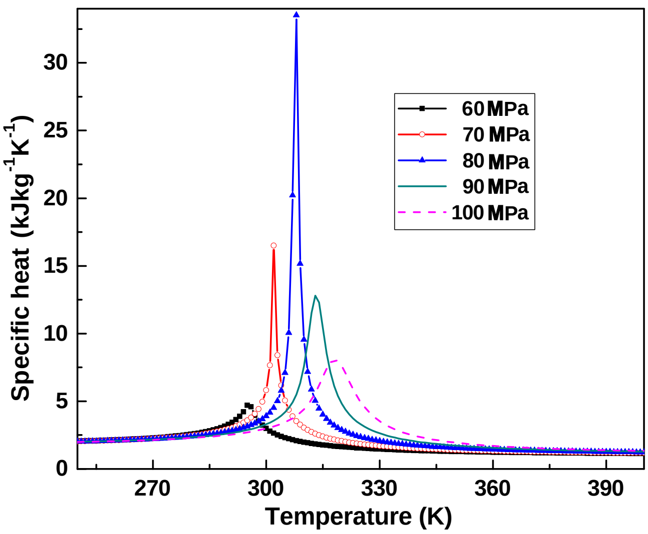

Figure 1.5: Variation of specific heat of CO_2 with temperature and pressure .

Supercritical CO_2 possess very low viscosity, very high coefficient of thermal expansion compared to other conventional working fluids. Three dimensional CFD research results of Yadav et al. (2014) reveals that for the same wall temperature and geometrical parameters the liquid CO_2 exhibits seven times higher heat transfer rate than water. Further similar rate of heat transfer is noticed when CO_2 is operated at near pseudo-critical region also. In an another 3-D CFD analysis of NCLs, Yadav et al. (2014) noticed that near pseudo critical region, the heat transfer rate is much higher in the case of supercritical phase than the subcritical phase, however for subcritical phase, higher heat transfer rate is noticed near saturated liquid state. Experimental results of Thippeswamy and Yadav (2020) on comparison of heat transfer performance of various conventional working fluids of NCL, like water and brine solution with the subcritical and sCO_2 at various loop fluid operating pressure and at various inlet temperatures to source & sink shows that the heat transfer rates in the case of subcritical vapour, subcritical liquid, two-phase sCO_2 based NCL are several times (4 to 9 times) higher than the water and brine-based NCLs. Study of Hahne (1968) on natural convection heat transfer of sCO_2 shows maximum thermal conductivity in the vicinity of pseudo critical temperatures/pressures, and it is more pronounced as critical point is approached. Computational simulations of Zhang et al. (2010) on the sCO_2 based NCLs show that higher Reynolds number mass flow can be established with sCO_2 as a working fluid, even for a small temperature difference ($\sim$25°) between source and sink.

1.7 Instability in natural circulation flow

Flow stability in natural circulation loop is very important as heat transport performance of system entirely depends on its stability behaviour. Flow instability is highly undesirable as it can lead to undesirable mechanical vibration in the system, which makes operation of system noisy and eventually components are susceptible to fail due to fatigue. It is very difficult to control the system if flow instability exists in the natural circulation and it can also affect the local heat transfer characteristics.

At supercritical state, sharp change in the density of the loop fluid near pseudo-critical point causes instability in mass flow rate. At supercritical condition in NCLs, the flow instability causes significant problem for the normal flow condition due to low flow rates.

The stability in NCLs can be defined based on the nature of the trend it follows in the system. If the mass flow rate oscillates in such a way that the amplitude of the oscillations is very small and direction of flow is same with respect to time, then the system is called as "neutral". On the other hand, if the oscillations in the loop keep growing in time and finally it leads to flow reversal then the system is called as "unstable".

The field of stability in fluid dynamics can be characterize as Static instability, Dynamic instability, Acoustic instability, Density wave instability or oscillation and Thermal instabilities. Time-dependent balanced conservation equations are essential to explain the dynamic instability as it characterizes wider class of instabilities. However static instabilities can be theoretically explained by steady state laws and without the aid of time-dependent conservation equations. In natural circulation, flow excursion static instability depends on the relationship between the pressure drop due to frictional forces and the driving forces due to gravity in the loop. Pressure drop oscillation is a dynamic type of oscillations and it occurs in the system due to compressible nature of the working fluid.

If the oscillation frequency in NCL reaches to acoustic range of frequency, then acoustic instability appears in the system and resonance of pressure waves is the prime cause for this instability. When there is a perturbation in the density of the working fluid of natural circulation system then density wave oscillation occurs and its characteristic speed depends on local conditions. The relationship between flow rate, density, and pressure drop causes density wave oscillation.

Thermal instabilities are identified by periodic time oscillations of various quantities in a system such as excursion of heated wall surface temperature.

Natural circulation loops are naturally susceptible to various instabilities, which are obviously due to the nonlinearity involved in natural convection process. Flow disturbance occurs in the NCLs for any disturbance in the driving force and it leads to oscillatory behaviour. Instabilities in NCLs can be well defined by taking ratios between the amplitude of two consecutive oscillations i.e., amplitude of the succeeding oscillation (A_2) to the amplitude of the preceding oscillation (A_1), as shown in Fig. 1.6. This ratio is popularly known as decay ratio and Fig.1.6. schematically depict the definition of decay ratio. Decay ratio is defined as,

$$DR = \frac{A_2}{A_1} \tag{1.1}$$

If this ratio is < 1, then system is stable,

If it is $= 1$ it indicates that the system is neutrally stable,

and finally if it is > 1 then the system is an unstable system. (as shown in Fig. 1.6).

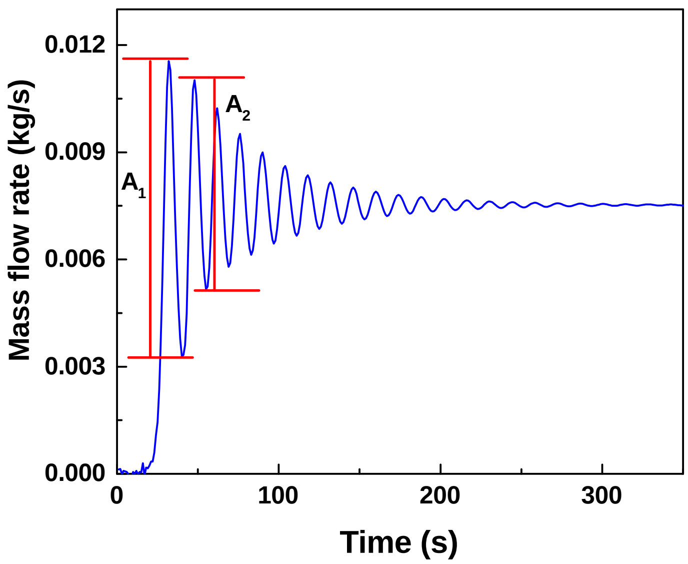

Figure 1.6: Definition of decay ratio (Vijayan and Nayak 2005).

Figure 1.7 (Vijayan and Nayak 2005) depicts the nature of Stable, naturally stable and unstable systems respectively. Instability is defined as sustainability of the natural circulation system against small perturbations of operating parameter. Flow oscillation, chaotic non-linear dynamic behaviour and a flow reversal are the adverse effect of instability in fluid flow. The instability can be quantified in terms of percentage oscillations amplitude variation with respect to steady-state condition. If, oscillations amplitude variation is greater than $\pm 10\%$ from the mean value then it is considered as indication of instability. In a study conducted on instability in NCLs by Mochizuki (1994) it is recommended to consider $\pm 30\%$ variation of amplitude as a cut-off value to declare system as unstable. In NCLs, flow instability is highly unacceptable as it can induce undesirable mechanical vibration in the system components. It may eventually lead to catastrophic incidences due to fatigue development in the system components. In power boilers, natural circulation instability will create huge fluctuation in steam drum water level and it is very difficult to control and maintain the water level. Further, efficiency and heat transfer characteristics will get deteriorate as flow oscillations persist in the system. Hence, in-depth analysis of instabilities in the natural circulation loop is mandatory before using it for a specific application as efficiency and heat transfer, as well as safety of the system are very important aspect of the design.

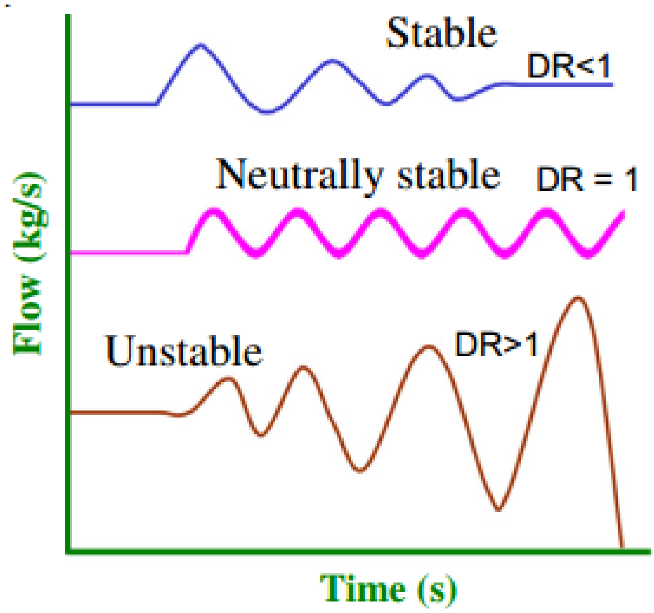

Figure 1.7: Types of instability (Vijayan and Nayak 2005).

1.8 Classification of instability

Theoretical and experimental studies reveal varieties of instabilities in natural circulation systems, which are mainly depends on various factors like, constructional feature of loop, prevailed transport mechanism in the loop, mode of oscillation, the nature of the instability threshold and methodology adopted in prediction of these oscillations. Based on this context, instabilities in natural circulation systems classified by Vijayan and Nayak (2005) into various categories, which helps in conceptualizing and mitigating the instabilities in NCLs mechanism. Instability analysis of NCLs using mathematical models reveal that the cause of all instabilities is due to the existence of challenging multiple solutions i.e., the system fluctuates from one solution to the other solution and hence it cannot nail down to any one perennial solution. Mathematically, an unstable oscillation in natural circulation system is characterized as shifting of one solution to another solution. This phenomenon is predominantly due to its inherent self-generated feedbacks, which makes every solution thus obtained to appear more attractive compare other solution. For a given operating conditions of a system, shifting of solution from one to another repeatedly results in endless oscillatory behaviour. In general, instabilities can be classified based on the following, Vijayan and Nayak (2005) Analysis method, Propagation method, Number of unstable zones, Nature of the oscillations, Loop geometry and Disturbances or perturbations. In this dissertation instability of the natural circulation loop is analyzed based on the nature of the oscillations of the prime parameters such as mass flow rate, temperature, velocity and pressure.

Instabilities in NCLs eventually take different oscillatory forms depending upon various dominating forces. Based on periodicity of these oscillations, it can be characterized as periodic and chaotic. Further, these oscillations can be classified as a fundamental mode or higher harmonic modes based on oscillatory mode it attains ultimately. Flow oscillates not only in a definite direction but it can change its direction during oscillations, i.e., it can be characterized as uni-directional, bidirectional, or switch between the two periodically or chaotically. Different oscillatory forms are depicted in the Figs. 1.8(a-c)).

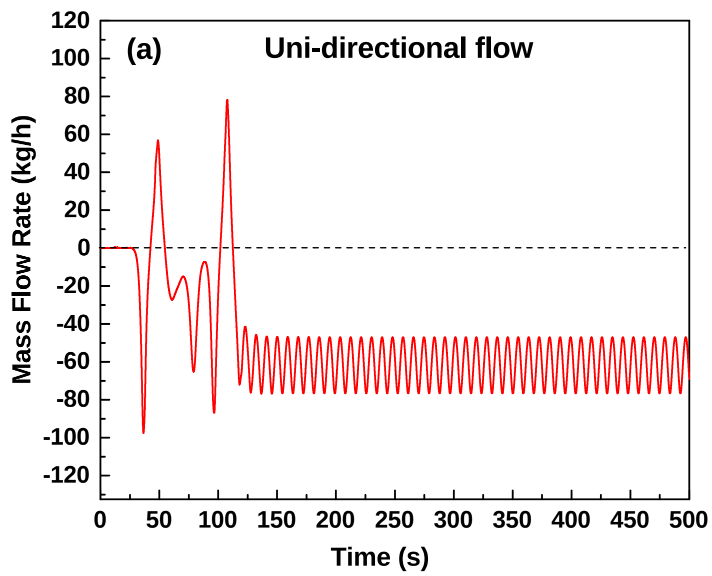

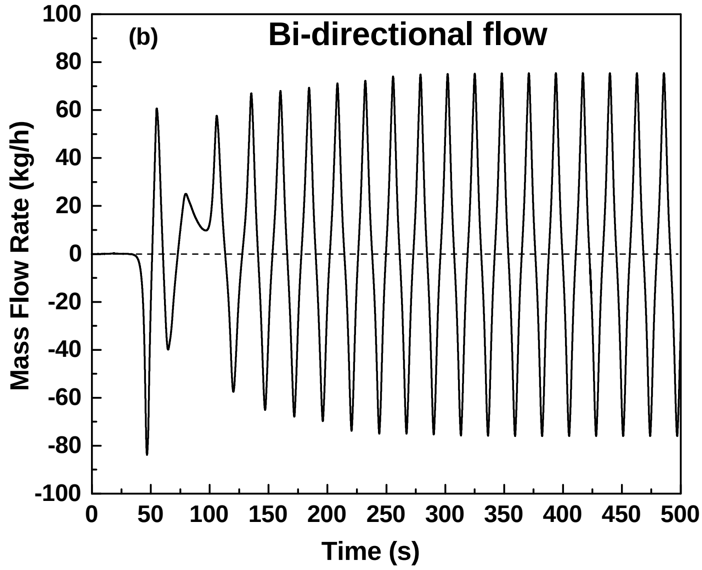

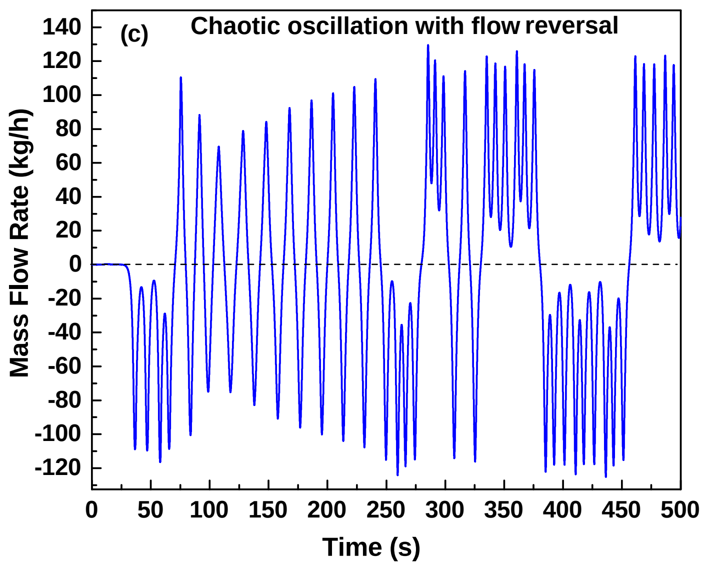

Figure 1.8: Nature of oscillation (a) Uni-direction flow (b) Bi-directional flow (c) Chaotic oscillations with flow reversal.

1.9 Structure of the thesis

Chapter 1 presents a brief introduction to Natural Circulation Loop, Classification of Natural Circulation loop, various application of Natural Circulation Loop, Working fluids etc.

Chapter 2 presents comprehensive literature review on Natural Circulation Loops, which comprises of survey on heat transport mechanism in NCL, Stability behavior of NCL, Various applications of NCL, research gap and research objectives.

Chapter 3 deals on comparative study on the dynamic performance between two different configurations of NCL, i.e., i) NCL with isothermal heater and a cold heat-exchanger, and ii) NCL with both side heat-exchangers. To explore this, two-dimensional transient computational fluid dynamics studies are carried out on the stability appraisal of sCO_2 based natural circulation loop.

Chapter 4 presents assessment of transient and stability behavior of sCO_2 based NCLs by using three-dimensional numerical analysis technique. In this study, three different configurations of NCL, which are exposed to three different kinds of heat sources by keeping the same kind of sink i.e., heater, hot heat exchanger (HHX) and isothermal wall (ISO) at the source and a cold heat exchanger (CHX) at sink, has been studied and the results thus obtained are compared.

Chapter 5 is an experimental investigations on supercritical CO_2 sCO_2 based Natural Circulation Loop. The loop is designed, fabricated and tested to conduct the high pressure and temperature experiment. Details on experimental setup of high-pressure natural circulation loop along with various instruments which are used to perform experiment are also presented in this section. Tests have been carried out to study the system performance and validate the numerical results.

Chapter 6 concludes with important findings based on computational fluid dynamics numerical simulations and experimental study. Further, the recommendations for future works are also presented in this dissertation.

CHAPTER 2

Literature Review

The current chapter depicts the detailed literature review on theoretical and experimental research activities conducted by various researchers in the field of Natural circulation phenomenon. This review mainly concentrated on outline of heat transfer phenomena and various instabilities involved in the natural circulation loop. The review also emphasizes the impact of various boundary conditions on the heat transfer mechanism and stability in NCLs. Further, this chapter concludes with the research gap and objectives of the study.

2.1 Natural circulation loop

Natural circulation loop (NCL) is considered to be one of the most promising and dominant mechanism in transporting heat energy from source to sink. The driving force develops naturally in NCLs as a result of thermally generated density gradient, which is generally accredited as buoyancy force. The concept of fluid motion due to heating at bottom and cooling in the top is evoked from the work of Rayleigh (1916). The first researcher who introduced the term natural circulation in the field of heat transfer is Japikse (1973).

Mertol et al. (1982) carried out one dimensional numerical analysis on NCL to investigate the behaviour of transient heat transfer, fluid flow and pressure. Result shows that in the initial stage the flow velocity will be very small and hence the fluid will be exposed to prolonged heating and hence it will over heat the fluid. Due to sudden release this accumulated heat overshoots the velocities and temperature in the loop.

Further, in an another study, Mertol et al. (1984) presented pressure, temperature and velocity distribution in NCL under laminar flow conditions by determining the variation of the friction and heat transfer coefficients.

In a toroidal thermosyphon, at steady-state regime, Stern and Greif (1987) measured the fluid temperature across the heating section for a range of heat fluxes and reported that in all the cases, the highest temperature occurred at the inner wall location and the greatest amplitudes of the fluctuations occurred at the locations near but not at the inner wall.

In NCLs, the heating section, designated as source, shall be embedded at the bottom and cooling section, designated as sink, shall be at the top of the loop. NCLs shall be fabricated to form a closed loop circuits and installed in a vertical position in order to reap the maximum benefits of gravity created buoyancy force. In a study conducted by Acosta et al. (1987) on single-phase NCL it is noticed that maximum fluid velocity can be achieved when loop is kept at near zero-degree tilt angle i.e., in a vertical position and fluid velocity decreases with the loop tilt angle. Further, experimental study of Acosta et al. (1987) shows that over a certain range of inclinations of the loop i.e., at around zero degrees, the flow could either clockwise or counter clockwise. If tilt angle exceeds certain limit, flow direction changes suddenly and at critical tilt angle it forms the boundary between stable single and multiple steady-states. At lower heat input at source the critical angle is found to be as large as 25° tilt from the vertical.

Nayak et al. (2000) assessed various void fractions and pressure drop correlations to predict the performance of NCLs and it is noticed that most correlations give predictions close to each other. Vijayan et al. (2007) studied rectangular NCL by changing the orientations of heater and cooler in the loop and noticed that for a given operating condition of a loop, maximum flow can be achieved when both the heater and the cooler oriented horizontally but loop found to be least stable compared to the loop with both heater and cooler oriented vertically.

The effect of wall thermal conductivity and wall thickness on heat transfer characteristics of a single-phase NCL is numerically investigated by Lin et al. (2008) and found existence of axial conduction through the thick and highly conductive wall of the loop, which tends to appreciably improve the buoyancy-induced circulating flow in the loop at lower modified Rayleigh number.

Influence of loop diameter, inlet temperature and system pressure on the performance of single-phase, two-phase and supercritical natural circulation system was analyzed by Vijayan et al. (2010) using a one-dimensional theoretical model. It was noticed that at all the three regions, the flow rate increases with an increase in loop diameter. When loop fluid is in single-phase and supercritical region, the flow rate found to be increased with increase in inlet temperature at source. Whereas when it is in two-phase region and beyond the pseudo critical value, the flow rate found to be increased initially and then decrease after reaching to a peak value. Pressure has a substantial impact on the flow rate in the two-phase region, marginal effect in the supercritical region, and virtually no effect in the single-phase region. Later, effect of loop diameter, loop height and ambient temperature on the performance of Natural circulation loops was parametrically analysed by Sadhu et al. (2016) and noticed that with increase in loop diameter the mass flow rate found to be increased which obviously due to lower frictional losses in the loop. Increase in loop height will increase the mass flow rate in the loop but it increase the loss of energy to the ambient.

One-dimensional mathematical model study of Cheng et al. (2017) shows that increase in loop diameter and temperature difference across the loop increases the steady state Reynolds number, however the modified Grashoff number and the heat transfer rate increases when temperature difference across the loop increases.

2.1.1 Applications of Natural Circulation Loop

Natural circulation technique is extensively incorporated in various industrial as well as domestic applications like Nuclear Reactor (Power Plant) Core Cooling, Natural Circulation Power Boilers, Gas Turbine Blades Cooling, Geothermal Energy Extraction, Electronic Devices Cooling, Electrical Transformers Core Cooling, Solar Heaters, Air-conditioning and Refrigeration, Internal Combustion Engine Cooling, etc.

Cohen and Bayley (1955) surveyed the gas-turbine rotor blades cooling system by adopting thermo-siphoning and found that it is the most attractive blade cooling technique as it is very simple and effective in cooling the root of the gas turbine blades. Kreitlow et al. (1978) analysis on the energy extraction from geothermal well shows that thermosyphoning is the only mechanism wherein the maximum energy extraction and flow rate can be achieved through the well.

The application of passive safety systems i.e., the system which operates under the influence of naturally governed forces such as convection and gravity, has been well recognized and accepted by the community of Nuclear Power plant designers since mid-1980s. This concept has been implemented in the new water cooled nuclear reactor designs. Design and implementation of passive system in the nuclear power plant will not only contributes to achieve simple, safe and highly reliable features in nuclear reactors but also potentially improves the economics in terms of operation and maintenance. NCLs are highly economical in terms of its operation and maintenance due to non-existence of active elements in the system.

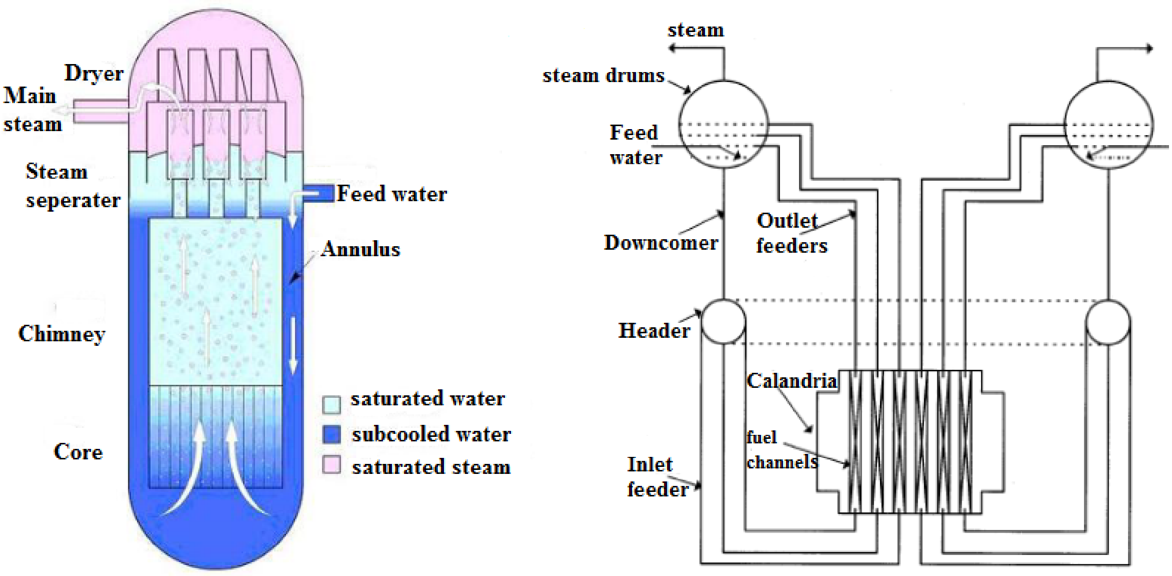

(a) ESBWR **(b)** AHWR

Figure 2.1: Natural circulation loop in nuclear power plants.

The emergency core cooling mechanism of Dodewaard nuclear reactor of Netherlands

(Hagen and Stekelenburg 1997), Economic Simplified Boiling Water Reactor (ESBWR) (Gamble et al. 2006) designed by General Electric and Advanced Heavy Water Reactor (AHWR) (Sinha and Kakodkar 2006) (shown above in Fig. 2.1) of India are fine examples of NCL in nuclear power applications.

Misale et al. (2007) experimentally analyzed the influence of loop height on the performance of NCLs, which could be used for cooling of electronic devices. Results show that, the velocities of the tallest loop are the lowest as increase in buoyancy forces enhances the shear stresses.

Solar collector using supercritical CO_2 as working fluid is experimentally analysed by Yamaguchi et al. (2009) and found that the average collector efficiency was more than 60.0% compared to the water-based solar collector.

Notwithstanding to all these applications and its popularity, the main drawback of NCLs is its very low Reynolds number, due to which the heat transfer rate in the system becomes low compared to forced circulation loop Yadav et al. 2014.

Theoretical studies of Kumar and Khalid (2019) on application of CO_2 based NCL in refrigeration system reveals that amount of heat absorbed in the evaporated is almost equal to the amount of heat rejection in the condenser.

2.2 Behavior of Carbon dioxide as a Loop fluid in Natural Circulation Loops

Kumar and Gopal (2009a) conducted a comparative study between CO_2 and conventional refrigeration / air conditioning fluids which can be used in NCLs as secondary fluids. The results show that for a given size of the system and heat input, the loop pipe diameter required for CO_2 is found to be very compact compared to most of the conventional secondary fluids due to its excellent thermo-physical and transport properties.

Using a simple analytical expression Kumar and Gopal (2009b) shown that use of CO_2 in place of water can result in a compact loop. Further, it is noticed that, the mass flow rate of external fluid does not influence the performance of loop but temperatures of external fluids strongly affect the loop performance.

Yadav et al. (2012b) carried out 3-dimensional CFD analysis to compare the CO2 and water based NCLs by exposing its source and sink to various isothermal wall temperatures. Results show that CO_2 at liquid state and also near pseudo-critical region exhibits approximately seven times higher heat transfer rate than water. Further, two new correlations are proposed for Reynold number in terms of modified Grashof number and Nusselt number in terms of Reynold number and Prandtl number from the data obtained.

Yadav et al. (2014) carried out comparative analysis between carbon dioxide and various other secondary loop working fluids at same operating conditions like same rate of heat transfer, pressure drop and also for the same rise and drop of secondary fluid temperature. Results show that the primary and secondary working fluids heat exchanger turn into compact and lightweight when carbon dioxide is employed as a secondary loop working fluid. Also for a given capacity of the forced circulation system, the CO_2 requires much smaller power compared with all other fluids. It is concluded that it possesses an exceptional secondary fluid characteristics, which are very much required for refrigeration and air conditioning applications.

Thippeswamy and Yadav (2020) experimentally compared the heat transfer performance of various conventional working fluids of NCL, like water and brine solution, with the subcritical and sCO_2 at various loop fluid operating pressure and at various inlet temperatures to source & sink. It was observed that the heat transfer rates in the case of subcritical vapour, subcritical liquid, two-phase and sCO_2 based NCL are several times (4 to 9 times) higher than the water and brine-based NCLs.

Hahne (1968) studied the natural convection heat transfer of sCO_2 and obtained maximum thermal conductivity in the vicinity of pseudo-critical temperatures/pressures, and noticed that it is more pronounced as the critical point is approached.

Yoshikawa et al. (2005) studied the Performance of supercritical fluids natural convection circulation system and found that for a temperature difference of 3-8 °C across heating and cooling source an average flow velocity as high as 4 m/min could be obtained.

In another 3-D CFD analysis of NCLs,Yadav et al. (2012b) noticed that near pseudo critical region, the heat transfer rate is much higher than the subcritical phase, however, for the subcritical phase, a higher heat transfer rate is noticed near-saturated liquid state.

Three-dimensional CFD analysis of a subcritical as well as supercritical CO_2-based NCL subjected to isothermal condition at source and sink has been carried out by Yadav et al. (2016) and developed correlations for obtaining optimum operating condition in supercritical region. At supercritical phase the heat transfer is much higher compared to subcritical phase, however when the liquid operated near saturation condition show higher heat transfer rate.

Janardhana Reddy et al. (2018) investigated the transient convection behaviour of CO_2 at subcritical, supercritical, and near-critical regions at different physical parameters by using numerical methods and noticed that at supercritical region the time required to reach steady-state condition increases with increasing the reduced temperature and pressure values.

2.3 Behaviour of Supercritical based Natural Circulation Loops

Misale et al. (2000) studied the influence of wall thermal capacity on the sCO_2 based NCL behaviour and noticed that the Reynolds number increases if the wall thermal capacity decreases. If the thermal capacity and the conductivity of the pipe material at heating section decrease, the average temperature of the pipe increases and hence the buoyancy force in the loop increases. At the supercritical region, the Nusselt number is found to have larger values than the near-critical and subcritical regions for CO_2.

A computational simulation has been carried out by Zhang et al. (2010) to study the flow and heat transfer behaviour of sCO_2 NCL subjected to constant temperature wall on both source and sink. Result show that with sCO_2 as a working fluid in the loop, higher Reynolds number can be achieved even for 25°C temperature difference across the source and sink. Due to higher Reynolds number (as high as 6x 10^4) and higher average Nusselt number (as high as 14) at super critical state obviously enhances the heat transfer rate in the loop.

CFD analysis of Yadav et al. (2012b) on single-phase CO_2 subcritical and supercritical based NCL with end heat exchangers show that velocity and temperature vary in all directions due to strong buoyancy effects. Further, it is notice that heat transfer rate in supercritical region is higher than that of subcritical region and it reaches maximum near the pseudo-critical region. Further a new correlation is proposed for Reynolds number and Nusselt number.

Numerical Transient analysis ofYadav et al. (2014) on subcritical and sCO_2 based natural circulation loop at various operating pressures and temperature shows that time required to reach steady state decrease with increase in operating pressure and heat transfer rate increases with increase in source temperature due to widening of temperature difference between Cold Heat Exchanger and Hot Heat Exchanger, which leads to a higher buoyancy force.

Archana et al. (2015) developed 2 dimensional CFD code to study the effect of pressure on heat transfer and steady state characteristics of sCO_2. Results show that mass flow increase with increasing the operating pressure of the loop due to increase in the density difference across the source and sink. Further, as the operating pressure increases the heat transfer coefficient decreases.

Liu et al. (2016) carried out experiments to investigate the effects of heat flux, pressure, buoyancy force on heat transfer behaviour of sCO_2 rectangular NCL and developed a heat transfer correlation for supercritical fluid based on obtained data. It is noticed that the heat transfer coefficient decreases to the maximum extant, if loop pressure and heat fluxes at source increases. Further, results indicated that reason for heat transfer deterioration in the loop is mainly due to the steep gradient of physical property variation over the tube cross-section.

To explore the transient behaviour of subcritical & sCO_2 based NCL, Yadav et al. (2014), conducted numerical study at various loop fluid operating pressure and loop tilt angle and also at various inlet temperatures to Hot heat Exchanger and a fixed inlet temperature to Cold Heat exchanger. The experimental results show that as the operating pressure of the loop fluid increases, the time duration required to reach steady state of the system decreases and the change in temperature across hot or cold heat exchanger also decreases. Change in temperature of loop fluid across hot or cold heat exchanger decreases as operating pressure increases. At a tilt angle of 45° in YZ plane, the Loop fluid temperature is found to be higher compared to tilt of loop in XY plane, this is due to reduction in effective height of the loop.

In experimental study conducted by Yadav et al. (2017) on sCO_2 based natural circulation loop, it is observed that loop fluid mass flow rate decreases with a change in tilt angle. However, the heat transfer rate increases with an increase in external water mass flow rate and hot water inlet temperature but decreases with a change in tilt angle. Further, the loop was found to be stable under the pulsating mass flow rate of external hot and cold water.

Sadhu et al. (2018) modeled high temperature sCO_2 based NCL, to investigate the effect of various operating variables and design parameters on loop performance. Result show that for a given heat input at source, the maximum loop fluid circulation could be achieved by increasing either the diameter and/or the loop height. Effect of Change in pipe diameter on the loop performance is more significant compared to change in height. Further, effect of axial conduction is found to be negligible.

Deng et al. (2019) conducted both numerical and experimental studies on sCO_2 based NCL to flow transition and noticed significant effect on the flow pattern during change in heat fluxes at source. In the transition region, sudden drop and increase in the Reynolds number is observed for every transition period. At supercritical state, during the transition period, the fluctuation in cooler temperature is found to be very minimal compared to heater temperature before it entering into the stable flow, which shows the prominent effect of cooler in the loop.

2.4 Applications of CO_2

Nekså (2002) used CO_2 based heat pump water heater and found that it has got significant advantage over conventional heaters, wherein water temperature can be increased up to 90°C without any operational difficulties. Adriansyah (2004) theoretically investigated CO_2 transcritical cycle based combined air conditioning and tap water heating plant and found improvement in the performance of the system. Pharmaceutical hydrates demonstrated very high solubility in sCO_2 compared to other anhydrous phases (Bettini et al. (2004)). Zhang and Yamaguchi (2008) Conducted experiment by using expansion valve in a CO_2 heat pump system to expand liquid CO_2 to a CO_2 solid-gas two phase flow and achieved cryogenic refrigeration temperature of -56.6°C, which is less than triple point temperature of CO_2. Conboy et al. (2013) has constructed a test-loop of sCO_2 based Closed-Brayton power conversion cycle to investigate the key areas of technological uncertainty and this experimental research result show that sCO_2 recompression cycle can achieve high efficiency at relatively low operating temperatures with extremely compact turbo machinery.

In view of reducing the sCO_2 operating pressure while retaining its thermal conversion efficiency and also to exploit its properties of very high Reynolds number natural convective flow at supercritical state, Chen and Zhang (2014) experimentally investigated the characteristics of solar thermal conversion using sCO_2-dimethyl ether mixtures. It is found that with this mixture the operating pressure successfully reduced and the mass flow rate and temperature are found to be more stable as supercritical fluid properties of CO_2 is moderated when DME is introduced. Despite its simplicity and compactness, a sCO_2 Rankine cycle can achieve high efficiency compared to a steam Rankine cycle if incorporated in the waste heat recovery system of a gas turbine

(Cho et al. 2015).

Kim et al. (2017) compared three cycles in terms of energy and exergy analyses and concluded that deployment of sCO_2 power cycle in a waste heat recovery system of gas turbine can achieve high efficiency in comparison to a steam cycle.

Li et al. (2018) noticed that by employing sCO_2 as a refrigerant in refrigeration and air-conditioning applications, maximum heat transfer coefficient can be achieved even at lower cooling pressure in the gas cooler. Wang et al. (2019) discussed the important characteristics of the transcritical CO_2 process applied to heat pumps, and compared theoretical and experimental results of several heat pump applications. The results show that CO_2 is an attractive alternative to the synthetic fluids.

2.5 Oscillatory Behaviour or Instabilities in Natural Circulation Loops

Natural circulation loops are inherently susceptible to instability due to its low driving force as well as its nonlinear flow nature. For the flow to get established in natural circulation loops, the driving force shall be dominating force compare to the collective force of all the resistive forces. Appropriated agreement between driving force and resistive force is the prerequisite for a stable state in the natural circulation loops. The instabilities in NCLs are highly vulnerable to any change in the operating parameters or perturbance in the loop. This inherent behaviour of Natural circulation flow is mainly due to the strong coupling between the flow and the driving force. Particularly in case of compressible fluids, the average loop density increases with increase in the loop pressure and it supplements buoyancy effect in the system due to lower viscosity and which in turn increases the mass flow rate. Resistive force in a loop is a function of friction factor, mass flow rate and average density. For any change in these parameters there will be a huge impact on the resistive forces, which is mainly due to viscous dissipation and friction between wall and fluid. The resistive force thus increased in the system due to higher density will counters the buoyancy force and suppresses the mass flow rate in the loop. Again, the buoyancy force strives to overcome the resistive force and this tug of war will continue between these two forces till there establishes a balance and it is the root cause for the instability/oscillation in the natural circulation loops. As discussed above, the loop fluid establishes only when the driving force dominates all the resistive forces of the system.

Further, due to the nonlinearity of the natural convection process, there will be change in flow pattern for any disturbance in the driving force and it leads to oscillatory behavior, even though steady-state is expected in the system eventually. Therefore, NCLs always require a precise assessment of its flow behaviour with respect to time and also the actual thermo-physical phenomenon which occurs in the NCL. The flow and temperature fields in the NCLs are inter-dependent, and hence it is not possible to have direct control over the circulation rate or direction of flow/circulation in the loop, this inherent nature of NCL propels the loop into instability. The small driving force, i.e., buoyancy force and its nonlinear nature of the natural convection, intrinsically make the NCLs more unstable than the forced circulation system. It is essential to comprehend the characteristics of NCL stability before integrating it into any practical applications. Both forced and natural circulation systems are susceptible to instability in case the flow is two-phase, however the natural circulation systems are more unstable compare to forced circulation systems. Further, forced circulation systems are more stable, as it is supported by external mechanical driving force.

Instability can be defined as stable, neutrally stable and unstable depending on the nature of oscillations. The mass flow stability can be categorized as neutral if the mass flow rate oscillates with smaller amplitude and the flow velocity remains in the same direction, and similarly, it can be categorized as unstable if the oscillations keep growing with time and lead to flow reversal. After any perturbation in the system, if the system reaches back to the original steady state condition, then the system is considered to be stable. If on the other hand the system continues to oscillate with the same amplitude, then the system is neutrally stable. If the system stabilizes to a new steady state or oscillates with increasing amplitude, then the system is considered as unstable. It is interesting to note that the amplitude of oscillations in both forced and natural circulation systems cannot go on increasing indefinitely in any of the cases defined above but it is limited to the extent of nonlinearities involved in the system. However, these limitations in cycle oscillations may be chaotic or periodic depending on stable, neutrally stable and unstable oscillations in the loop. Instability is highly undesirable as it can induce mechanical vibration in system components, if the flow oscillations are persistent in nature. The sustained oscillations in the system may leads to premature exposure of heating section of the loop to a critical heat flux as well as other secondary effects like power oscillations in power generation systems. Instability can also interrupt the control systems and which can lead to operational difficulties in power generation system.

In the supercritical region, the loop experiences mass flow rate instability due to sharp changes in the density of loop fluid near pseudo-critical points. Flow instability at the supercritical state is even more critical compare to the other states as it can induct more harmful effect on components of the system, and eventually it may lead to catastrophic incidences due to fatigue development in the components. Further, if oscillations get augmented, it can affect the heat transfer characteristics, which will be detrimental to the system efficiency. Many investigators profoundly studied the natural circulation system to comprehend the nature of instability, and some of the observations of a few researchers are given below.

In a one-dimensional rectangular-shaped model, Keller (1966) first observed and reported a periodic oscillatory motion of the loop fluid when certain parameter in loop exceeds certain limits and interestingly it is noticed that the flow oscillation was always unidirectional throughout the operation. Further, it is concluded that these oscillations depend on the interaction between frictional and buoyancy forces but independent of inertial forces. In a theoretical discussion, Welander (1967) mentioned that the solution of differentially heated loop fluid is susceptible to instability in an oscillatory manner, i.e., a weaker instability will be in the form of pulsations with a unidirectional motion, while a stronger instability will be bidirectional and also these oscillations are found to be irregular. Thermal anomalies in the fluid create an unstable fluid motion in the loop and these anomalies amplify with flow rate variations. It is noticed that flow is maximum while fluid flowing in the riser and minimum flow in the down comer. Similarly the flow passes quicker through the heat sink than through the heat source.

Experimental study of Creveling et al. (1975) on single-phase free convection loop show that at higher and lower rates of heat-transfer, the loop fluid flow was found to be steady but it was highly oscillatory at intermediate ranges of heat-transfer. Chen (1985) carried out an analytical and numerical investigation to study the flow instability in single-phase thermosyphons over a range of loop aspect ratios and expressed the steady-state results in terms of a single dimensionless parameter. When this parameter is less than a critical value, the flow is stable, and above this value, the flow is unstable. Further, it is observed that when the aspect ratio of the loop approaches unity, the flow is least stable. Lifshitz and Zvirin (1993), performed comprehensive work to study the characteristics of natural circulation loop at steady state and transient condition and developed a five region stability chart. The first region is monotonic instability region, wherein a small disturbance grows monotonically and finally reaches to the steady stable state. Second one is global stability region, wherein it approaches to rest state from any initial conditions i.e., a small perturbation to the rest state and other three regions are oscillatory instability i.e., small perturbations grow to long term periodic flow and finally decay to rest. Based on this chart it is concluded that, for transferring maximum heat from the source to the sink, i.e. to remove maximum heat from the core of nuclear reactor, the NCL parameters shall operate in the first region of the stability chart.

Schuster et al. (2000) investigated the thermo-hydraulic properties of integrated reactor concepts with a natural circulation driven primary loop and concluded that it is not possible to reach a stable two-phase flow in the loop without passing through flow instabilities. Further, when the loop is at thermal equilibrium i.e., quantity of heat addition and rejection at source and sink are equal then the flow oscillations are found to be at nearly constant frequencies and amplitudes.

Furuya et al. (2001) experimentally investigated the effect of inlet restriction on thermal-hydraulic stability. Results show that the driving force of the natural circulation at the stability boundary is a function of heat flux and inlet sub-cooling but independent of inlet restriction. In a natural-convection-driven flow, Dimmick et al. (2002) found that the flow instabilities introduce due to large variations in fluid properties near the critical point. It can occur only under certain conditions and it is very prominent at low powers.

The steady state flow in uniform or non-uniform diameter single-phase natural circulation loops studied by Vijayan (2002) and result shows that, the stability behaviour of a non-uniform diameter loop is found to be depend on a large number of geometric parameters in addition to the modified Stanton number. Jain et al. (2008) numerically studied flow instabilities in a supercritical CO_2 based NCL at steady-state and dynamic conditions and determined stability boundaries under different operating conditions. Parametric studies reveal the similarity of stability characteristics between supercritical conditions and two-phase flows under different operating conditions.

Chen et al. (2010) carried out numerical simulations to investigate flow transitions and instabilities in a sCO_2 based NCL and found that at certain heat source temperature i.e., at around 375 K, which is near the second pseudo-critical temperature, the loop fluid in the system changes from unstable bidirectional flow into stable unidirectional flow as the fluid properties experience major transitions. Here the fluid properties experience major transitions with the increase of temperature. Chen and Zhang (2011) numerically studied the effect of pipe diameter on the heat transfer and stability of sCO_2 based natural convective circulation system and found that the flow get stabilized in larger diameter pipe due to enhanced heat transfer and highly developed flow field. Further, heat transport can be enhanced further at higher operating temperature.

An experimental study by Kapitz and Wiesche (2012) showed that the nucleation sites in the NCLs will strongly impact stability behaviour, especially for low heat flux levels. Misale (2016) experimentally investigated the behavior of single-phase NCL by imposing constant and variable power input at source, the result show that for both type of inputs the loop found to be unstable i.e., temperature oscillations across the source. It is observed that oscillation frequency and amplitude increases with increase in power input.

Stability behaviour of the NCL at various pressure & temperature levels, at various flow regions i.e., laminar, transition & turbulent, at various phase i.e., single, two & multi-phase flow etc., can be clearly visualized when it is mapped in a systematic method. In view of this various researchers developed a stability maps and revealed the inherent stability behaviour of natural circulation loops.

Jiang et al. (2001), used one-dimensional two-phase flow drift model to analyze both static and dynamic behaviour of natural circulation loop by varying the loop pressure, inlet sub-cooling and heat flux parameters. The results show that sub-cooled boiling in the source and void flashing in the adiabatic riser section have significant influence on the distribution of the void fraction, mass flow rate and flow instability of the loop, particularly at low pressure. Based on the results, stability map of the system is developed and distinctly marked the various regions in it. One-dimensional linear stability analysis was performed by Mousavian et al. (2004) for the single-phase natural circulation loop and developed the stability map.

Rao et al. (2005) studied the one-dimensional transient stability behavior of NCL with end heat exchangers using the finite element program by imposing finite perturbation to the loop circulation rate and constructed the stability envelope based on variation of two non-dimensional parameters. Sharma et al. (2010) developed computer codes to analyze the linear and nonlinear stability behaviour of supercritical water in the natural circulation loop and developed the stability maps. Seyyedi et al. (2019) numerically studied a simple rectangular single-phase NCL with an asymmetric heater and developed a stability map which is valid for all the three regions of flow i.e., laminar, transition, and turbulent. Manthey et al. (2020) experimentally studied the influence of the flow resistance on the two-phase flow stability and their oscillatory behavior in an open natural circulation system, and summarized its variation in stability maps.

2.6 Mitigation of instability in NCLs

Over time, numerous researchers have developed plenty of solutions techniques to tackle or at least to mitigate the instability issue in the NCLs; however, this enigma is yet to be resolved completely. The following section is attributed to the consummate contribution of such researchers to the NCL turf.

Chen (1985) presented analytical and numerical solutions to investigate the stability of natural convection flows in single-phase rectangular shaped thermosyphons. The study results conducted at different aspect ratios and radii are expressed in terms of dimensionless parameter. When this parameter value less than certain critical value the flow is found to be in stable state, however above this value the flow will be oscillatory instability. When flow aspect ratio of the loop approaches unity the flow found to be least stable.

Zvirin (1985) analytically investigated the effects of through-flow on the flow rates and temperature distributions in a natural circulation loop at various loop parameters by employing a one-dimensional spatial model and found that the through-flow stabilizes the motion in the loop. Manero et al. (1987) observed that, in the two phase NCLs during bubble boiling, the frequency of oscillations is inversely proportional to the cut-off time of a single vapour bubble formation and breaking. For a small inclinations of the loop, the frequency of oscillation of the temperature and pressure is higher as the time of formation and breaking of a single bubble is smaller, however for larger inclinations the time required for the same is larger and thus the frequency of oscillation of the temperature and pressure is lower.

Cammarata et al. (2004) experimentally examined the effect of change in gravity and thermal boundary conditions on the dynamics of natural circulation loops and validated obtained dynamical behaviour with the mathematical model results, which is previously validated under terrestrial gravity condition. Further, it is concluded that the dynamics of natural circulation loops stabilizes with the reduction of the gravitational field but it enhances the thermal stresses on the system. Cammarata et al. (2003) developed a control strategy by employing mathematical model along with the standard P.I.D. control to counteract instabilities in NCL and verified this strategy both by numerical simulation and experimental tests. The strategy control thus developed found to be suitable for avoiding the flow inversion of the working fluid inside the NCL.

Jiang and Shoji (2003) conducted a three-dimensional nonlinear model study on NCL by incorporating the flow modes and proposed an algorithm to control the flow stability and distribution by varying the thermal boundary condition. Chen et al. (2014) carried out numerical simulations to investigate the influence of heater orientations on the performance of supercritical CO_2 based NCLs. Vertically orientated heater is found to be stable in a wide range of heat flux whereas horizontally oriented heater shown oscillatory behaviour. Further, the heat transfer and stability of loop is significantly affected by the cooler heat transfer behaviour. However, the heat transfer characteristics will not get influenced by location of heat source. Yadav et al. (2016) developed a three-dimensional CFD models for both subcritical and supercritical CO_2 based NCLs to study the effect of loop tilting in different planes at different operating pressures and temperatures and found that changing the orientation of the loop can tackle the flow instability issues elegantly and effectively in the NCLs. A significant effect is also observed on heat transfer and mass flow rate in the loop with the tilt angle of the loop. Bidirectional flow in NCLs is a very common phenomenon, and it adversely affects the heat transfer performance of the loop. To address the flow reversal issues in the NCLs,Wahidi et al. (2020) carried out a two-dimensional CFD simulation by introducing a modified Tesla valve in the riser of a sCO_2 based NCL and achieved unidirectional fluid flow circulation in the loop. Further, with the Tesla valve in NCLs, the velocity and temperature oscillations were also found substantially mitigated without reducing the heat transfer performance. In the process of combating the instability issues in NCLs,Wahidi and Yadav (2021) incorporated tesla valve in both riser and downcomer of loop and found further mitigation of velocity and temperature oscillation but at the cost of 3% reduction in the heat transfer performance of the loop.

2.7 Research gap

The above discussion gives a broad overview of research work carried out so far on natural circulation systems based on CO_2 and water. NCLs can be configured with various heat source and heat sink combinations depending on the application requirement and the available resources to transport heat energy from higher to lower energy levels. Natural circulation loops incorporated with various mechanisms of heat addition and rejection at source and sink, respectively, show different instability nature. Flow direction reversal and oscillatory nature of working fluid in the loop are major disadvantages of natural circulation loop. It is mandatory to comprehend the dynamic behaviour of various combinations of NCL before implementing it in a specific application. Based on intensive literature review carried out, following observations are made:

- Majority of studies have been conducted on forced circulation loops.
- Though in recent times there is a growing interest in CO_2 based secondary loops, it is observed that there are no systematic studies available on these systems.
- Even though some investigations have been carried out on stability analysis of natural circulation loops, those are mostly related to specific to stand-alone NCLs. Comparative analysis of instability behaviour of NCLs with various boundary conditions are relatively scarce.
- Research have been carried out on the stability analysis of different types of

NCLs considering different geometrical designs (toroidal, rectangular loops etc.), different working fluids (water, brine solution, CO_2 etc.), a different state of working fluid (Subcritical and supercritical state) etc., by various researchers.

Comparison of the instability of natural circulation loop based on sCO_2 is a novel idea. 2-D and 3-D numerical comparative study of oscillatory instability of supercritical CO_2 with different geometries and boundary conditions are not found in the literature. This research focused mainly on transient 2-D and 3-D numerical analysis of sCO_2 based NCLs configured with various kinds of heat inputs at the source of the NCL like Heater, a Heat exchanger (HHX) and Isothermal wall (ISO), and cold heat exchanger at the sink (CHX) by changing the intensity of heat input at source and operating pressure of the loop fluid.

2.8 Objective of the present work

The main objectives of the present study are:

1. Two dimensional instability behavior study for sCO_2 based natural circulation loop by imposing different boundary conditions at source.

2. Three dimensional instability behavior study for sCO_2 based natural circulation loop at different boundary conditions at source.

3. To design and fabricate experimental test Loop of the rectangular Natural Circulating system.

4. To conduct experiment to study the behavior of sCO_2 based natural circulations loop at different pressure, temperature and heat input at source.

CHAPTER 3

Comparative Computational Appraisal of Supercritical CO_2 based Natural Circulation Loop: Effect of Heat-Exchanger and Isothermal Wall

Natural circulation loop (NCL) is a geometrically simple heat transfer device in which fluid flow occurs due to density gradient of loop fluid, induced by the temperature difference between the source and the sink. NCL has an inherent problem of instability caused by the combined effect of buoyancy, friction and inertia forces at varying operating conditions, and hence it requires an elegant solution of instability. The primary objective of the present work is to do a comparative study on the dynamic performance between two different configurations of NCL based on supercritical CO_2, i.e.; (i) NCL with isothermal heater and a cold heat-exchanger (ISO-CHX), and (ii) NCL with hot and cold heat-exchangers (HHX-CHX). To explore these NCLs, two-dimensional transient computational fluid dynamics studies have been carried out on the stability of supercritical CO_2-based natural circulation loop. Results are obtained for different operating pressures and temperatures in the form of mass flow rate and velocity variation with respect to time. Results show the higher instabilities in both side heat-exchanger loop than an isothermal heater with heat-exchanger loop. At a lower rate of heat input at source in the HHX-CHX loop, the mass flow is bidirectional, whereas it is unidirectional in the ISO-CHX loop at all level of heat input. It is also observed that as pressure increases, flow instability also increases. Obtained results are validated with the published experimental and numerical data and found in good agreement.

3.1 Physical Model of NCL

A 2-D geometry as shown in Figs. 3.1 have been prepared by using ANSYS Fluent version 19.0.

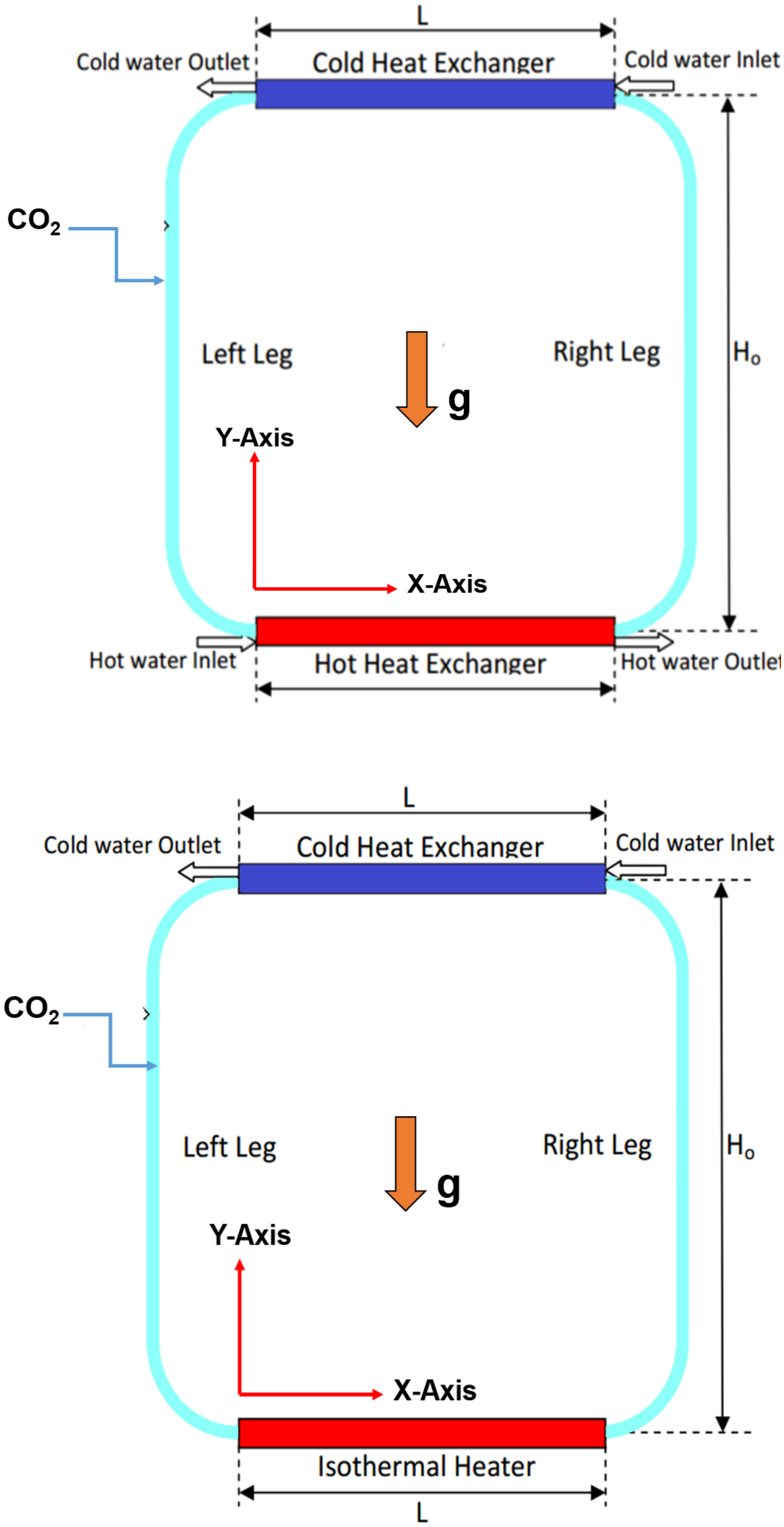

Figure 3.1: Schematic of (a) The Schematic of HHX-CHX NCL design (b) The Schematic of ISO–CHX NCL design.

sCO_2 based NCL with both side heat exchangers, named as HHX-CHX (as shown in Fig.3.1(a)), and isothermal wall (as source) with heat-exchanger (as sink), named as ISO-CHX (as shown in Fig. 3.1(b)) with sCO_2 the computational domain are investigated to comprehend the influence of temperature and loop pressure on the flow. All the geometrical and material specifications for the model is given in Table 3.1.

Table 3.1: Geometrical specification of loop used in present study.

Parameters	**Values**
CHX	
Inner tube diameter	15 mm
outer tube diameter	20 mm
HHX	
Inner tube diameter	15 mm
outer tube diameter	20 mm
Length of heat-exchanger (L)	660 mm
Height of loop (H_0)	1 m mm
Length of Isothermal heater (L)	660 mm
Width of the loop (L_w)	1 m
Diameter of loop (d)	15 mm
Curvature radius of the bend (R)	50 mm
Total length of loop (L_t)	4 m
Material of loop	Stainless steel

3.2 Grid independence study

To achieve the solution's independence from the chosen grid, a sensitivity analysis is carried out for a grid independence study (as shown in Fig.3.2). CHX is kept at 1.15 kg/min and the heater section temperature is maintained at 353 K to get the grid independence. Mass flow rate is recorded at the centre of the pipe for the grid independence test (as shown in Fig.3.2) to ensure the reliability of obtained results.

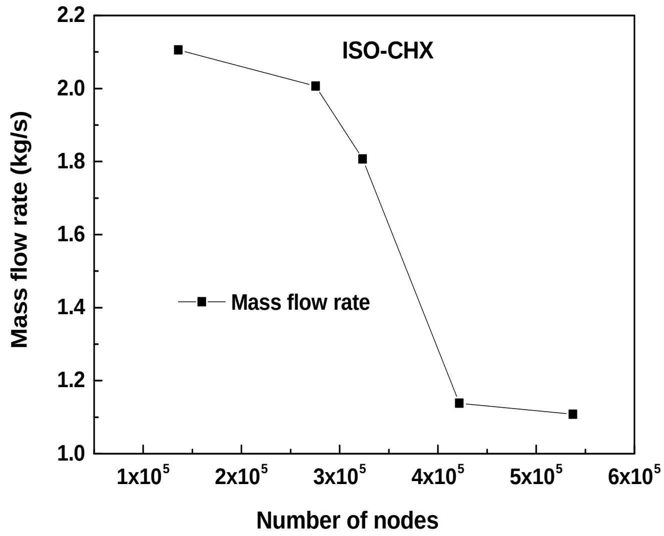

(a) ISO-CHX

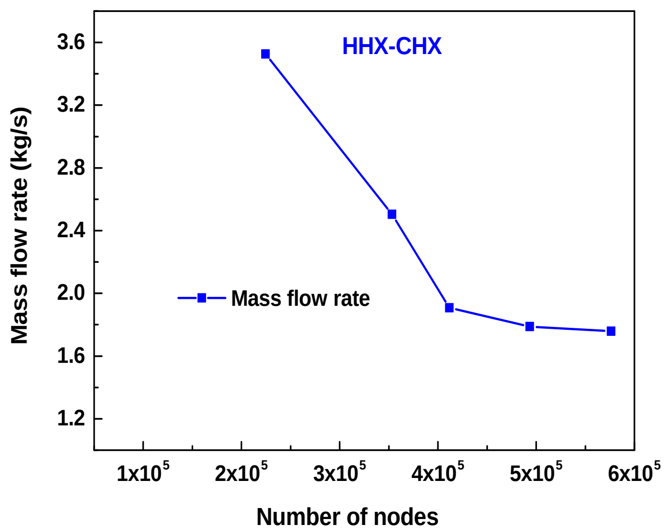

(b) HHX-CHX

Figure 3.2: Grid independence study for supercritical CO_2 based natural circulation loop for (a) ISO-CHX and (b) HHX-CHX.

3.3 Mathematical formulations

The fundamental conservation equations (mass, momentum and energy) solved for the simulation are given below. The commercial software ANSYS (FLUENT) V-19.0 is employed to solve these equations with the associated boundary specifications for two-dimensional geometry. The mass conservation equation can be given as:

$$\frac{\partial}{\partial t}\rho + \frac{\partial}{\partial x}\rho u + \frac{\partial}{\partial y}\rho v = 0 \tag{3.1}$$

Momentum Conservation:

In X-direction

$$\frac{\partial}{\partial t}\rho u + \frac{\partial}{\partial x}\left[\rho u u - \frac{4}{3}(\mu + \mu_T)\frac{\partial u}{\partial x}\right] + \frac{\partial}{\partial y}\left[\rho u v - (\mu + \mu_T)\frac{\partial u}{\partial y}\right] = -\frac{\partial p}{\partial x} - \frac{2}{3}\frac{\partial}{\partial x}\left(\mu\frac{\partial v}{\partial y}\right) + \frac{\partial}{\partial y}\left[(\mu + \mu_T)\frac{\partial v}{\partial x}\right] - \frac{2}{3}\frac{\partial}{\partial x}(\rho\kappa) + \rho g_x \tag{3.2}$$

In Y-direction

$$\frac{\partial}{\partial t}\rho v + \frac{\partial}{\partial x}\left[\rho v u - (\mu + \mu_T)\frac{\partial v}{\partial x}\right] + \frac{\partial}{\partial y}\left[\rho v v - \frac{4}{3}(\mu + \mu_T)\frac{\partial v}{\partial y}\right] = -\frac{\partial p}{\partial y} - \frac{2}{3}\frac{\partial}{\partial y}\left(\mu\frac{\partial u}{\partial x}\right) + \frac{\partial}{\partial x}\left[(\mu + \mu_T)\frac{\partial u}{\partial y}\right] - \frac{2}{3}\frac{\partial}{\partial y}(\rho\kappa) + \rho g_y \tag{3.3}$$

Energy equation is given as

$$\frac{\partial}{\partial t}\rho h + \frac{\partial}{\partial x}\left[\rho h u - \frac{\mu_T}{\mathrm{Pr}_T}\frac{\partial h}{\partial x}\right] + \frac{\partial}{\partial y}\left[\rho h v - \frac{\mu_T}{\mathrm{Pr}_T}\frac{\partial h}{\partial y}\right] = \frac{\partial p}{\partial t} + u\frac{\partial p}{\partial x} + v\frac{\partial p}{\partial y} + \frac{\partial}{\partial x}\left(\lambda\frac{\partial T}{\partial x}\right) + \frac{\partial}{\partial y}\left(\lambda\frac{\partial T}{\partial y}\right) \tag{3.4}$$

Turbulence Model

As found in previous studies for sCO_2 (Chen et al. (2010); Yadav et al. (2012a); Chen et al. (2014)), the flow Reynolds number can be as high as 10^4 for even a smaller temperature difference (8 K) between source and sink. However, turbulence models for supercritical fluids are less developed and still under intense study (Chen et al. (2014)). Therefore, in the present simulation, a general Renormalization group (*RNG*) k-ε model is selected as the first step to introduce the turbulent effect. The RNG k-ε turbulent model is used together with standard wall function and no-slip condition near the wall. In previous studies, Chen et al. (2010); Yadav et al. (2012a); Chen et al. (2014) have used the Renormalization group (*RNG*) k-ε for sCO_2-NCL and achieved accurate results.

The variation in thermo-physical properties of supercritical CO_2 near the critical point is substantial, so it is vital to capture the property variation owing to changes in temperature adequately. Hence, the properties of CO_2 at any point in the loop are calculated at the fixed operating pressure and local temperature. The required properties of CO_2, including density, specific heat, thermal conductivity and viscosity, are obtained from the NIST Standard Reference Database (REFPROP) Version V9.1.

To capture the turbulence quantum, a series of simulations have been done before finalizing the finalizing type of turbulence. In simulations, Turbulence model is selected in such as a way that it should capture the area of fully developed turbulent flow away from the wall and near the walls too. To deal with the near-wall region, wall functions are used. Wall functions are equations empirically derived and used to satisfy the physics in the near-wall region. The first cell center needs to be placed in the log-law region to ensure the accuracy of the results. Wall functions are used to bridge the inner region between the wall and the turbulence fully developed region. When using the wall functions approach, there is no need to resolve the boundary layer causing a significant reduction of the mesh size and the computational domain. First grid cell needs to be 30 < y+ < 300 (If this is too low, the model is invalid, if this is too high, the wall is not properly resolved). However, 38.39 is the minimum y+ value mentioned in the manuscript.

Governing equations for the RNG k-ε model include two equations.

Turbulent kinetic energy equation

$$\frac{\partial\left(\rho\kappa\right)}{\partial t}+\frac{\partial\left(\rho u_i\kappa\right)}{\partial x_i}=\frac{\partial}{\partial x_j}\left[\left(\mu+\sigma\kappa\mu_t\right)\frac{\partial\kappa}{\partial x_j}\right]-\rho\varepsilon+\beta^* P_\kappa\frac{\partial U_i}{\partial x_i} \tag{3.5}$$

where

$$G = \mu_T \left(2 \left[\left(\frac{\partial u}{\partial x} \right)^2 + \left(\frac{\partial v}{\partial y} \right)^2 \right] + \left(\frac{\partial u}{\partial y} + \frac{\partial v}{\partial x} \right)^2 \right) \tag{3.6}$$

Turbulent kinetic energy dissipation equation

$$\frac{\partial}{\partial t}\rho\varepsilon + \frac{\partial}{\partial x}\left(\rho u\varepsilon - \frac{\mu_T}{\sigma_\varepsilon}\frac{\partial}{\partial x}\varepsilon\right) + \frac{\partial}{\partial y}\left(\rho v\varepsilon - \frac{\mu_T}{\sigma_\varepsilon}\frac{\partial}{\partial y}\varepsilon\right) = c_1\frac{\varepsilon}{\kappa}G - c_1\rho\frac{\varepsilon^2}{\kappa} - R \tag{3.7}$$

where

$$R = \frac{c_\mu \eta^3 \rho \left(1 - \frac{\eta}{\eta_0}\right) \varepsilon^2}{\kappa \left(1 + \beta\eta^3\right)} \tag{3.8}$$

$$\eta = \frac{S\kappa}{\varepsilon} \tag{3.9}$$

$$S = \frac{1}{\sqrt{2}}\left(\frac{\partial u}{\partial x} + \frac{\partial v}{\partial x}\right) \tag{3.10}$$

where the values of constants are as follows :

$$\eta_0 = 4.8, \beta = 0.012, c_\mu = 0.0845, \sigma_\varepsilon = \sigma_\kappa = 0.7178, c_1 = 1.42, c_2 = 1.68 \tag{3.11}$$

Turbulent viscosity (μ_T) is a concept used in turbulence modeling to represent the effect of turbulent fluctuations on the momentum transfer in a fluid. In turbulent flows, the motion of the fluid is characterized by chaotic and irregular fluctuations in velocity. The Reynolds-averaged Navier-Stokes (RANS) equations, which are commonly used for simulating turbulent flows, include an additional term to account for the turbulent viscosity. The term $\mu_T$is introduced to model the additional viscous-like effects arising from the turbulence.

The following terms are defined to describe the fluid flow and heat transfer phenomena. Mass flow rate at any cross section is defined as,

$$m = \int_0^A \rho V dA \tag{3.12}$$

Local velocity can be given as,

$$u_x = \frac{\int_0^A u_r \left|\rho_r \bar{V}.dA\right|}{\int_0^A u_r \left|\rho_r \bar{V}.dA\right|} \tag{3.13}$$

Steady-state modified Grashof number [49]are defined as

$$Gr_m = \frac{g\beta d^3 \rho^2 Q H_0}{A\mu^3 C_p} \tag{3.14}$$

All the properties are calculated at the bulk mean temperature (Tm) of loop fluid, defined as:

$$T_m = \frac{\sum_{i=1}^{n} T_i}{n} \tag{3.15}$$

Where, n is the number of cross-sections considered in the loop.

The average temperature of the loop is defined as,

$$T_{avg} = \frac{T_C + T_H}{2} \tag{3.16}$$

Where T_C and T_H are the temperatures at the heat sink and heat source respectively. For heat exchangers, it is considered.

3.4 Simulation detail

In this research, a supercritical CO_2-based NCLs with different heating boundary conditions, as shown in Fig. 3.1 are investigated. External walls are considered adiabatic. The wall thickness is kept zero for simulation. To resolve the coupling between velocity and pressure, the pressure- implicit with the splitting of operators (*PISO*) algorithm is used (Yadav et al. (2012a)). The momentum and energy parameters in the governing equations are iterated with a second-order upwind scheme. Turbulence parameters (k,ε etc.) are iterated with an upwind scheme of second-order.To discretize the pressure term, PRESTO (Pressure staggering option) (Chen et al. (2010)) is used. For pipe walls, the no-slip boundary condition isused.

A general Renormalization Group (*RNG*), the k-, ε model, is selected to account for turbulence. The axial conductivity and viscous dissipation in the fluid are taken into account, and convergence is obtained when residuals of the continuity and momentum equations are less than 10^{-3}, and for energy, k and ε are less than 10^{-6}. Loop fluid, i.e., CO_2 is kept in the supercritical region having operating pressure 80, 90 and 100 bar. All the standard properties of CO_2 were obtained from the NIST REFPROP property tables (NIST (2018)). The loop fluid is heated from bottom at heater with constant heat input, and is cooled sensibly at top by rejecting heat to the external fluid (water) in the cold heat-exchanger (CHX). Circulation of the loop fluid is maintained due to the buoyancy effect caused by heating at the bottom and cooling at the top. At the heat-exchanger, water is used as a coolant at a fixed rate of 1.15 kg/min to ensure the turbulent flow. Data were updated for every interval of 2 K temperature, and piecewise-linear interpolation was used to obtain property between two data points.

3.5 Validation

The validation of obtained CFD results as shown in Fig. 3.3 for 90 bar is carried out using two correlations based on an experimental study by Vijayan (2002) and numerical study by Yadav et al. (2012b). The correlations involve non-dimensional parameters like $Re - Gr_{\mathrm{m}}$ calculated at heater section. Good agreement was found between the generated results and existing correlations, as shown in Fig. 3.2. Obtained results are closer to Yadav et al. (2012b) as they used the same working fluid i.e., CO_2. The differences in the results could be due to the use of different types of heat sources; Yadav et al. (2012b) used isothermal heat source and sink, whereas in present study heat exchanger is used as sink. The maximum discrepancies are found to be less than 7% with the correlation.

Correlation suggested by Vijayan (2002)

$$Re = 1.96(Gr_m d/L_t)^{1/2.75} \tag{3.17}$$

Correlation suggested by Yadav et al. (2012b)

$$Re = 2.066(Gr_m d/L_t)^{1/2.77} \tag{3.18}$$

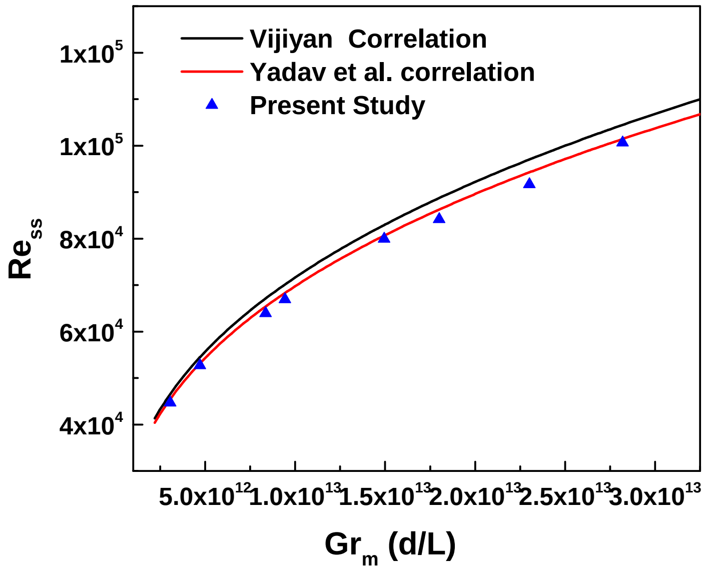

Figure 3.3: Validation of the obtained result with correlations Re and $(Gr_m d/L_t)$.

3.6 Results and discussion

Two dimensional CFD study is carried out to obtain the transient behaviour of supercritical CO_2 at various loop pressure and source temperature. The loop pressure was kept at 80, 90, 100 bar and the source temperature at Hot heat exchanger and isothermal heater wall is varied, for each pressure level, from 323 K to 353 K in a pace of 10 K difference. During the study, mass flow rate of water in CHX is kept constant at 1.15 kg/min and the CHX inlet temperature is maintained at 305 K for all the cases. Initial temperature of the loop is kept at 305 K throughout the loop in all the cases. The results thus obtained are discussed in the following sections.

3.6.1 Transient variation of mass flow rate

Figure 3.4(a-b) show the transient variation of the mass flow rate of supercritical CO_2 at various inlet temperatures of the heat source at a loop pressure of 90 bar. Results are obtained at the center of right leg by considering the area-weighted average across the cross-section.

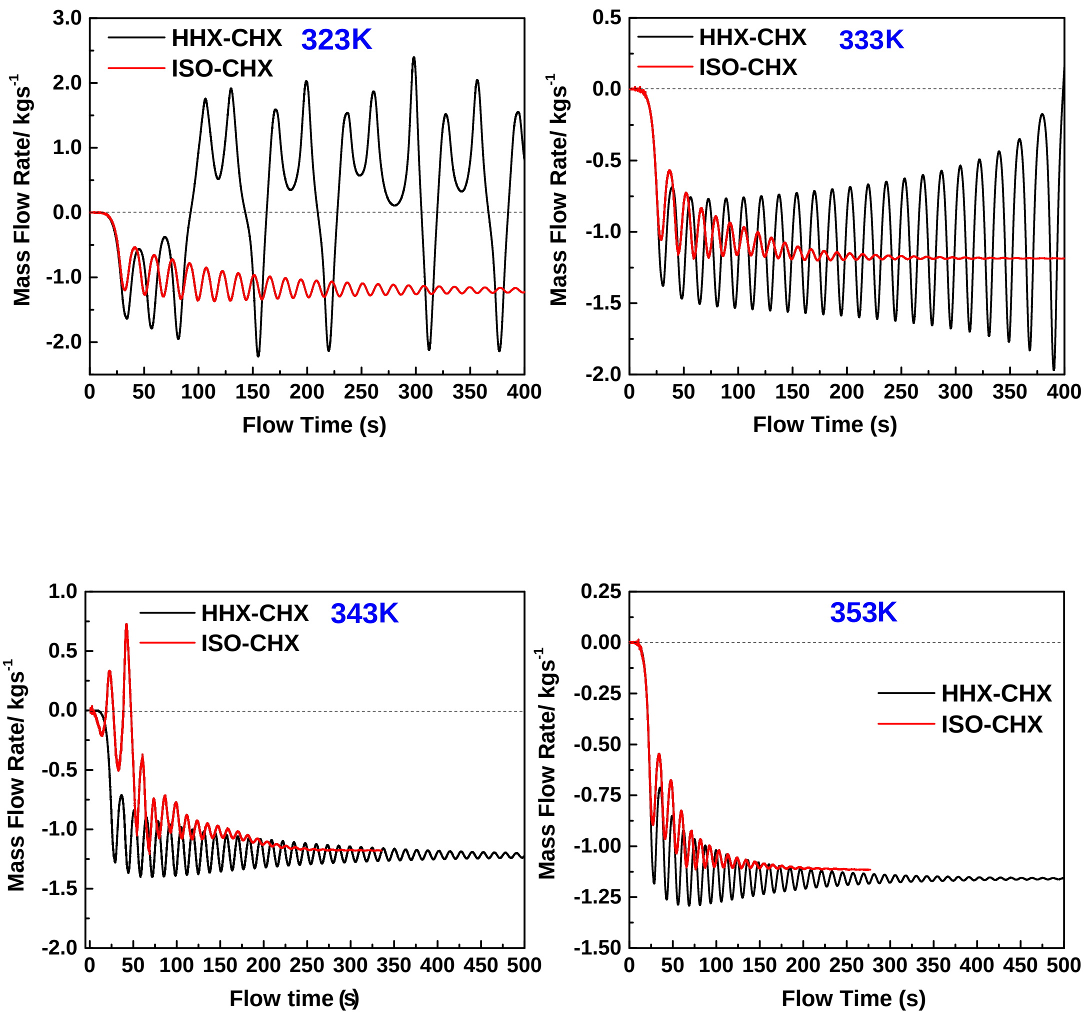

Figure 3.4: Mass flow rate variation of supercritical CO_2 at 90 bar for different heat source temperatures (a) 323 K (b) 333 K (c) 343 K and (d) 353 K

For lower heat input in HHX-CHX loop i.e. at temperatures 323 K, fluid flow is bidirectional and the amplitude of oscillations keep on increasing with time. It indicates that the flow is very unstable at lower heat input. The average loop fluid temperature for these lower heat input cases is close to the pseudo-critical temperature, which may be the probable reason for instability in the form of mass flow oscillations and chaotic nonlinear dynamic behaviours for these cases, whereas for higher heat input, i.e. at temperatures 343 K and 353 K, the mass flow oscillation of loop fluid dampens gradually and converges to a stable and steady state in due course. At all level of heat input in ISO-CHX loop, the flow is unidirectional and the amplitude of oscillations keep on converging with time. It indicates that the mass flow rate is very stable at all level of heat input. Further, the amplitude of mass flow rate oscillation is very subdued in case of ISO-CHX loop compared to HHX-CHX loop.

For a given operating pressure, the instability decreases with increasing heat input. It is interesting to note that, the instability convergence is gradual for a heat input at a temperature of 343 K in comparison with heat input at a temperature of 353 K, wherein the instability converges drastically. This may be occurring due to decrease in differential density of the loop fluid across the heat source (i.e. at the bottom of the right and left leg) with an increase in heat input at source, which in turn elevates the fluid loop temperature as water mass flow rate and temperature at CHX are kept constant. Further, the decrease in buoyancy force is highly significant towards a higher range of heat input thus leading to a substantial reduction in flow oscillations. It is evident from the graph that instability dampens much faster in case of ISO-CHX loop compared to HHX-CHX loop, this phenomenon could be because of the very fast response of isothermal heater for the sudden change in heat input at source, which in turn decreases the gradient of buoyancy as inferred above. It can also be observed that HHX-CHX loop has the highest flow rate compared to ISO-CHX loop in all level of heat inputs, because of its higher instability feature.

3.6.2 Velocity variation

Figure 3.5 shows the transient variation of velocity (m/s) for both HHX-CHX and ISO-CHX loops. Significant variation in density induced buoyancy with temperature causes changes in the magnitude of velocity. The viscosity of supercritical fluid will be extremely low compared to subcritical CO_2 fluid, and a slight variation in the temperature of the supercritical loop fluid will have a drastic influence on the mass flow rate. As the temperature of the heat source increases, the loop fluid temperature also increases, which gives rise to an increase in flow velocity, which is very evident from the graphs.

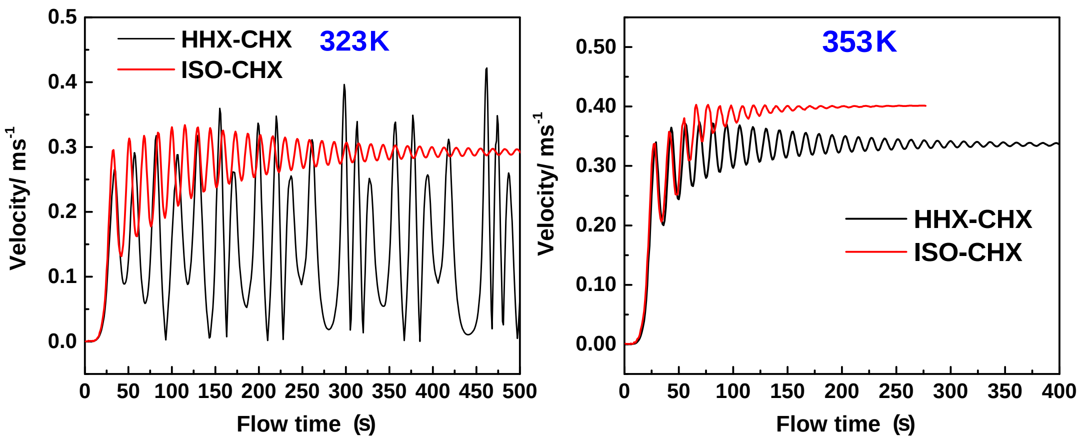

Figure 3.5: Velocity variation of supercritical CO_2 at 90 bar for different heat source temperatures (a) 323 K and (b) 353 K.

In case of HHX-CHX loop, at lower heat input rate, the velocity fluctuation is very high, and the system never reaches to the stable state, whereas in case of ISO-CHX loop, velocity fluctuation in the initial stage will be high but reaches to stable stage in due course. At a higher rate of heat input, in both the cases, velocity oscillates in the initial stage but reaches to stable stage eventually. However, ISO-CHX loop reaches to stable state at a faster rate mainly due to higher veloc- ity of loop fluid compared to HHX-CHX loop. At a high velocity of the fluid, induced by high temperature, flow momentum will be more and hence it makes flow reversal difficult, and the system gets stabilizes at a faster rate. This phenomenon can be observed in both HHX-CHX loop as well as in ISO-CHX loop but at a different interval of time. Further, due to sudden change in density and viscosity of supercritical CO_2 in ISO-CHX loop, strong local buoyancy effect can be observed that causes higher radial/azimuthal velocity than HHX-CHX loop.

3.6.3 Effect of operating pressure on flow instability

Figure 3.6 shows transient behaviour of mass flow rate with different operating pressures for both HHX-CHX and ISO- CHX loops. The mass flow rate in both the loops increases with increase in operating pressure of the loop. In case of HHX-CHX loop at higher pressure, the mass flow shows a directional instability i.e. the flow direction changes frequently from clockwise direction to counter clockwise direction in the loop. In case of ISO-CHX loop, the flow direction is stable at all levels of operating pressure i.e. the flow follows a definite direction in the loop.

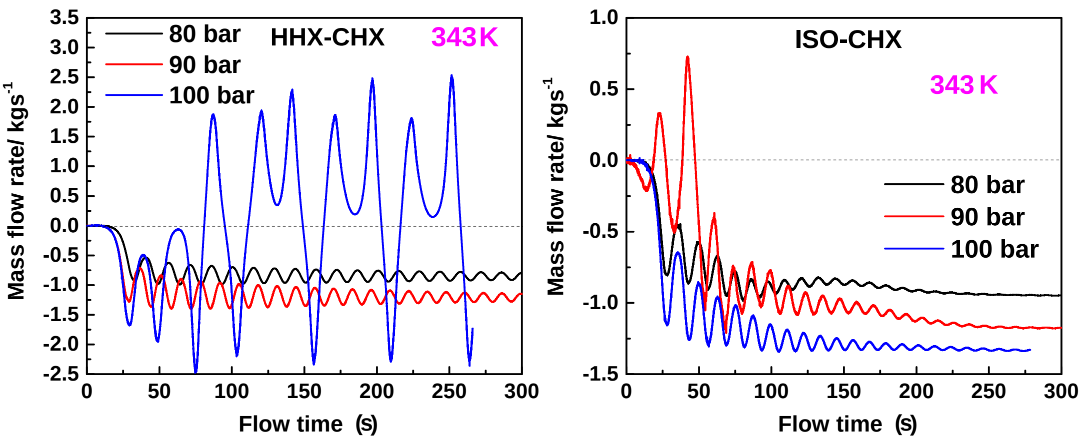

Figure 3.6: A variation on mass flow rate with different operating pressures for (a) HHX–CHX Case and (b) ISO–CHX Case.

Transient analysis of mass flow rate as shown in Fig. 3.6 implies that with an increase in pressure, the magnitude of oscillation of mass flow rate or the degree of instability is more. To explain this, the transient variation of the driving force and resistive force in the loop is to be thoroughly analysed. For a loop to operate in a stable condition, good agreement between the two forces has to be found. The resistive force in the loop is a function of friction factor, mass flow rate and average density along the loop. Yadav et al. (2012b) developed a correlation for friction factor given as:

$$f = (0.7907 lnRe - 1.868)^{-2} \qquad (27000 \leq Re \leq 180000) \qquad (3.19)$$

Average Reynolds number obtained from the simulation is between 40,000 and 90,000, thus leading to a very small friction factor. This very low friction factor undermines the effect of change in mass flow rate and average density with operating pressure and hence, changes in resistive forces with loop operating pressure are insignificant. However, there are significant changes in the driving forces with pressure, due to an increase in density with increase in pressure. This shows that for higher operating pressures, the driving force is high, and hence the difference between driving and resistive forces is significant. This is the reason for increased instability in loops operating at higher pressure.

The magnitude of fluctuations for HHX-CHX loop is more due to exponential increase or decrease in the temperature in heat-exchangers, which increases the response time for the loop fluid to decrease the gradient of buoyancy, whereas for ISO-CHX loop, the sudden change in temperature dampens the flow fluctuations, which stabilizes the flow at the earliest.

3.6.4 Variation of turbulence kinetic energy

Figure 3.7 shows the variation in turbulence kinetic energy for 90 bar at 343 K temperature for both the configurations. Turbulence kinetic energy for fluid dynamics is the average kinetic energy per unit mass associated with chaotic oscillations of fluid. Higher magnitude of turbulence indicates the high amount of heat transfer rate. Due to more temperature gradient in ISO-CHX loop than the HHX-CHX loop, the turbulence energy is found more in ISO-CHX loop which imparts the higher Nusselt number for the loop.

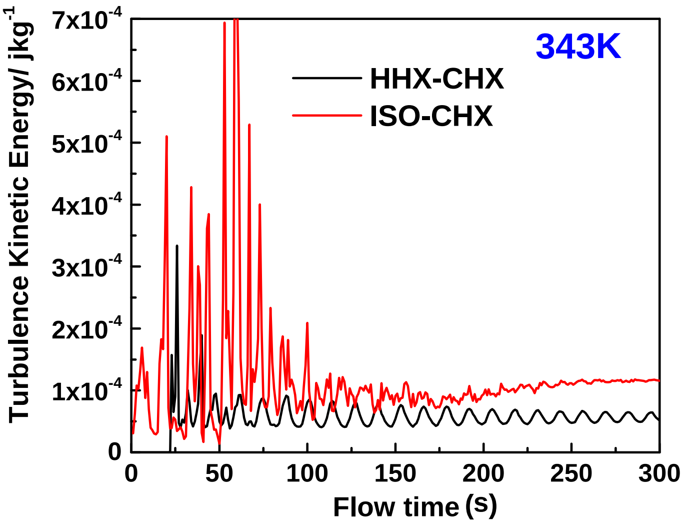

Figure 3.7: Turbulence Kinetic Energy for Supercritical CO_2 based Heater-CHX and ISO-CHX natural circulation loop.

3.6.5 Nusselt number

Figure 3.8 shows the variation of Nusselt number with increase in the heat input at source for both HHX-CHX loop and ISO-CHX loop.

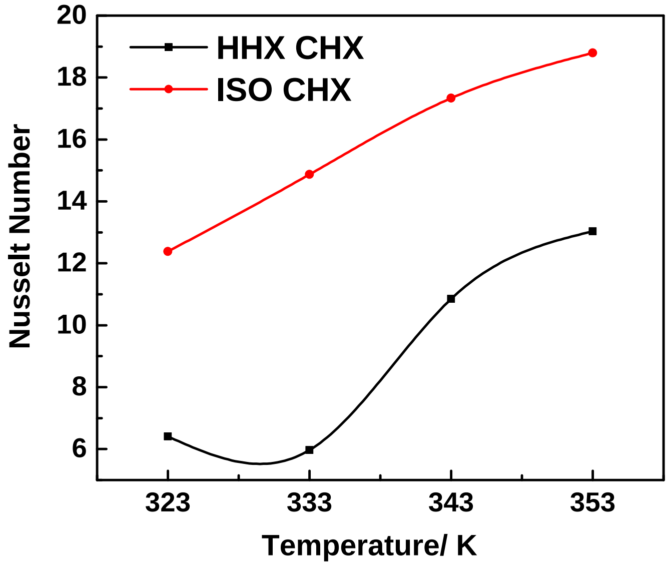

Figure 3.8: Variation of Nusselt number at different heat inputs and operating pressures.

Nusselt number is a function of Reynolds number and Prandtl number (Pr), and it is revealed that the magnitude of Reynolds number increases with increasing temperature for both the cases. Higher Nusselt number indicates a higher heat transfer coefficient and hence more effective natural convection phenomenon. The Nusselt number in case of ISO-CHX loop is very high compared to HHX-CHX loop; it may be due to higher turbulence kinetic energy and uniform heat input throughout the source of ISO-CHX loop. In ISO-CHX loop, for all the heat source temperature conditions, stable flow inside the loop is achieved.

3.7 Summary

The following conclusions are drawn from the present work:

- At a lower rate of heat input, the instability in mass flow rate and velocity grows abruptly in the *HHX-CHX* loop, whereas in the *ISO-CHX* loop, the instability dampens comparatively at a faster rate.
- At a lower rate of heat input in the *HHX-CHX* loop, i.e., at temperatures 323 K, fluid flow is bidirectional and the amplitude of mass flow rate oscillations keep on diverging with time. Whereas, at all level of heat input at source in the *ISO-CHX* loop, the mass flow is unidirectional and the amplitude of mass flow rate oscillations keep on converging with time.
- At higher operating pressure, in case of *HHX-CHX* loop, the mass flow shows a directional instability. Whereas, in case of *ISO-CHX* loop, the mass flow direction is stable at all levels of operating pressure i.e., the flow follows a definite direction in the loop. Further, the mass flow rate in both the loops increases with increase in operating pressure of the loop.
- As the heat input at source increases beyond a certain threshold, the instability of mass flow and velocity in the *HHX-CHX* loop keeps dampening at a definite rate and in due course it gets stabilized to a steady state flow in the loop. However, *HHX-CHX* loop stabilizes at a slower pace when comparing the same scenario

with the *ISO-CHX* loop. It is very interesting to note that the mass flow rate is almost same in both the cases for a given pressure but the magnitude of velocity in *ISO-CHX* loop prevails over HHX-CHX loop.

- At all level of heat input, the Nusselt number is on a higher side for *ISO-CHX* loop than *HHX-CHX* loop, which is mainly due to higher turbulence and comparatively stable flow.

- In the supercritical CO_2 based NCL, the energy transport from source to sink is more stable in *ISO-CHX* loop compared to *HHX-CHX* loop.

CHAPTER 4

Numerical Assessment of Stability Behaviour in Supercritical CO_2 based NCLs Configured with Heater, Heat exchanger and Isothermal wall as Heat Sources

In this chapter, a three-dimensional numerical analysis is presented to assess the transient and stability behavior of supercritical CO_2 (sCO_2) based NCLs configured with three different types of heat sources i.e., heater, hot heat exchanger (HHX) and isothermal wall (ISO) at the source, and a cold heat exchanger (CHX) at sink in all three NCLs. Unsteady three-dimensional conservation equations (mass, momentum and energy equations) are solved to assess the transient and stability behavior of sCO_2 mass flow rate, temperature and velocity as a function of time. Further, the effect of pressure on sCO_2 mass flow rate is also assessed to compare the loops performance. Performance of the loop has been studied for various heat inputs at source by keeping constant mass flow rate and temperature at sink. It is observed that for any nature of boundary condition at source, the loop experiences some initial disturbances or instabilities before reaching to the steady state. However, time needed for the attainment of steady state varies with the nature of heat input employed at source. Results show a higher magnitude of instabilities in Heater-CHX loop than HHX-CHX and ISO-CHX loops, and these instabilities mitigate at a faster rate in the ISO-CHX loop at all levels of heat input and operating pressure of the loop. It is also observed that as loop fluid operating pressure increases, the instability of the system decreases and the loop fluid mass flow rate increases. Further, the Nusselt number in case of Heater-CHX loop is more compared to other loops because of its high turbulent kinetic energy.

4.1 Physical model of NCL

Comparative analysis has been conducted between three different sCO_2 based NCLs, i.e., one configured with Heater-CHX loop (Fig. 4.1a), the second one configured with HHX-CHX loop (Fig. 4.1b) and the third one with ISO-CHX loop (Fig.4.1c).

In these loops the effect of heat input on the mass flow rate, temperature and velocity of the loop fluid (sCO_2) have been studied along with the effect of pressure on the mass flow rate. For all the NCLs the magnitude of heat input at source varied for all the operating pressure of the loop fluid, which is varied from 80 to 100 bar in a step of 10bar. For all the cases of operating pressure and heat input, the loop sink temperature i.e., CHX inlet temperature has been kept constant at 305 K. Both the right and left legs are assumed to be adiabatic. The Loops are kept in a vertical plane to ensure maximum mass flow rate of loop fluid Vijayan et al. (2007). All the geometrical and material specifications of the model are given in Table 4.1.

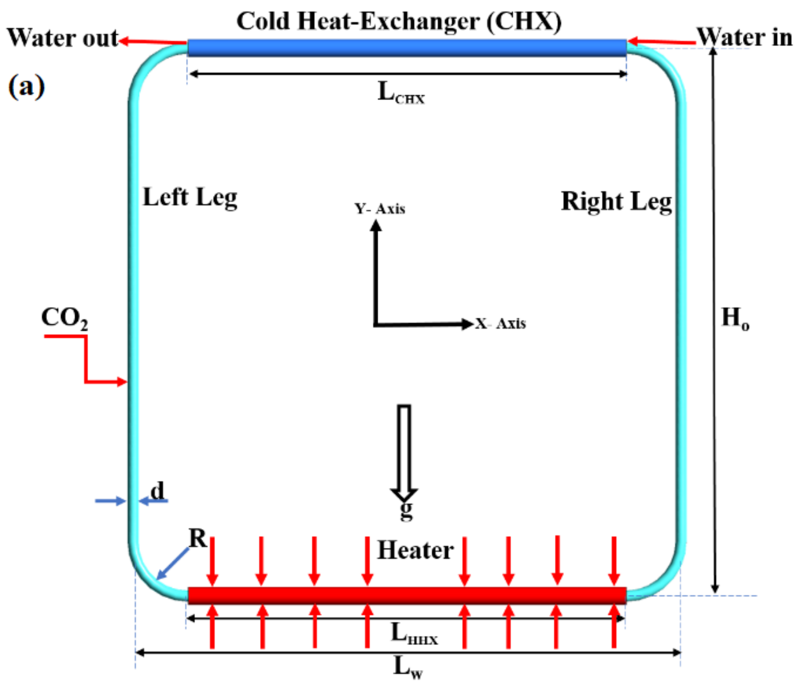

Figure 4.1 shown is a rectangular NCL schematic consisting of a heating source, a left leg, a cold heat exchanger (CHX), and a right leg.

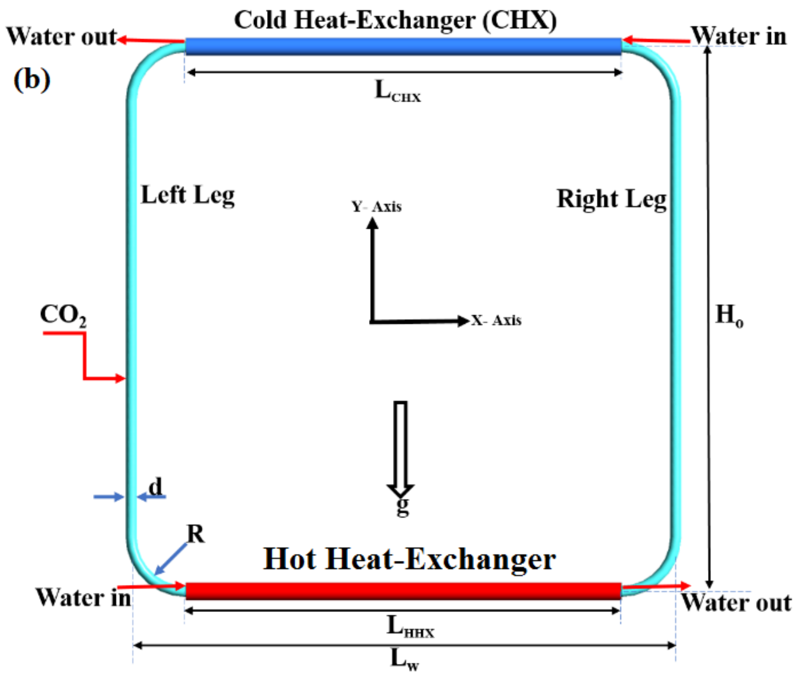

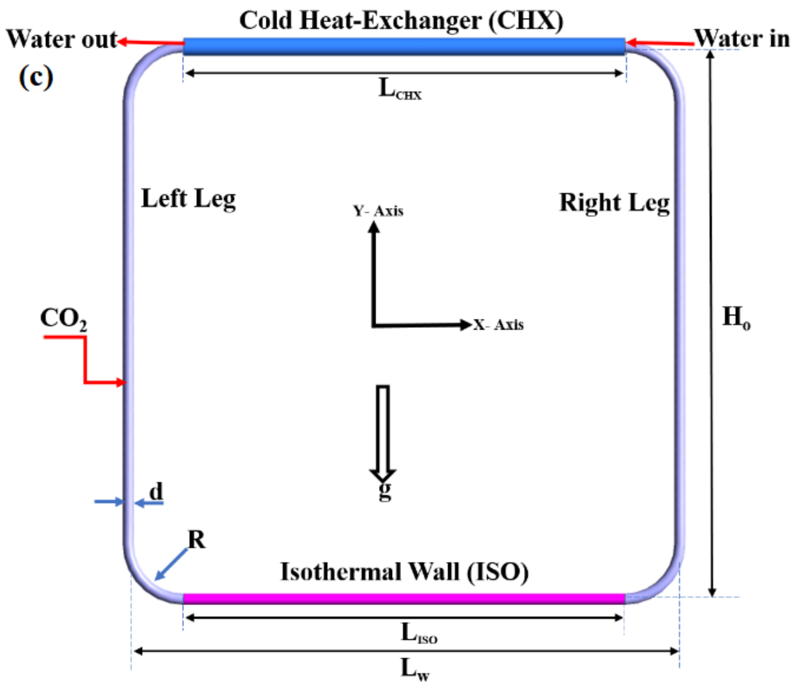

Figure 4.1: Schematic of (a) Heater-CHX (b) HHX-CHX and (c) ISO-CHX natural circulation loops

The loop fluid is heated from below at heater with constant heat inputs and is cooled sensibly by rejecting heat to the external fluid (water) in the CHX.

Table 4.1: Geometrical specification of loop used in present study.

Parameters	Values (mm)
CHX	
Inner tube diameter	10 mm
outer tube diameter	16 mm
HHX	
Inner tube diameter	10 mm
outer tube diameter	16 mm
Length of heat-source ($L_{HHX/ISO}$)	400 mm
Height of loop (H_0)	500 mm
Width of the loop (L_w)	500 mm
Diameter of loop (d)	10 mm
Curvature radius of the bend (R)	50 mm
Total length of loop	1914 mm
Material of loop	Stainless steel

4.1.1 Grid independence study

Grid independence study conducted at 1500 W of heat input at source for Heater-CHX loop and for the same quantum of heat input, the evaluated corresponding temperature at inlet of HHX-CHX loop is 317.5 K and similarly at Isothermal wall of ISO-CHX loop is 311.5 K. The loop fluid operating pressure is kept at 90 bar and constant temperature of 305 K is maintained at inlet of CHX of all the loops. The geometrical model considered for 3-dimentional CFD simulation of NCLs comprises of loop fluid (sCO_2) in the loop primary side of fluid region, wall thickness of pipe and cooling fluid (water) in the secondary side of fluid region i.e., in the cold heat exchanger.

A sensitivity analysis has been carried out in the modelled grid to study the grid independence, in order to obtain the solution which is independent from the adopted grid and time. Initially coarse meshing is framed and then it is progressively refined until an independent mesh result was obtained. For meshing the three-dimensional loop geometry, design modeler of the ANSYS 19.0 software is employed.

Figure 4.2 shows the cross-sectional view of the CHX, wherein meshing is carried out for sCO_2 region, cooling water region and in the piping.

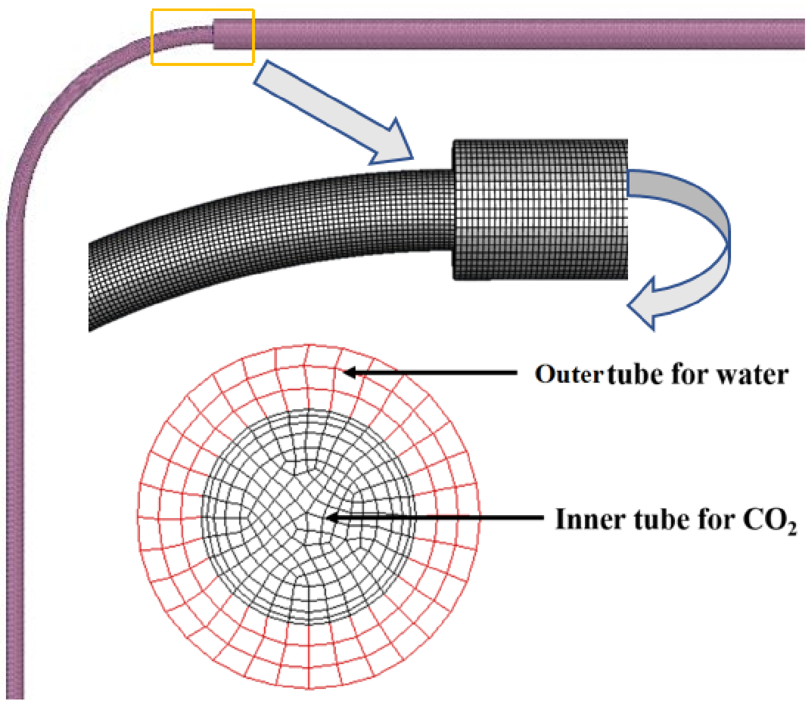

Figure 4.2: Mesh generated for the computational domain.

For the CO_2 region, in a radial direction close to the wall, grid sizing is kept as minimum as of 0.25 mm and moving farther from the wall, it is increased to maximum size of 1mm. Since the property variation is very minimal for water, a uniform grid sizing of 1 mm is envisaged in this region. In the axial direction i.e., in horizontal pipes including bends, coarse meshing of grid size 1.0 mm is adopted and in vertical pipes 2.0 mm grid size is considered. With this mesh generation, a yield of total 400,704 nodes are obtained. To deal with the turbulence models near-wall region is to use the wall functions. Wall functions are equations empirically derived and used to satisfy the physics in the near-wall region. The first cell center needs to be placed in the log-law region to ensure the accuracy of the results. Wall functions are used to bridge the inner region between the wall and the turbulence fully developed region. When using the wall functions approach, there is no need to resolve the boundary layer causing a significant reduction of the mesh size and the computational domain. First grid cell needs to be $30 < y^+ < 300$ (if this is too low, the model is invalid, if this is too high, the wall is not properly resolved). To ensure the optimal choice of fineness of the grid, a minimum value of 38.39 for Y^+ value has been used with standard wall function near the wall.

To check the reliability of obtained results, grid-independence test (as shown in Fig. 4.3a for Heater-CHX & ISO-CHX loops and Fig. 4.3b for HHX-CHX loop) is carried out. The grid convergence index (GCI) method proposed by Roache (1994) is utilised for performing the grid-independent study. GCI method is based on the application of Richardson's extrapolation, in which the spatial and temporal (in unsteady numerical simulations) discretisation errors approach to zero asymptotically as the grid is refined i.e., grid cells become smaller and the number of cells in the flow domain increase. With the GCI method of Roache (1994) the estimated error is 1.6 % for the mesh generated using 400,704 nodes in the NCLs.

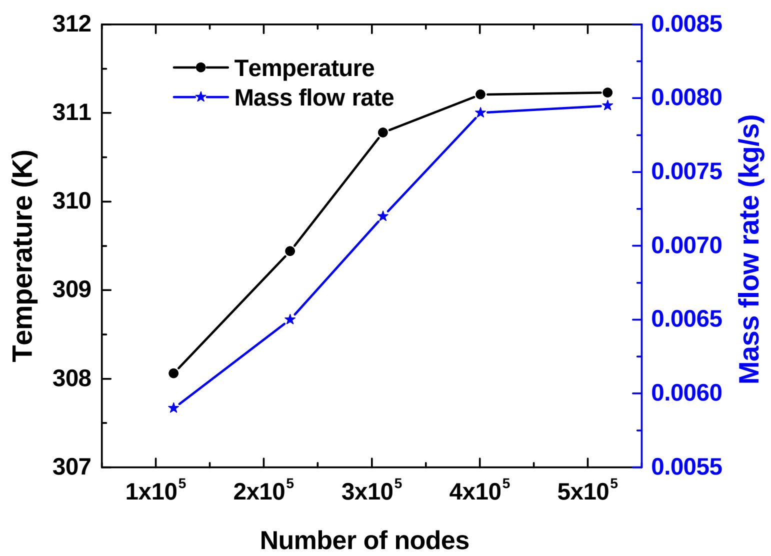

(a) Heater-CHX

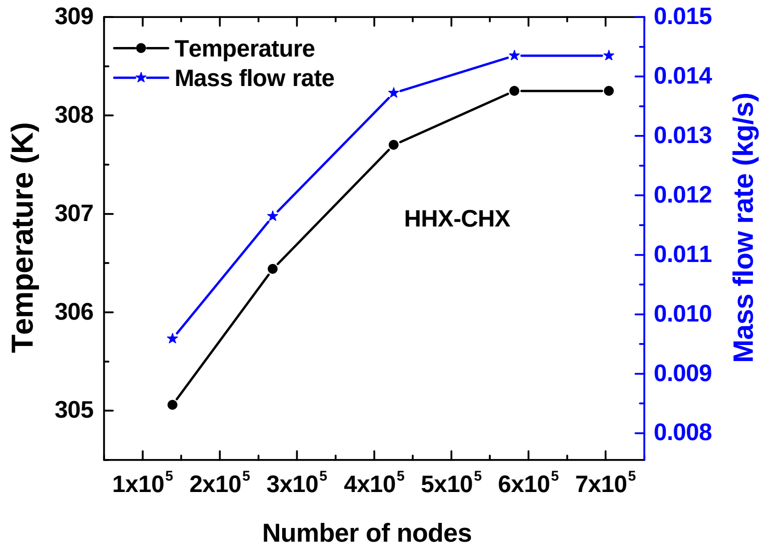

(b) HHX-CHX

Figure 4.3: Grid independence study for supercritical CO_2 based natural circulation loop for (a) Heater-CHX and (b) HHX-CHX.

The time step independence study is also performed on Heater-CHX loop for the mesh as generated above i.e., for the 400,704 nodes.

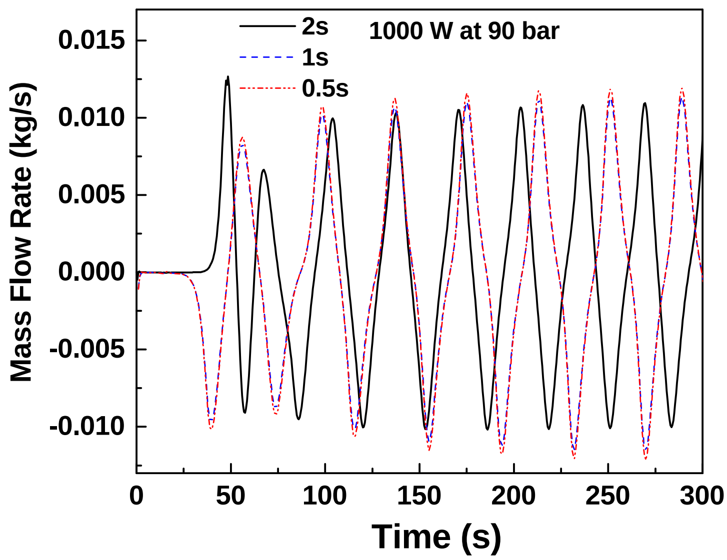

Figure 4.4: Time independent study for supercritical CO_2 based natural circulation loop at operating pressure of 100 bar for a heat input of 1000 W.

For the heat input of 1000 W at source and loop fluid operating pressure of 90 bar, the flow initiation transient in the model configuration was computed with time steps of 0.5 s, 1 s and 2 s and the result thus obtained is depicted in Fig. 4.4. It is evident from the graph that there is hardly any difference between results of 0.5 s and 1 s. Hence for employing better computational efficiency, the time step of 1 s is finally chosen.

4.2 Mathematical Formulation

The fundamental conservation equations (mass, momentum and energy) solved for the simulation are given below. The commercial software ANSYS (FLUENT) V-19.0 is employed to solve these equations with the associated boundary specifications.

The mass conservation equation can be given as:

$$\frac{\partial}{\partial t}\rho + \frac{\partial}{\partial x}\rho u + \frac{\partial}{\partial y}\rho v + \frac{\partial}{\partial z}\rho w = 0 \tag{4.1}$$

Momentum Conservation:

In X-direction

$$\begin{aligned} \frac{\partial}{\partial t}\rho u + \frac{\partial}{\partial x}\left[\rho uu - \frac{4}{3}(\mu+\mu_T)\frac{\partial u}{\partial x}\right] + \frac{\partial}{\partial y}\left[\rho uv - (\mu+\mu_T)\frac{\partial u}{\partial y}\right] + \frac{\partial}{\partial z}\left[\rho uw - (\mu+\mu_T)\frac{\partial u}{\partial z}\right] = -\frac{\partial p}{\partial x} \\ -\frac{2}{3}\frac{\partial}{\partial x}\left[\mu\left(\frac{\partial v}{\partial y}+\frac{\partial w}{\partial z}\right)\right] + \frac{\partial}{\partial y}\left[(\mu+\mu_T)\frac{\partial v}{\partial x}\right] + \frac{\partial}{\partial z}\left[(\mu+\mu_T)\frac{\partial w}{\partial x}\right] - \frac{2}{3}\frac{\partial}{\partial x}(\rho\kappa) \end{aligned} \tag{4.2}$$

In Y-direction

$$\begin{aligned} \frac{\partial}{\partial t}\rho v + \frac{\partial}{\partial x}\left[\rho vu - (\mu+\mu_T)\frac{\partial v}{\partial x}\right] + \frac{\partial}{\partial y}\left[\rho vv - \frac{4}{3}(\mu+\mu_T)\frac{\partial v}{\partial y}\right] + \frac{\partial}{\partial z}\left[\rho uw - (\mu+\mu_T)\frac{\partial v}{\partial z}\right] = -\frac{\partial p}{\partial y} \\ -\frac{2}{3}\frac{\partial}{\partial y}\left[\mu\left(\frac{\partial u}{\partial x}+\frac{\partial w}{\partial z}\right)\right] + \frac{\partial}{\partial x}\left[(\mu+\mu_T)\frac{\partial u}{\partial y}\right] + \frac{\partial}{\partial z}\left[(\mu+\mu_T)\frac{\partial w}{\partial y}\right] - \frac{2}{3}\frac{\partial}{\partial x}(\rho\kappa) - \rho g \end{aligned} \tag{4.3}$$

In Z-direction

$$\frac{\partial}{\partial t}\rho w + \frac{\partial}{\partial x}\left[\rho w u - (\mu + \mu_T)\frac{\partial w}{\partial x}\right] + \frac{\partial}{\partial y}\left[\rho w v - (\mu + \mu_T)\frac{\partial w}{\partial y}\right] + \frac{\partial}{\partial z}\left[\rho w w - \frac{4}{3}(\mu + \mu_T)\frac{\partial w}{\partial z}\right] = -\frac{\partial p}{\partial z} - \frac{2}{3}\frac{\partial}{\partial y}\left[\mu\left(\frac{\partial u}{\partial x} + \frac{\partial v}{\partial y}\right)\right] + \frac{\partial}{\partial x}\left[(\mu + \mu_T)\frac{\partial u}{\partial z}\right] + \frac{\partial}{\partial y}\left[(\mu + \mu_T)\frac{\partial v}{\partial z}\right] - \frac{2}{3}\frac{\partial}{\partial z}(\rho\kappa) \tag{4.4}$$

Energy equation is given as

$$\frac{\partial}{\partial t}\rho h + \frac{\partial}{\partial x}\left[\rho h u - \frac{\mu_T}{\mathrm{Pr}_T}\frac{\partial h}{\partial x}\right] + \frac{\partial}{\partial y}\left[\rho h v - \frac{\mu_T}{\mathrm{Pr}_T}\frac{\partial h}{\partial y}\right] + \frac{\partial}{\partial z}\left[\rho h w - \frac{\mu_T}{\mathrm{Pr}_T}\frac{\partial h}{\partial z}\right] = \frac{\partial p}{\partial t} + u\frac{\partial p}{\partial x} + v\frac{\partial p}{\partial y} + w\frac{\partial p}{\partial z} + \frac{\partial}{\partial x}\left(\lambda\frac{\partial T}{\partial x}\right) + \frac{\partial}{\partial y}\left(\lambda\frac{\partial T}{\partial y}\right) + \frac{\partial}{\partial z}\left(\lambda\frac{\partial T}{\partial z}\right) \tag{4.5}$$

Turbulence Model

Turbulence models for supercritical fluids are in a developing stage. In previous studies, Chen and Zhang (2011), Lisboa et al. (2010) and Yadav et al. (2012b) have used the Renormalization Group (*RNG*) k-ε model for sCO_2-NCL and achieved accurate results. Governing equations for the RNG k-ε model include two equations.

Turbulent kinetic energy equation

$$\frac{\partial}{\partial t}\rho k + \frac{\partial}{\partial x}\left(\rho u k - \frac{\mu_T}{\sigma_\kappa}\frac{\partial \kappa}{\partial x}\right) + \frac{\partial}{\partial y}\left(\rho v \kappa - \frac{\mu_T}{\sigma_\kappa}\frac{\partial \kappa}{\partial y}\right) + \frac{\partial}{\partial z}\left(\rho w \kappa - \frac{\mu_T}{\sigma_\kappa}\frac{\partial \kappa}{\partial z}\right) = G - \rho\varepsilon \tag{4.6}$$

where

$$G = \mu_T\left(2\left[\left(\frac{\partial u}{\partial x}\right)^2 + \left(\frac{\partial v}{\partial y}\right)^2 + \left(\frac{\partial w}{\partial z}\right)^2\right] + \left(\frac{\partial u}{\partial y} + \frac{\partial v}{\partial x}\right)^2 + \left(\frac{\partial u}{\partial z} + \frac{\partial w}{\partial x}\right)^2 + \left(\frac{\partial v}{\partial z} + \frac{\partial w}{\partial y}\right)^2\right) \tag{4.7}$$

Turbulent kinetic energy dissipation equation

$$\frac{\partial}{\partial t}\rho\varepsilon + \frac{\partial}{\partial x}\left(\rho u\varepsilon - \frac{\mu_T}{\sigma_\varepsilon}\frac{\partial}{\partial x}\varepsilon\right) + \frac{\partial}{\partial y}\left(\rho v\varepsilon - \frac{\mu_T}{\sigma_\varepsilon}\frac{\partial}{\partial y}\varepsilon\right) + \frac{\partial}{\partial z}\left(\rho w\varepsilon - \frac{\mu_T}{\sigma_\varepsilon}\frac{\partial}{\partial z}\varepsilon\right) = c_1\frac{\varepsilon}{\kappa}G - c_2\rho\frac{\varepsilon^2}{\kappa} - R \tag{4.8}$$

where

$$R = \frac{c_\mu \eta^3 \rho \left(1 - {}^{\eta}\!/_{\eta_0}\right) \varepsilon^2}{\kappa \left(1 + \beta \eta^3\right)} \tag{4.9}$$

$$\eta = \frac{S\kappa}{\varepsilon} \quad and \quad S = \frac{1}{\sqrt{2}} \left(\frac{\partial u}{\partial y} + \frac{\partial u}{\partial z} + \frac{\partial v}{\partial x} + \frac{\partial v}{\partial z} + \frac{\partial w}{\partial x} + \frac{\partial w}{\partial y} \right) \tag{4.10}$$

where the values of constants are as follows :

$$\eta_0 = 4.8, \beta = 0.012, c_\mu = 0.0845, \sigma_\varepsilon = \sigma_\kappa = 0.7178, c_1 = 1.42, c_2 = 1.68 \tag{4.11}$$

$$\mu_T = c_\mu \rho \frac{\kappa^2}{\varepsilon} \tag{4.12}$$

The following terms are defined to describe the fluid flow and heat transfer phenomena. Mass flow rate at any cross section is defined as,

$$\dot{m} = \int_0^A \rho_r \overline{V_r}.dA' \tag{4.13}$$

The local flow velocity can be given as:

$$u_x = \frac{\int_0^A u_r \left|\rho_r \bar{V}.dA\right|}{\int_0^A \left|\rho_r \bar{V}.dA\right|} \tag{4.14}$$

The local temperature is given as:

$$T_x = \frac{\int_0^A T_r \left|\rho_r \bar{V}.dA\right|}{\int_0^A \left|\rho_r \bar{V}.dA\right|} \tag{4.15}$$

Modified Grashof number **?** are defines as follows:

$$Gr_m = \frac{g \beta d^3 \rho^2 Q H_0}{A \mu^3 C_p} \tag{4.16}$$

The local Nusselt number for heating or cooling wall is defined as:

$$Nu_x = \frac{h_x D}{\lambda_x} \tag{4.17}$$

The local heat transfer coefficient h_x is given by

$$h_x = \frac{q_x}{T_{wall} - T_{b,x}} \tag{4.18}$$

The heat flux q_x on the wall is defined as:

$$q_x = \lambda_x \left(\frac{\partial T}{\partial y}\right)_w \tag{4.19}$$

The Nusselt number of heat transfer wall is

$$Nu = \frac{\int_0^L Nu_x dx}{L} \tag{4.20}$$

All the properties are calculated at the bulk mean temperature (T_m) of loop fluid, defined as:

$$T_m = \frac{\sum_{i=1}^{n} T_i}{n} \tag{4.21}$$

4.3 Simulation detail

A three-dimensional transient simulation is performed for the geometries shown in the Fig. 4.1 by using ANSYS Fluent research version 19.0. Both right and left legs of loop are considered to be perfectly insulated to ensure adiabatic condition. The wall thickness at the source and sink is considered as 3 mm for simulation. A Navier-Stokes equation, wherein the pressure-velocity are coupled, have been solved by using SIMPLE (Semi-Implicit Method for Pressure-Linked Equations) algorithm. The velocity and temperature parameters in the momentum and energy governing equations are iterated with a second-order upwind scheme. Similarly the turbulence parameters ($k - \varepsilon$ etc.) are also iterated with second-order upwind scheme. The pressure term in the momentum equation is discretized by using PRESTO (Pressure staggering option). No-slip boundary condition is considered for pipe walls. A general Renormalization Group *RNG* $k-\varepsilon$ model is used to account turbulence in the loop fluid. Further, the axial conductivity and viscous dissipation in loop fluid are considered in the simulation. Convergence is achieved when residuals of the all-governing equations are less than 10^{-3} except the energy equation which was less than 10^{-6}. For simulation, the operating pressure of sCO_2 i.e., loop fluid was kept at 80, 90 and 100 bar, to ensure it at supercritical region. A NIST REFPROP property table NIST (2018) was utilized to obtain all the standard properties of CO_2 for every interval of 2 K temperature & piecewise-linear interpolation was used to obtain property between two data points. While the following assumptions/boundary conditions are considered in the analysis is given in Table 4.2.

Table 4.2: Assumptions/boundary conditions are considered in the analysis.

S.No.	**Description**
1.	The internal and external fluids are in single-phase throughout the loop.
2.	Loop fluid is supercritical CO_2 (Pressure varies from 80 bar to 100 bar).
3.	Left and right leg wall are assumed to be adiabatic.
4.	No-slip condition near wall.
5.	Wall thickness is kept 3 mm.
6.	CHX inlet water temperature is supplied at 305 K.

4.4 Validation

Obtained 3D CFD results are validated with correlation of Reynolds Number and modified Grashof number i.e., $Re - Gr_{\mathrm{m}}$ in two different ways:

i. Numerical correlation validation with $Re - Gr_{\mathrm{m}}$ developed by Chen and Zhang (2011).

ii. Experimental correlations validation with $Re - Gr_{\mathrm{m}}$ developed by Swapnalee et al. (2012)

The correlations available in the literature have been selected to validate the obtained results i.e., the numerical correlation developed by Chen and Zhang (2011), and the experimental correlation developed by Swapnalee et al. (2012). These correlations relate two non-dimensional parameters i.e., Reynolds number (Re) and modified Grashof number ($Gr_m d/L_t$), and it is calculated at the heating section of the loop. CFD simulation results obtained for 90 bar are validated using these correlations. Good agreement was found between the generated results and existing correlations, as shown in Fig. 4.5.

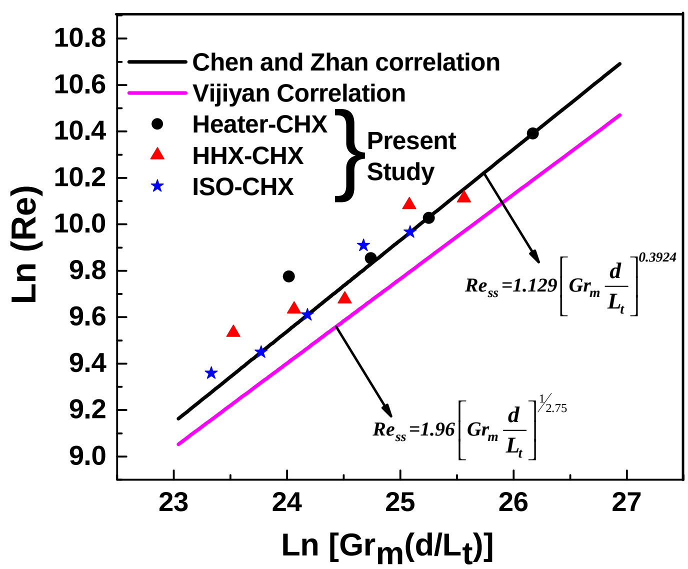

Figure 4.5: Validation of the obtained result with correlations $lnRe$ and $ln(Gr_m d/L_t)$.

The maximum discrepancies are found to be less than 2% with the numerical correlation Chen and Zhang (2011) and less than 6% with experimental correlation Swapnalee et al. (2012)

Numerical Correlation by Chen and Zhang (2011)

$$Re = 1.129(Gr_m d/L_t)^{0.3924}$$

Experimental Correlation by Swapnalee et al. (2012)

$$Re = 1.907(Gr_m d/L_t)^{0.364}$$

4.5 Results and discussion

To compare the transient and instability behaviour of sCO_2 in square-natural circulation loops, three-dimensional CFD simulation is carried out for three different NCL loop configuration. These loops are subjected to same quantum of heat at source but with varying conditions of boundary i.e., first loop is exposed to heater, the second loop is exposed to hot heat exchanger and the third loop to Isothermal wall at their respective sources. The heating section of Heater-CHX loop is exposed to 250 W, 500 W, 1000 W, 1500 W and 2000 W heat fluxes at various pressures i.e., 80, 90 and 100 bar. Whereas, equal quantity of heat is injected to HHX-CHX loop, by circulating hot water of corresponding temperature at the inlet of HHX. Similarly, corresponding constant temperature is maintained throughout the Isothermal wall of ISO-CHX loop. The ISO-Wall temperature and HHX inlet/outlet temperature, corresponding to heat input at 250 W to 2000 W heat fluxes is tabulated in the Table 4.3.

Table 4.3: Heat fluxes imposed at heater and its corresponding temperature derived at HHX and ISO

S.No.	**Heat Input at Heater (W)**	**Corresponding temperature**		
		Hot Heat Exchanger		**Isothermal Wall**
		Inlet to HHX	Outlet from HHX	
1	250	308.50	307.81	306.00
2	500	310.75	309.38	308.00
3	1000	314.25	311.50	309.75
4	1500	317.50	313.38	311.50
5	2000	320.75	315.25	313.50

These values are derived from the steady state condition of Heater-CHX loop for ISO-CHX loop and evaluated analytically for HHX-CHX loop. Further, in order to maintain the similarity in heat rejection process, all these three loops are configured with a cold heat exchanger at their respective sinks. The heating section of loops receives the heat energy from three different kind of boundary conditions but the cooling section of all these loops rejects the heat through a cold heat exchanger, which is being maintained at a constant temperature of 305 K at the inlet of the cooler. The heating section of the loop is exposed to the following three boundary conditions at heat source.

- **Loop:1** Heater: Heat energy is transferred to the loop fluid by exposing entire heating section of the loop to a constant Heat fluxes.
- **Loop:2** Heat Exchanger: The loop fluid receives the heat energy through hot heat exchanger, wherein the intensity of heat input to the loop fluid depletes across the length of the heating section of the loop.
- **Loop:3** Isothermal heat addition: The loop fluid is exposed to uniform temperature throughout the heating section of the loop.

The loops which are configured with the above three boundary conditions are depicted in the Fig. 4.1. Further, in all the simulation cases, the initial temperature of the loop fluid at all the sections of the loop is kept at 305 K. The transient variation in loop fluid mass flow, temperature and velocity at various pressures and heat input along with the effect of pressure on mass flow rate have been recorded at the mid of left vertical leg and discussed in the following sections.

- **Loop:1** Heater: Heat energy is transferred to the loop fluid by exposing entire heating section of the loop to a constant Heat fluxes.
- **Loop:2** Heat Exchanger: The loop fluid receives the heat energy through hot heat exchanger, wherein the intensity of heat input to the loop fluid depletes across the

length of the heating section of the loop.

- **Loop:3** Isothermal heat addition: The loop fluid is exposed to uniform temperature throughout the heating section of the loop.

The loops which are configured with the above three boundary conditions are depicted in the Fig. 4.1. Further, in all the simulation cases, the initial temperature of the loop fluid at all the sections of the loop is kept at 305 K. The transient variation in loop fluid mass flow, temperature and velocity at various pressures and heat input along with the effect of pressure on mass flow rate have been recorded at the mid of left vertical leg and discussed in the following sections.

4.5.1 Transient variation of temperature

Figure 4.6 below shows the variation of loop fluid temperature in three differently configured NCLs i.e., Heater-CHX, HHX-CHX and ISO-CHX natural circulation loops. The initial temperature of the loop fluid of all the loops is kept at 305 K in order to maintain the uniformity in all the loops. At lower level of heat input, the temperature fluctuation is very high in all NCLs and it never reaches to a steady state throughout the operation of the loop. Whereas, at higher heat input, the fluctuation in temperature gets mitigated over a period of time and reaches to steady state eventually. Further, at the lower level of heat input, in all the loops, temperature fluctuation maintains the same pattern and amplitude throughout the operation of the loop. However, in case of Heater-CHX loop, at 500 W and 1000 W heat fluxes, the amplitude of temperature fluctuation keeps on increasing with time.

At lower level of heat input, the temperature difference across source and sink will be very less and hence the driving force will be obviously very less. This weak driving force strives to overcome the all opposing forces in the loop and if driving force is greater than the opposing forces then the flow establishes.

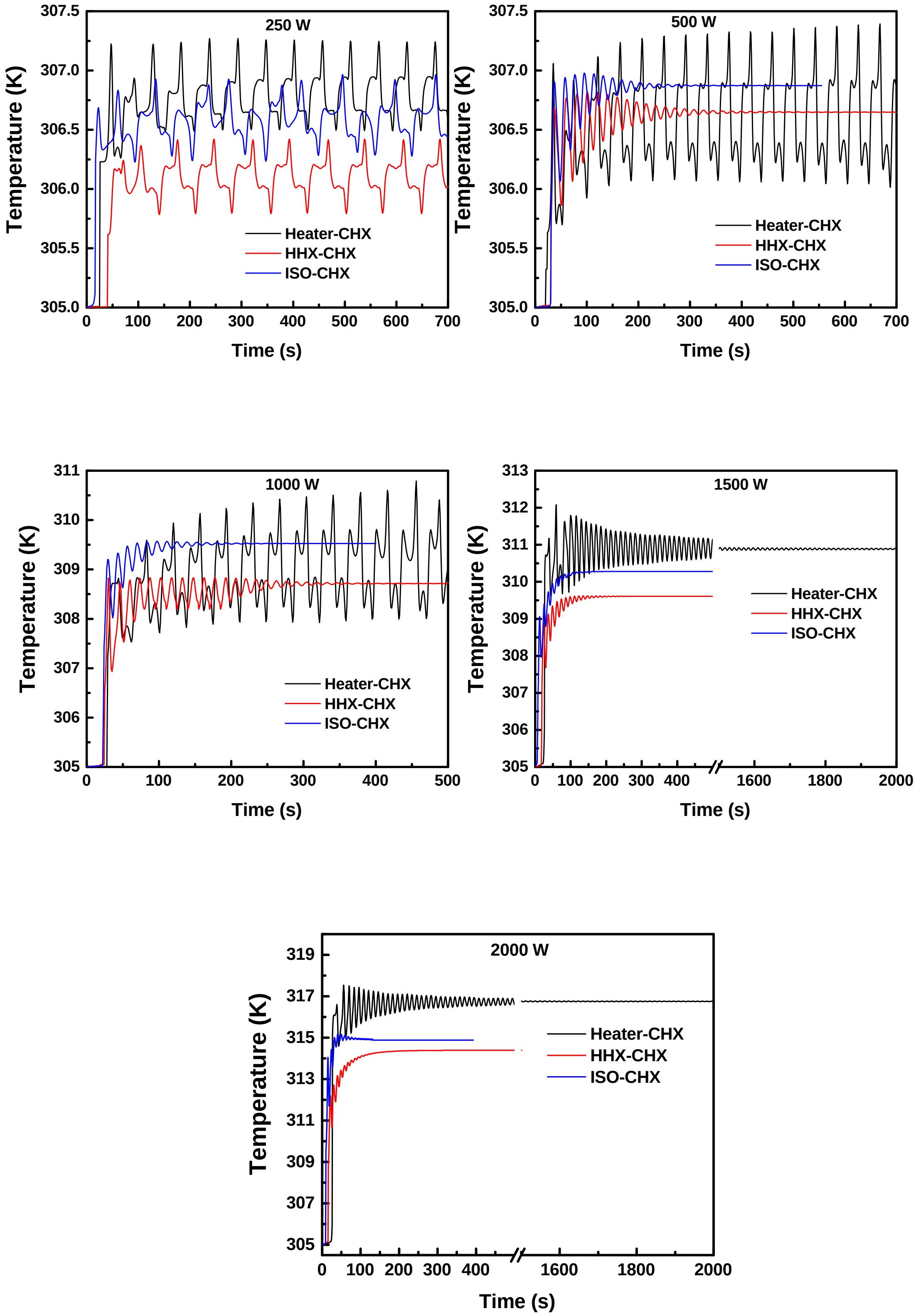

Figure 4.6: Variation of temperature at Heater-CHX, HHX-CHX and ISO-CHX for Supercritical CO_2 based natural circulation loop at different heat inputs.

Since the driving force is very weak at lower heat input, at one point of time it fails to drive the fluid in the loop and the velocity slides down.

This tug-of-war in the loop continues or reaches to a steady state depending upon the imposed boundary conditions. Further, the time required to reach to a steady state is also dictated by the quantum of heat input and boundary conditions at source. At higher heat put, the driving force will be very strong due to stretched differential temperature across the source and sink. Higher the differential temperature higher will be the buoyancy effect and hence higher circulation rate Cheng et al. (2017). It is very clearly visible in the graphs that as the temperature difference increase, the mass flow increases.

The amplitude of temperature fluctuation is very vigorous in case of Heater-CHX loop and it takes longer duration to get mitigated at higher level of input. Whereas, in case of ISO-CHX loop, the amplitude of temperature fluctuation is insignificant in nature and also reaches a steady state at a shorter time duration.

For a given boundary conditions the operating temperature of the loop fluid is highest in case of Heater-CHX loop and it is lowest in case of HHX-CHX loop.

4.5.2 Transient variation of mass flow rate

Figures 4.7a-e show the comparison of loop fluid mass flow rate (transient) in sCO_2 based NCLs configured with Heater-CHX, HHX-CHX and ISO-CHX, at source and sink respectively, by varying the heat input at source keeping loop pressure fixed at 90 bar and sink temperature at 305 K. Results are extracted at the centre of the right leg by considering the area-weighted average across the cross-section of the loop. The amplitude of mass flow fluctuation is very high at lower level of heat input in all the loops and never reaches to a stable state throughout the operation. However, at higher level of heat input, the amplitude of mass flow fluctuation reduces considerably and reaches to a steady state eventually. At the lower level of heat input, in addition to mass flow fluctuation, the flow reversal occurs very frequently in all the loops.

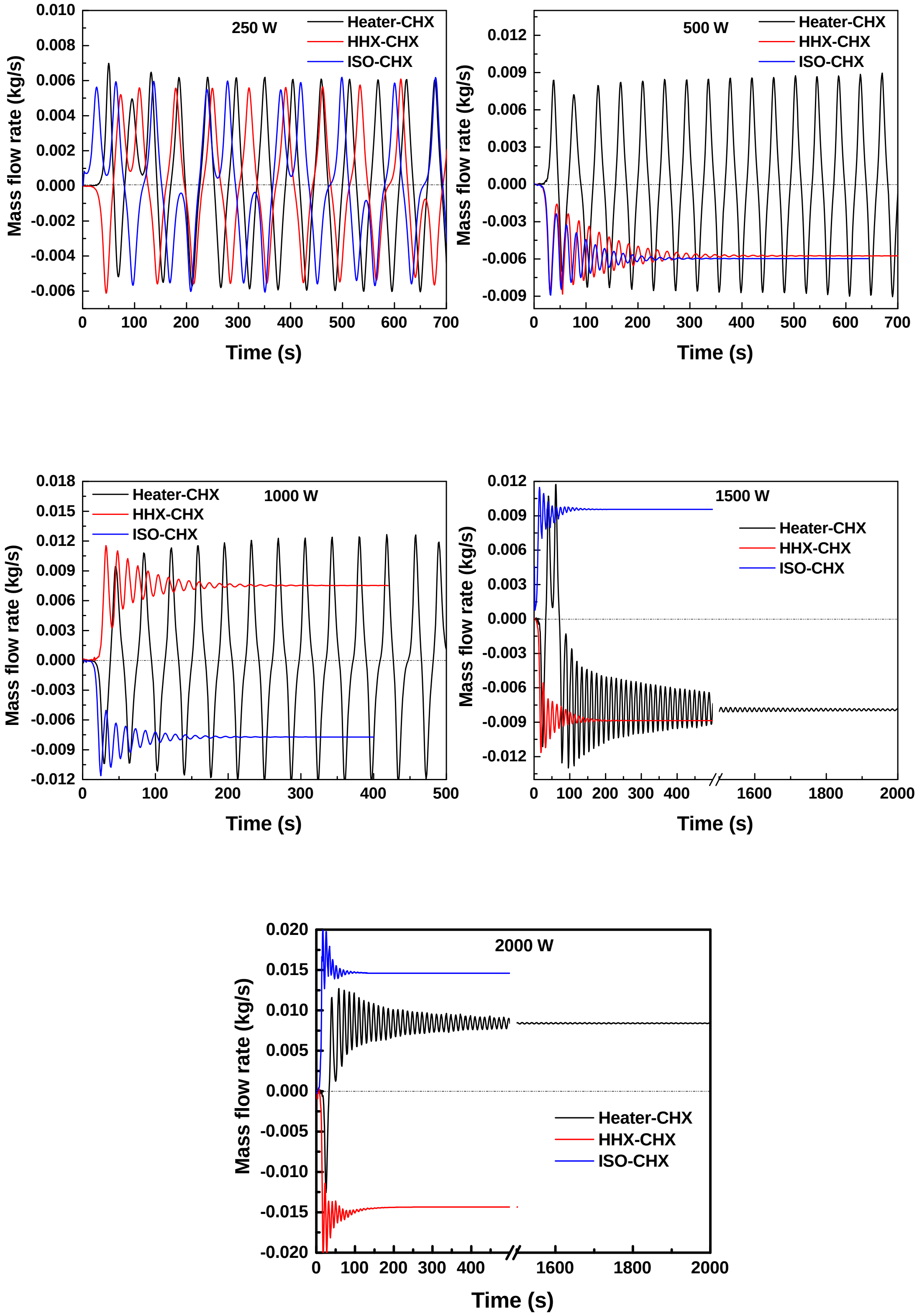

Figure 4.7: Variation of mass flow rate at Heater-CHX, HHX-CHX and ISO-CHX for Supercritical CO_2 based natural circulation loop at different heat inputs.

It is to be noted that, in case of Heater-CHX loop, mass flow reversal phenomenon is common at all level of heat input, but its severity and duration of fluctuation reduces as heat input at source increases. Whereas, no such reversal of mass flow is noticed in other two loops except at lowest level heat input i.e., at 250 W. At all level of heat input to the loop, the severity of mass flow oscillation is very high in the Heater-CHX loop compared to other two loops. Further, it is to be noted that the mass flow rate, at steady state, is very low in case of Heater-CHX loop compared to other two loops at all level of heat input to the loop. Further, at all level of heat input, in case of HHX-CHX and ISO-CHX loops, the magnitude of mass flow rate, at steady state, is found to be virtually in the same level and it is greater than the Heater-CHX loop.

It is obvious from the graphs that in NCLs the direction of mass flow is highly inconsistent and extremely unpredictable. It is interesting to note that, the direction of mass flow is independent of the type of the boundary conditions on which NCLs are subjected and also quantum of heat input at source. In case of Heater-CHX loop, from 250 W to 1000 W of heat input the mass flow reversal occurs frequently throughout the operation and never reaches to steady state. This phenomenon of flow reversals, at lower level of heat input, may be due to very low velocity of loop fluid. However, at 1500 W and 2000 W of heat input, the mass flow takes a definite direction after initial reversal but direction is opposite to each other, however eventually it reaches to a steady state condition. Similarly, in case of HHX-CHX loop, at lower as well as higher level of heat inputs, mass flow takes anticlockwise direction and at moderate level of heat input it takes clockwise direction. In a similar way, in case of ISO-CHX loop, at lower level of heat input, mass flow takes anticlockwise direction and at higher level of heat input it changes to clockwise direction. This unpredictable behaviour of flow reversals and the direction of flow could be due to bilaterally symmetrical geometry of NCLs in its vertical axis. Due to this geometrical symmetry of loop, the resistance to flow in either directions will be identical and hence the flow of loop fluid takes the precedence and queue from the initial movement of the molecules at heating section of the loop.

4.5.3 Transient Variation of Velocity

Figure 4.8 shows the velocity transient behaviour of loop fluid in Heater-CHX, HHX-CHX and ISO-CHX natural circulation loops. The loop fluid magnitude of velocity is a direct function of density difference between the source and the sink of the loop. Differential density in the loop is a function of temperature difference between the source and sink, which in turn will have a direct impact on the mass flow rate of loop fluid in the loop.As the differential temperature increases across source and sink, the density difference between heating and cooling sections also increases. Impact on mass flow rate and velocity due to widening of differential temperature is more pronounced in case of supercritical fluids as its viscosity is inherently lower compared to subcritical fluid. It is clearly visible in the graph i.e., at lower level of heat input (250 W/308.5 K/306 K), the loop fluid average velocity is approximately in the rage of 0.05 m/sec to 0.06 m/sec and at higher level of heat input (2000 W/320.75 K/313.5 K) it increases to a range of 0.19 m/sec to 0.24 m/sec, in the Heater-CHX, HHX-CHX and ISO-CHX loops respectively in ascending order. For a given boundary conditions, among these three loops, the loop fluid velocity is very high in case of ISO-CHX loop and it is lowest in case of Heater-CHX loop.

During the initial stage of heat input, the loop experiences very high fluctuation in the velocity due to non-uniform heat distribution in the loop. The non-uniform distribution of heat creates uneven accumulation of heat pockets at various locations in a system. These pockets suddenly release its accumulated heat when it moves to the cold region in the system. This sudden release of accumulated heat energy creates a huge density difference across the loop and it leads to very high velocity fluctuation in the initial period. Over a period of time once the system reaches to the equilibrium state i.e., when the quantity of heat addition and rejection is equal and driving force overcomes all the opposing forces in the system then the steady state and unidirectional flow will establish. Similarly, any variation in the heat input or a pressure the system will experience initial glitches and eventually settles down to steady state.

At lower rate of heat input, in all loops, the oscillation of velocity is very high and it never reaches to a steady state. In all three loops, the magnitude of velocity oscillation is considerably higher at lower heat input and it gradually decreases with the increase in the heat input. Further, the magnitude and frequency of velocity oscillation in case of Heater-CHX is predominantly more at all level of heat input compare to HHX-CHX and it is considerably subdued in case of ISO-CHX loop.

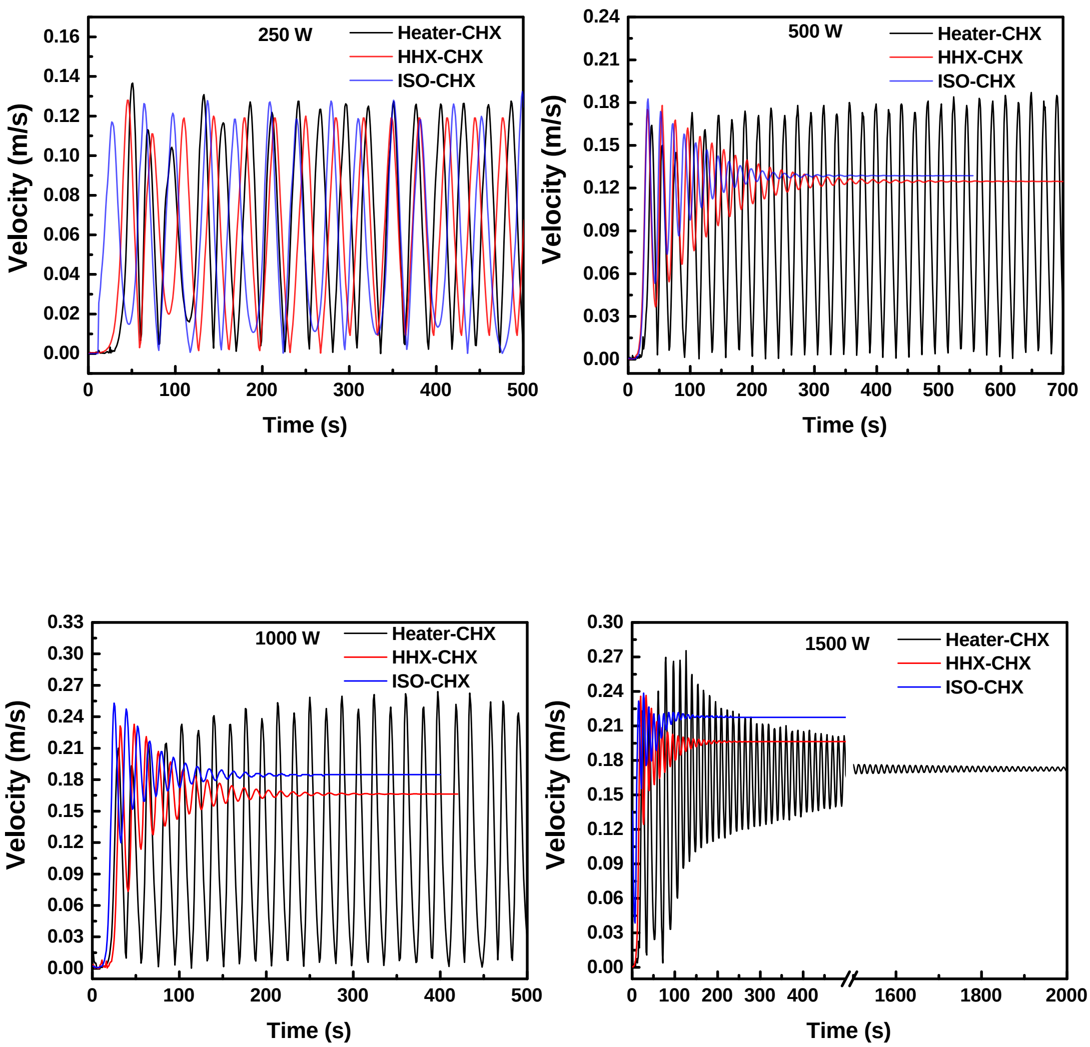

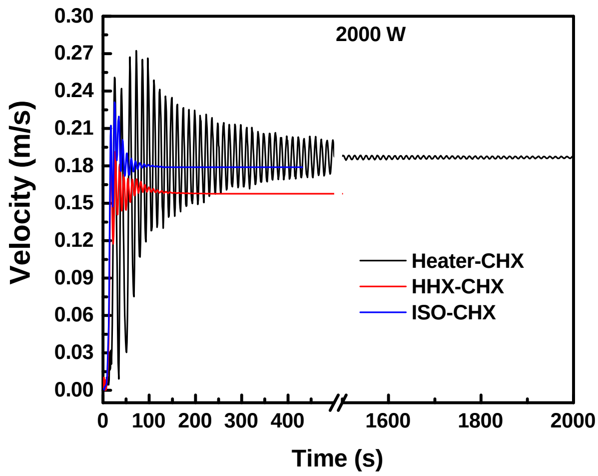

Figure 4.8: Variation of velocity for Heater-CHX, HHX-CHX and ISO-CHX for Supercritical CO_2 based natural circulation loop at different heat inputs.

In case of ISO-CHX loop, the magnitude of velocity oscillation gets converges to a steady state at a faster rate compare to other two loops. Whereas, in case of Heater-CHX loop, the magnitude of velocity oscillation is very high and it take considerably longer duration to get converge to a steady state compare to other two loops. In all NCLs configurations, as the heat input increases at source, the amplitude of velocity decreases and it reaches to steady state at a faster rate.

4.5.4 Effect of operating pressure

Figure 4.9 shows the transient behaviour of mass flow rate at various loop fluid pressure for all three loops i.e., Heater-CHX, HHX-CHX and ISO-CHX loops. From the graphs, it can be inferred that the magnitude and frequency of mass flow oscillation decrease with an increase in loop pressure for all three loops. It is very interesting to note that as the operating pressure of the sCO_2 increases, the time duration required to reach steady state of the system decreases, the same results are observed in the experimental study of Yadav et al. (2017). Further, the pressure has a significant effect on the mass flow rate in all three loops i.e., mass flow rate increases with increase in the loop fluid pressure, the same phenomenon is observed in a CFD analysis of Archana et al. (2015) on sCO_2 based NCL.

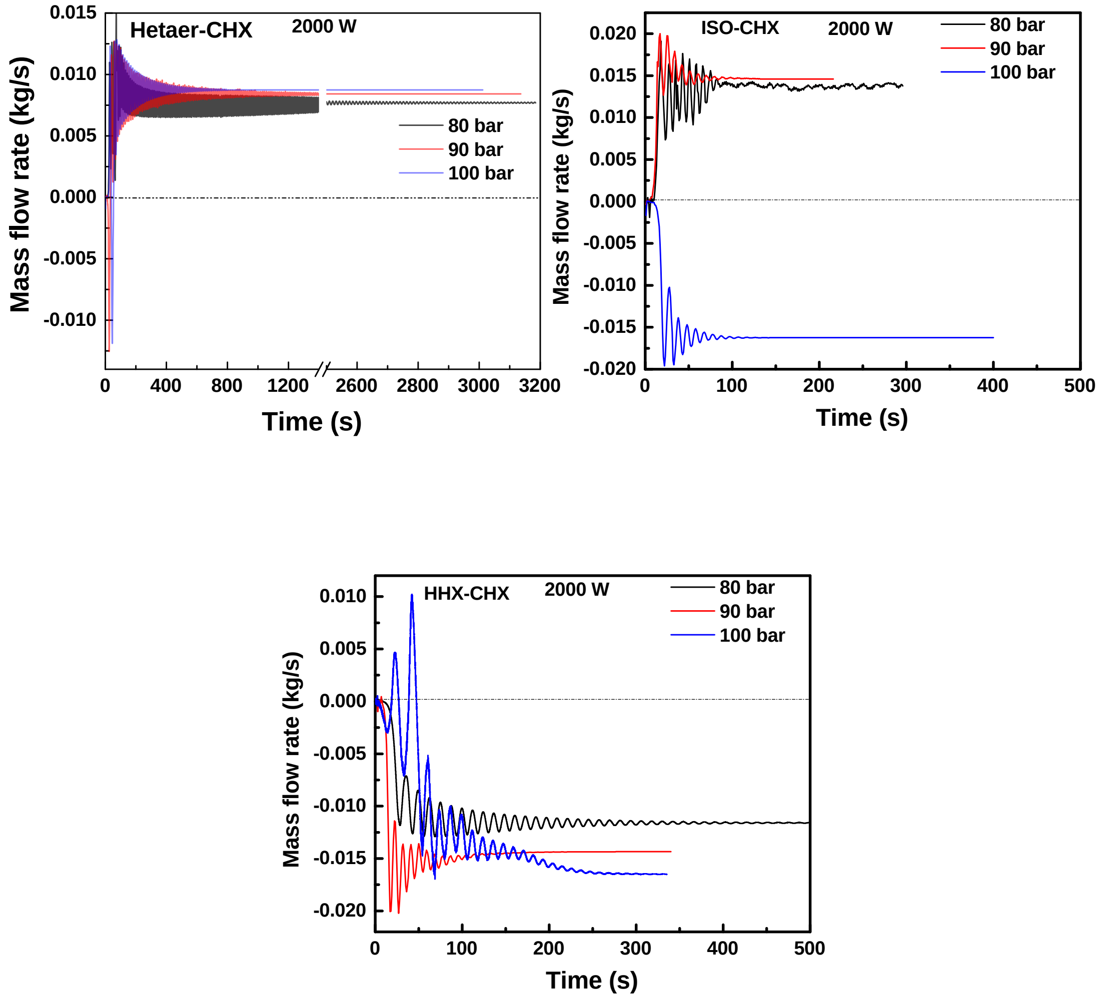

Figure 4.9: Effect of operating pressure 80 bar, 90 bar and 100 bar for Supercritical CO_2 based natural circulation loop at different heat inputs for (a) Heater-CHX (b) HHX-CHX and (c) ISO-CHX.

In general, the supercritical fluids attain a maximum density when it reaches to its critical temperature and pressure. Around the critical region, the impact on the density of the fluid will very huge even for a small variation in the temperature and pressure. The fluid keeps reaching to its peak density and reverts very frequently, which in turn induce density waves in the system. In natural circulation system these density waves will affect various operating parameters and create imbalance among the natural driving force, frictional forces and other forces. If the variation in density reaches to a very high value, then it leads to flow reversal in the loop.

In natural circulation systems, the driving force shall balance with the resistive force for the flow to get established. Appropriated agreement between driving force and resistive force is the prerequisite for a stable state in the natural circulation loops. The resistive force is a function of friction factor, mass flow rate and average density along the loop. In compressible fluids, the average loop density increases with increase in the loop pressure and it supplements buoyancy effect in the system due to lower viscosity and which in turn increases the mass flow rate. Further with the increase in density and hence the mass flow rate, the resistive forces in the loop increases (i.e., viscous dissipation and friction between wall and fluid). The resistive force thus increased counters the buoyancy force and suppresses the mass flow rate in the loop. Again, the buoyancy force strives to overcome the resistive force and this tug of war will continue between these two forces till there establishes a balance between these two forces and it is the root cause for the instability/oscillation in the natural circulation loops (Wang et al. (2015)). This concept is very much visible from the following graphs i.e., increase in mass flow rate with increase in loop pressure.

The flow instability in the Heater-CHX loop is very high compared to the other two loops and also it takes a longer time to reach steady state at lower pressure compared to higher pressure. It may be due to direct impact of heat fluxes on the loop fluid at source of the loop. In case of Heater-CHX loop, at lower pressure, the mass flow is unidirectional, whereas at higher pressure, as soon as the loop is exposed to heat energy at source, for a small period of time in the initial stage, the mass flow takes bidirectional path and after that it follows unidirectional path.

The influence of operating pressure on the loop fluid mass flow oscillation is moderate in case of HHX-CHX loop compared to other two loops. At all operating pressure of the loop fluid, in Heater-CHX loop, the mass flow takes clockwise direction and on contrary to this occurrence, in HHX-CHX loop, it takes anticlockwise direction.

The influence of operating pressure of the loop fluid on the mass flow oscillation is very mild in case of ISO-CHX loop compared to other two loops. This may be due to impulsive response of isothermal wall for any change in heat input at source, as temperature distribution is uniform throughout the heating section of loop. This uniform temperature distribution effectively dampens the mass flow fluctuations faster, leading to a faster rate of stabilization of system. Further in this loop, as the loop fluid's operating pressure increases, the mass flow changes its flow direction from clockwise to anticlockwise direction. It is very unique in ISO-CHX loop compared to other two loops under study.

4.5.5 Variation of turbulence kinetic energy

Figure 4.10 depicts the profile of turbulence kinetic energy variation in all three NCL configurations at 90 bar pressure for the heat input of 2000 W heat fluxes at source in Heater-CHX loop and for the temperature of 320.75 K at the hot heat exchanger inlet of HHX-CHX loop and for the uniform temperature of 313.50 K at the Isothermal wall of ISO-CHX loop. Turbulent flow is a property of the fluid flow but not a fluid physical characteristic. Velocity, pressure and other parameters irregular fluctuations causes turbulent flow in the loop.

Turbulent flow is characterized by fluctuating velocity fields in the flow region, which is highly chaotic in nature as both velocity and pressure varies randomly with time. Random quantities are generally four-dimensional functions of the space-time. Turbulence kinetic energy is the average kinetic energy per unit mass which is associated with oscillatory fluid flow. The turbulence energy generates in the flow is proportional to shear stresses i.e., frictional forces and buoyant forces. In general, Renormalized Group (*RNG*) i.e., $k-\varepsilon$ equations of turbulent models are used to evaluate the turbulence energy in flow field. The ANSYS FLUENT standard $k-\varepsilon$ of turbulence is considered in the present study to compare turbulence kinetic energy profile in various

NCLs as it ensures reasonably fair accuracy for a wide range of turbulent flows.

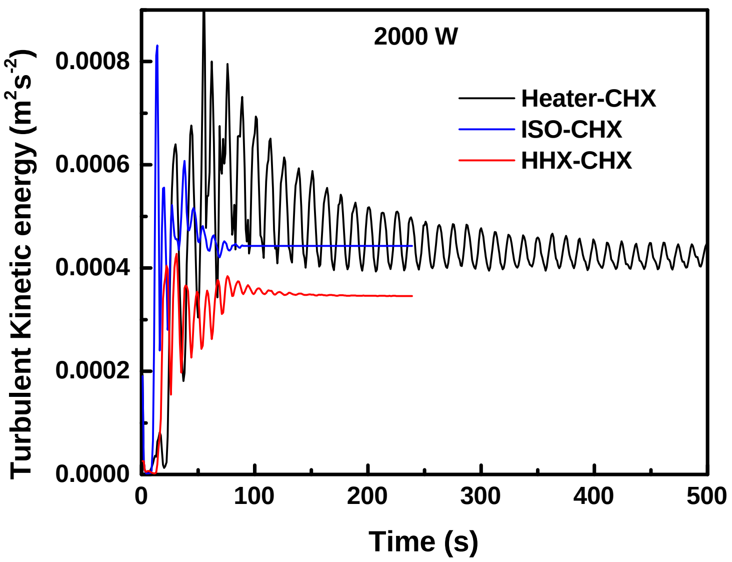

Figure 4.10: Turbulence Kinetic Energy for Supercritical CO_2 based Heater-CHX, HHX-CHX and and ISO-CHX natural circulation loop.

It is to be noted from the temperature profiles of NCLs that, for a given boundary conditions, the operating temperature of the loop fluid is highest in case of Heater-CHX loop compared to other loops. Flow turbulence is a function of temperature and hence higher the temperature indicates higher turbulence in the loop. Further, higher the turbulence energy in the fluid flow field indicates higher heat transfer rate. Exceptionally excellent Turbulence kinetic energy in Heater-CHX loop exhibits a better heat transport property compared to other loops. Further, higher Nusselt number in the Heater-CHX loop also supplements its better heat transport property.

4.5.6 Nusselt number

Figure 4.11 shows the effect of heat input on the Nusselt number for all three NCLs i.e., Heater-CHX, HHX-CHX and ISO-CHX loops. The Nusselt number, a non-dimensional form of heat transfer coefficient, is a function of Reynolds number and Prandtl number (Pr), i.e., in the loop, the Nusselt number increases with an increase in Reynolds number. The magnitude of Reynolds number increases with increase in the loop differential temperature, which indicates the increase in turbulence and hence the higher rate of heat transfer. Nusselt number in the Heater-CHX loop is very high compared to the other two configurations at all level of heat input and it keeps on increasing with an increase in the heat input at source in all NCLs. HHX-CHX NCL configuration demonstrated the least level of Nusselt number among the cluster of NCLs considered for analysis. The performance of ideal NCL i.e., ISO-CHX loop lies in between the two practical NCLs.

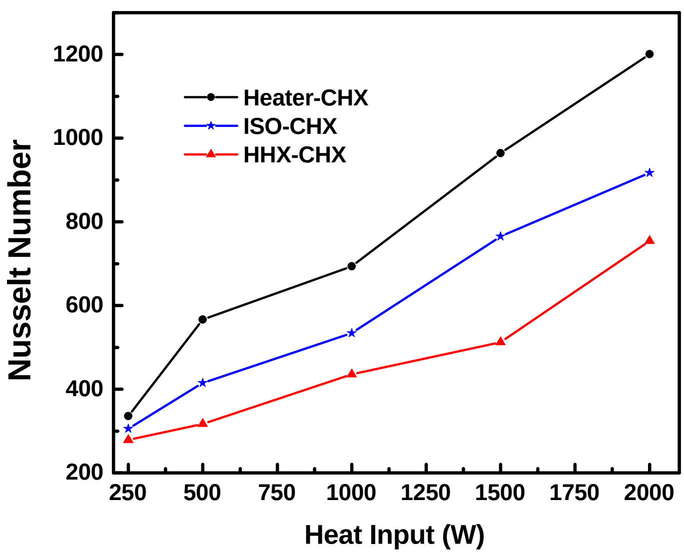

Figure 4.11: Variation of Nusselt number with heat input for CO_2 based Heater-CHX, HHX-CHX and ISO-CHX natural circulation loop.

4.6 Summary

Three-dimentional CFD simulation were conducted on three different combinations of source and sink in sCO_2 based square NCLs to study the influence of change in boundary condition and operating pressures on transient and instability behaviour of loop reveals the following:

1. NCLs show instability in the form of oscillation or both oscillation, flow reversal and the time required for these instabilities to attain a steady state depend on the

nature of boundary condition chosen or quantum of heat input applied at source.

2. The Loop fluid mass flow rate, temperature and velocity oscillation in Heater-CHX loop is very high compared to ISO-CHX loop. This difference in the behaviour of loops is inherently due to heat transfer rate is fixed and independent of loop fluid temperature in heater, but in other cases heat transfer rate depends on loop fluid temperature. Stability performance of HHX-CHX loop sets in between these two loops.

3. In ISO-CHX loop, the mass flow and temperature instabilities stabilized at a faster rate compared to Heater-CHX and HHX-CHX loops, as its response at source is instantaneous due to constant temperature throughout the heating section.

4. For a given boundary conditions, the operating temperature of the loop fluid is highest in case of Heater-CHX loop and it is lowest in case of HHX-CHX loop.

5. In all configurations of NCLs considered in the present study, the mass flow rate increases with an increase in loop fluid operating pressure, whereas, flow instabilities decrease with an increase in loop fluid operating pressure. It is found that as the operating pressure of the sCO_2 increases, the time duration required to reach steady state of the system decreases.

6. At all levels of heat input at source, the average mass flow rate is lower and the time taken for the velocity oscillations to dampen is very high in case of Heater-CHX loop compared to other two loops. Whereas, the amplitude of flow oscillation is very mild and velocity oscillations convergence at a shorter time duration in case of ISO-CHX loop compared to other two loops.

7. In all configurations of NCL, at lower heat input, the loop fluid flow takes bidirectional path at regular intervals. However, at higher heat input, it follows unidirectional path except for inconsequential initial glitches in case of Heater-CHX loop. Further, the direction of flow is highly inconsistent and extremely

unpredictable in all configurations of NCL considered. The direction of mass flow is independent of the type of the boundary conditions and quantum of heat input.

8. Nusselt number in case of Heater-CHX loop is very high compared to HHX-CHX and ISO-CHX loops because of its high turbulent kinetic energy and it leads to better heat transport property in case of Heater-CHX loop.

CHAPTER 5

An Experimental Investigation with Supercritical CO_2 based Natural Circulation Loops

Unless otherwise the theoretical findings are validated with experimental results, the authenticity of such findings will be always liable for dispute. The theoretical or numerical approach offers only direction in which the conceptualization process shall progress, however practical approach is the only way to reach the actual destination. In view of this a simple square natural circulation experimental loop has been designed and fabricated to conduct the test at various operating conditions. This section depicts experimental investigations on single phase sCO_2 based Natural Circulation Loop subjected to various pressures and temperatures. Details on experimental setup of high-pressure natural circulation loop along with various instruments which are used to perform experiment are also presented.

5.1 Natural circulation loop experimental set up design

A typical schematic representation of NCL experimental setup which is used to carry out the practical investigation is shown in Fig. 5.1. The experimental setup consist of loop which is fabricated with 15 mm diameter and 3 mm thick SS316 tube, electrical heater, cold heat-exchanger, Thermostatic bath, CO_2 Changing Cylinder, CO_2 accumulator, Data logger, Mass flow meter, Differential pressure transmitter, Pressure reliving valve, Rotameter, Pressure Gauge and Thermocouples.

Loop : A 1000 mm x 1000 mm square consist of two horizontal circular pipes (heat transfer sections) and two vertical circular pipes (circulation driving sections) connected with four bends, as shown in Fig. 5.2 is fabricated with the SS316 tube of diameter 15 mm. SS Grade 316 is a standard molybdenum-bearing grade austenitic stainless steel, which contains 6-18.5% Cr, 10-14% Ni, 2-3% Mo. The Molybdenum ($^{93}Mo_{42}$) gives 316 better overall corrosion resistant properties and Chromium ($^{52}Cr_{24}$) increases the oxidation resistance capacity. A tube in tube type of heat exchanger having 660 mm length, the outer diameter of 32 mm and thickness of 3 mm is used. The loop is designed to withstand 210 bar working pressure and after fabrication it is subjected to 150 bar hydraulic pressure (which is 1.5 times the operating pressure) to ensure the mechanical strength of the tube and the weld joints. This loop is kept in a vertically upright position at zero degree inclination to the horizontal floor plane, in order to reap the maximum benefits of the gravitational influence. The Cold heat-exchanger and the Electrical heater are integrated with the loop at the top and bottom section of the loop respectively.

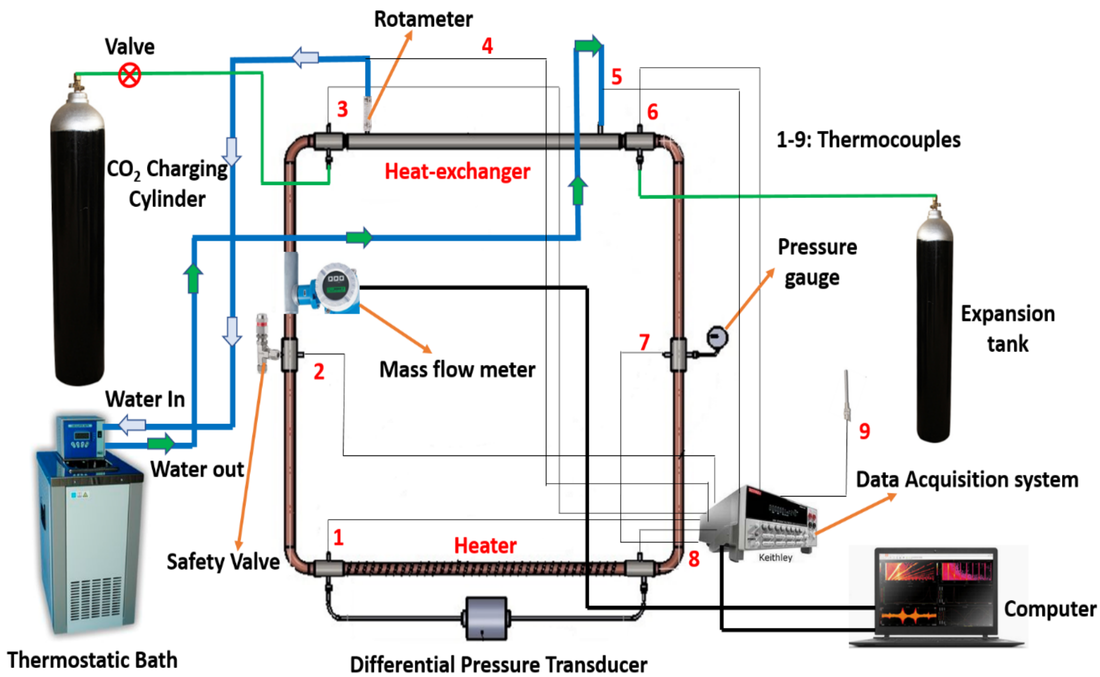

Figure 5.1: Schematic of the NCL with instruments used in the experiment.

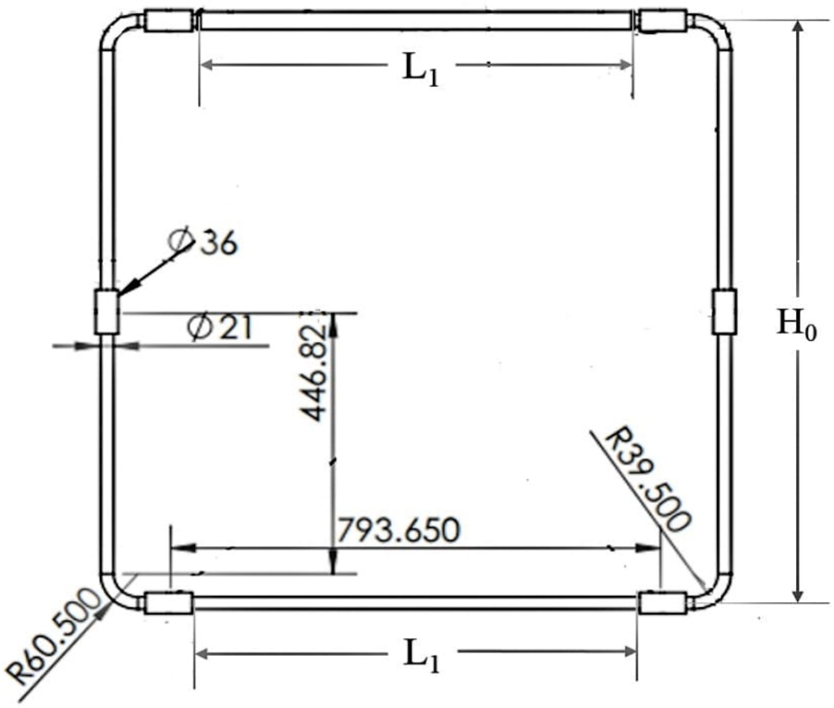

Figure 5.2: Design of fabricated regular natural circulation loop.

The vertical legs which are designated as a raiser and down comer interconnect the Cold heat-exchanger and the Electrical heater and these legs are well insulated with an asbestos rope to make it adiabatic. Further, to minimize the heat loss from the loop to ambient, the entire loop is insulated with asbestos and a 3 mm thick foam insulating material. The geometrical detail of NCL is given in Table 5.1.

Figures 5.3(a) and (b) show the photographic view of the setup without insulation and with one-layer asbestos rope insulation, respectively.Six pre-calibrated T-type thermocouples are located at different locations along the loop to monitor the inside temperature of loop fluid, i.e., CO_2. The thermocouples are directly connected to loop by using nut and ferrule arrangement, in such a way that its probe directly touches the the loop fluid. (shown in Fig. 5.3(a)).

Table 5.1: The geometrical dimensions of NCL.

Loop detail	**Size (mm)**
Inner diameter of the loop pipe	15
Outer diameter of the loop pipe	21
Thickness of the loop pipe	3
Length of heater and heat-exchanger (L_1)	660
Length of right leg and left leg (H_0)	1000
Radius of bend (outer)	60.5
Radius of bend (inner)	39.5
Outer diameter of heat-exchanger	32
Annulus distance (radial)	2.5

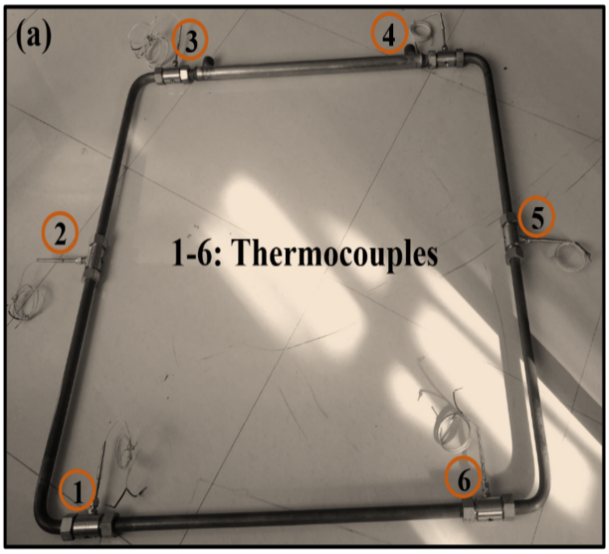

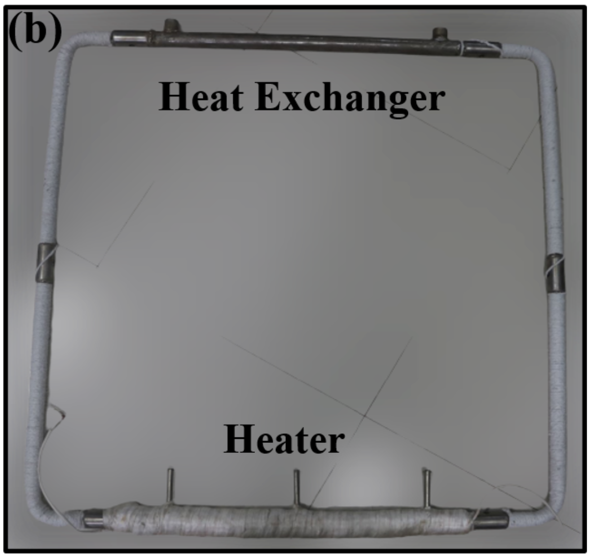

Figure 5.3: Photographic view of the experimental setup (a) Without insulation and (b) With one layer insulation (asbestos rope).

5.2 Data collection and instrumentation of NCL

a. Cold Heat-Exchanger Pulse Thermostatic Bath: Tube in tube cold heat exchanger is embedded on the top section of the loop. It is fabricated by using 3 mm thick tube of internal diameter 26 mm and length of 600 mm, which is embedded on the loop tube to form a concentric tube in tube heat exchanger configuration. The cooling surface area of tube in tube heat exchanger covers 60% of loop top section. Inlet and outlet of the exchanger is connected to the 2 kW capacity heating/cooling thermostatic bath (Thermo scientific PC200) thorough a flexible hoses, to feed a constant temperature fluid at inlet to the exchanger. Thermocouples are installed at inlet and outlet of the exchanger to monitor the cooling fluid temperature at the relevant locations. Further, rotameter of arrange 0-2 LPM is located at the out of the cooling fluid outlet to monitor the constant mass flow rate of the cooling fluid.

b. Electrical Heater Pulse Thermostat: Electrical coil of 2000 kW capacity is uniformly winded on the bottom section of the loop, to impart constant heat flux on the heating section. The electrical coil covers 600mm length of loop bottom section. The electrical coil is energized through the thermostat, which regulates constant power supply to heating coil to ensure a constant heat flux at heating section of the loop.

c. Data logger: Data acquisition system, Model: KEITHLEY-2700, with an accuracy of ± 0.1 % is integrated with the computer using Kickstart software (LabVIEW software) for the monitoring on line real time thermocouples temperatures and pressure readings.

d. Differential Pressure Transducer: Honeywell make differential pressure transducer of range 0-1000 mbar is equipped across the heating section to measure the loop fluid pressure drop across the heater.

e. Pressure Reliving Valve: To study the instability behavior of the system, experimental study is conducted at various pressure in the super critical pressure region of CO_2 i.e., at 80 bar, 90 bar and 100 bar. Safety of men and equipment is given at most importance while operating the system at such a high pressure. To ensure safety, a foolproof mechanical pressure reliving system is mandatory in the loop. Hence safety valve is incorporated on the loop right leg and the pressure relieving is set at 140 bar, which is very less compared to the mechanical design pressure of 210 bar.

g. Mass flow meter: Coriolis type mass flow meter: Model Rheonik RHE16, of range 0–500 kg/hr and full MODBUS capability is hook-up at the right vertical leg of loop to measure the mass flow rate of loop fluid i.e., sCO_2. This mass flow transmitter is a state-of-the-art multifunction DIN rail mount Coriolis transmitter.

h. CO_2 charging Cylinder: The loop fluid, CO_2, is initially changed into the vacuum pulled (to evacuate the air from the loop) loop through the CO_2 charging cylinder.

i. CO_2 Accumulator: It is integrated in the loop to dampen the pressure fluctuation in the loop due to unwarranted or uncontrolled heating i.e., over or under heating at heating section of the loop. The volumetric capacity of the expansion cylinder is designed 100 times to that of the loop volume.

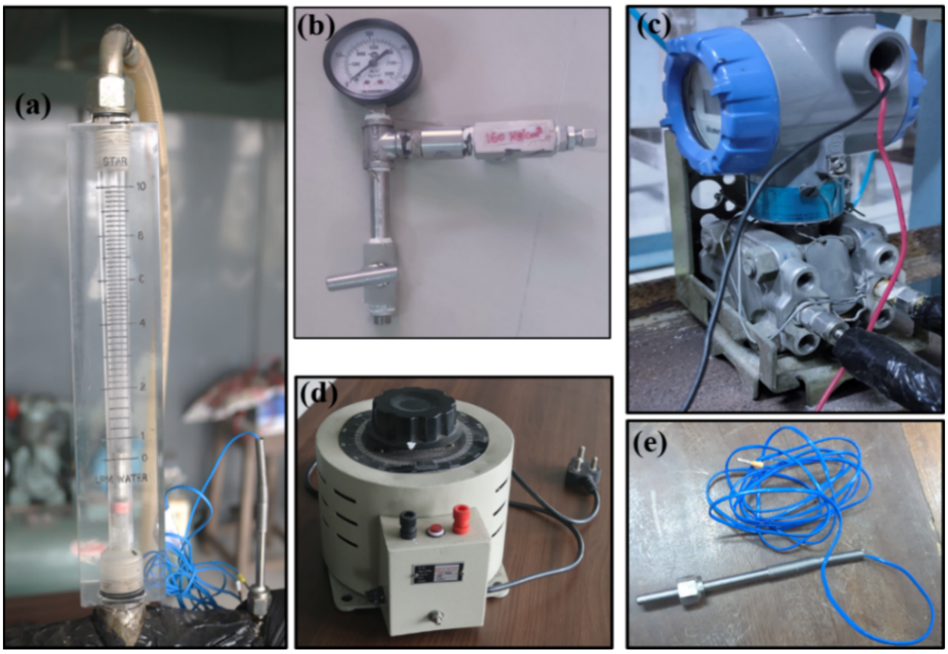

Figure 5.4: Equipment used for test facility (a) Rotameter (b) Safety valve (c) Differential Pressure transducer (d) Dimmerstat (e) Thermocouple.

Figure 5.5: Equipment used for test facility (a) Thermostatic bath (b) Data acquisition system (c) Vacuum pump (d) Mass flow meter.

j. Thermocouples: To monitor the temperature distribution at various locations in loop, 9Nos. T-Type pre-calibrated thermocouples are installed in the loop (shown in Fig. 5.1.

Figure 5.4 and Fig.5.5 show the various equipment used in the experiment. Table 5.2 shows the equipment details, operating range and accuracy.

Table 5.2: Equipment details used for experimentation.

Equipment	Make/Type	Range	Accuracy
1. Thermostatic bath with inbuilt pump and heat exchanger	Thermo scientific PC200	-60 to 150 °C Heating /cooling capacity 2 kW	±0.01 °C
2. Thermocouple	T-type	-270°C -370 °C	±0.25 °C
3. Data Acquisition System	KEITHLY-2700	———	±0.01 °C
4. Differential Pressure transducer	Honeywell	0-1000 mbar	±0.1 mbar
5. Mass flow meter	Rheonik, RHE 16	0-500 kg/h	±0.1 kg/min
Rotameter	——	0-10 LPM	±0.1 LPM
6. Watt Digital Meter	HTC PM-03	5-2200 W	±1 W
7. Pressure Gauge	Delta/Bourdon tube	0-150 bar	±1 bar

5.3 Pre experimental Activities

After fabrication, the photographic view of the assembled test facility for R-NCL is shown in Fig. 5.6. To ensure the quality of the weld joint, the loop was exposed to Non Destructive Tests (NDT) like dye penetration test (all the joints) and radiography (Two nos. weld joints) are conducted. NDT results confirmed that the weld joints are flawless i.e., no weld cracks and weld blow holes are detected. Further, to confirm the weld joint strength the loop was subjected to hydrotest for an hour at 150bar pressure and found no pressure drop in the loop. With this tests it is confirmed that loop tube and weld joints are safe at operating pressure of the loop. After completion of NDT and hydrotest, the loop is blown with the dry air to remove the weld debris, dirt and moisture.

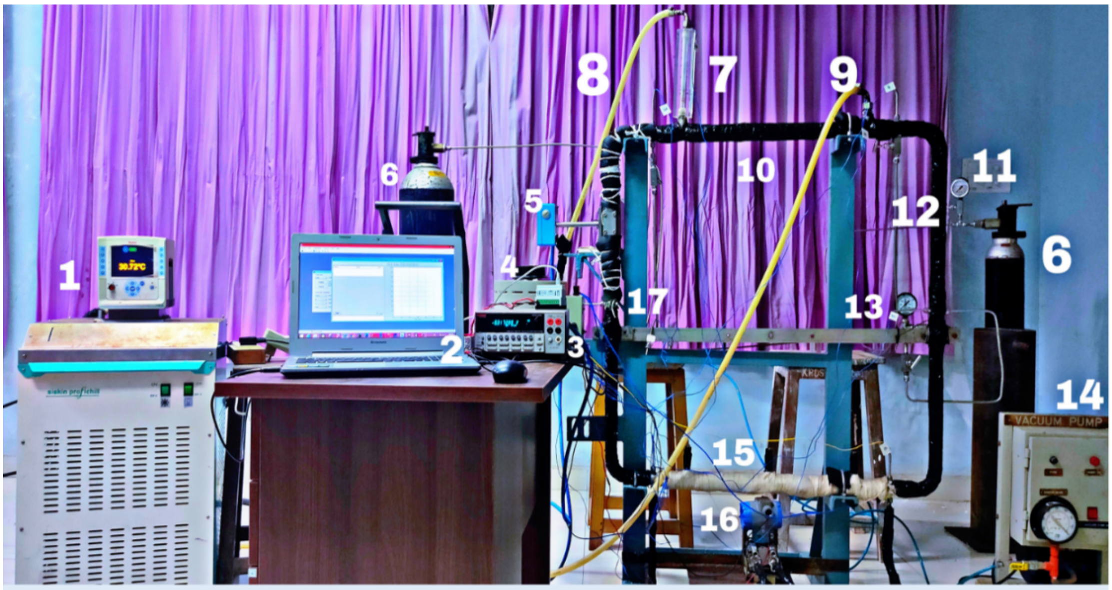

1. Thermostatic bath **2.** Laptop **3.** Data acquisition system **4.** Dimmer stat **5.** Mass flow meter **6.** CO_2 Cylinder **7.** Rotameter **8.** Water outlet **9.** Water inlet **10.** Heat-exchanger **11.** Pressure gauge **12.** Right leg **13**. Safety valve **14.** Vacuum pump **15.** Heater **16.** Differential pressure transducer **17.** Left leg

Figure 5.6: Experimental setup of natural circulation loop.

After performing the required tests, all the measuring instruments viz Thermocouples, Pressure gauge, DP transmitter, Mass flow meter are threaded into its respective tapings points and the loop was subjected to pneumatic test to ensure no leak from the instruments tapings. The bottom section of the loop i.e., heater section is winded with the electrical coil of 2 KW capacity. Then entire loop is insulated with the asbestos rope and the foam insulation to ensure adiabatic condition. The tube in tube cold heat exchanger is connected to the thermostatic bath thought the hose pipe and the rota-meter. All the thermocouples are connected to the data logger and which in turn connected to the lap top.

5.4 Experimental procedure

After connecting all the required instruments, safety devices in the loop and also conducting the entire prerequisite test, the loop is charged with CO_2. To ensure the required purity of CO_2 in the loop, before charging the CO_2 into the loop, air inside the loop is completely evacuated by using a vacuum pump and the purity of CO_2 in the loop is ensured by checking the sample at lab. Temperature of CO_2 in charging cylinder and the loop is cooled to the very low temperature by using the thermostatic bath (calculated from NIST (2018) REFPROP software V 9.1). The CO_2 pressure in the loop as well as the CO_2 accumulator is slowly increased up to CO_2 charging cylinder pressure. Once the pressure is equalized in all the three components i.e., charging cylinder, loop and accumulator, isolation valve between charging cylinder and the Loop is isolated. For safety reasons the CO_2 charging cylinder is kept disconnected from the loop. The loop fluid temperature is slowly brought back to the room temperature (initial temperature (T_0) of 32°C) by circulating the water in the cold heat exchanger. After working fluid temperature reached to the laboratory temperature, the loop pressure is fine tuned to (P_0) i.e., 80 bar by releasing the pressure through atmospheric vent. After reaching the require pressure in the loop the cooling water flow to the cold heat exchanger is fine tuned to 1.15 kg/minute by throttling the out let regulating valve. By keeping the thermostat at lowest position, the power supply to the heating coils is switched-on. In order to avoid sudden pressure shoot-up of loop fluid, due to heat input to the loop, power supply to heater coil is slowly increased at incremental rate with the support of the thermostat. Constant pressure is maintained in the loop with the assistance of accumulator/expansion sink (cylinder) by dampening the increased pressure due to change is temperature of the loop. The transient behaviour of pressure, mass flow rate and temperatures are recorded at various level of heat input i.,e at 250, 500, 750 and 1000 W. Further, experiment is repeated at elevated pressure of loop fluid i.e., at 90 and 100 bars and transient behaviour of the loop is noted down. The experimental readings thus recorded through various measuring instruments and data loggers, are tabulated and plotted the graph. In the following section, these graphs are analyzed based on the basic physics involved in the transient behaviour of the loop. Further these experimental transient behaviour of the loop fluid is compared with the CFD results.

5.5 Uncertainty analysis

Every measurement is subject to some uncertainty. A measured result is only complete if it is accompanied by a statement of uncertainty in the measurement. Error is usually defined as the difference between the actual value and the calculated or measured value. Uncertainty refers to a possible value that the error may have. Measurement uncertainties can come from measuring instruments, ambient conditions or various parameters/variables considered during experiments. Such uncertainties can be estimated using statistical analysis of a set of measurements and other kinds of information about the measurement process.

In this study, the heat transfer rate is an important parameter that depends on the mass flow rate ($\dot{m}$), temperature difference ($\triangle T$), and specific heat of the external fluid. Since specific heat of external fluid is considered to be constant, the functional dependency of the various performance parameters relation formula is given as:

$$Q_{CHX} = f\left(\dot{m}_w, \Delta T_{CHX}\right) \tag{5.1}$$

Uncertainty in heat transfer rate:

Minimum mass flow rate (rotameter) measured in 3 LPM and least count is 0.1 LPM. Hence maximum uncertainty in the case of mass flow rate measurement is

$$\frac{\Delta m_w}{m_w} = \frac{0.1}{3} = \pm 0.033 = \pm 3.3\% \tag{5.2}$$

For the Coriolis mass flow meter

$$\frac{\Delta m_l}{m_l} = \frac{0.1}{30} = \pm 0.0033 = \pm 0.33\% \tag{5.3}$$

The minimum temperature measured is 32 °C, and the least count is 0.25 °C. Hence, the maximum uncertainty in the case of temperature measurement with a data acquisition system is

$$\frac{\Delta T}{T} = \frac{0.25}{32} = \pm 0.0078125 = \pm 0.78125\% \tag{5.4}$$

Uncertainty in calculating heat transfer rate based on external fluid flow

$$\frac{\Delta Q}{Q} = \left[\left(\frac{\Delta m_w}{m} \right)^2 + 2 \left(\frac{\Delta T}{T} \right)^2 \right]^{1/2} \tag{5.5}$$

$$\frac{\Delta Q}{Q} = \left[(0.033)^2 + 2(0.0078125)^2 \right]^{1/2} = 0.034 = 3.4\%$$

Uncertainty in calculating heat transfer rate based on internal fluid flow

$$\frac{\Delta Q}{Q} = \left[\left(\frac{\Delta m_w}{m} \right)^2 + 2 \left(\frac{\Delta T}{T} \right)^2 \right]^{1/2} \tag{5.6}$$

$$\frac{\Delta Q}{Q} = \left[(0.0033)^2 + 2(0.0078125)^2 \right]^{1/2} = 0.0034 = 0.34\%$$

However, the heat transfer rate is an input in the experiment and measured using Wattmeter having uncertainty,

$$\frac{\Delta W}{W} = \frac{1}{250} = \pm 0.004 = \pm 0.4\% \tag{5.7}$$

Uncertainty of correlation used for validation:

Correlation by Chen and Zhang (2011),

$$Re = 1.129(Gr_m d/L_t)^{0.3924} \tag{5.8}$$

This correlation consists of mass flow rate and heat input as main variables, considering other thermophysical properties and geometrical parameters constant. Hence, total uncertainty (X) involved in the correlation,

$$X = \left[\left(\frac{\Delta m}{m} \right)^2 + \left(\frac{\Delta Q}{Q} \right)^2 \right]^{1/2} = \pm 0.00518 = \pm 0.5\% \tag{5.9}$$

5.6 Results and discussion

Experimental study is carried out to obtain the transient behaviour of sCO_2 at different pressure (80, 90, 100 bar) and at different heat input (250, 500, 750 and 1000 W). Mass flow rate and temperature of cooling water at the inlet to CHX is kept 1.15 kg/min and 305 K respectively for all the cases. Whereas the heat input at source i.e., at HHX is varied from 250 W to 1000 W and initial temperature of the loop is kept at 305 K throughout the loop in all the cases.

5.6.1 Transient variation of mass flow rate in the loop

Figures 5.7(a-d) shows the transient variation of mass flow with respect to time at 250, 500, 750 and 1000 W of heat input at source. Rate of fluid mass flow is a function of strength of the driving force in a system, in NCLs which in turn depends on the differential temperature of working fluid across the out let of both source and the sink. This is clearly visible in the graphs that as the heat input at source increases, the fluid flow rate increases. The NCLs considered in the current study are bilaterally symmetrical geometrical structures and also the loop receives uniform heat energy throughout the heating section. This geometrical as well as thermal symmetry of the loop makes the flow direction more chaotic and it will be very high at low heat input due to very weak driving force in the loop. At lower heat fluxes, i.e., at 250 W and 500 W, in the initial few seconds the mass flow rate is very sluggish due to lower driving force. After few seconds later, the loop fluid gathers momentum and mass flow establishes in the loop but the flow direction keep on changes very frequently. However, at higher heat input the mass flow takes a baby steps immediately after the heating section is exposed to heat fluxes and it keep on increase and reaches to a saturation level for a given heat put. Further it is very obvious from the graph that the mass flow rate never reaches to a steady state even at higher rate of heat input, however the amplitude of fluctuation keep on reduces with higher heat input. The mass flow reversal phenomenon is very frequent in the loop at lower heat input, however at higher heat input, it takes unidirectional path due to stronger driving force in the loop.It is interesting to note that as the heat input increases the amplitude of mass flow fluctuation also keep on decreases.

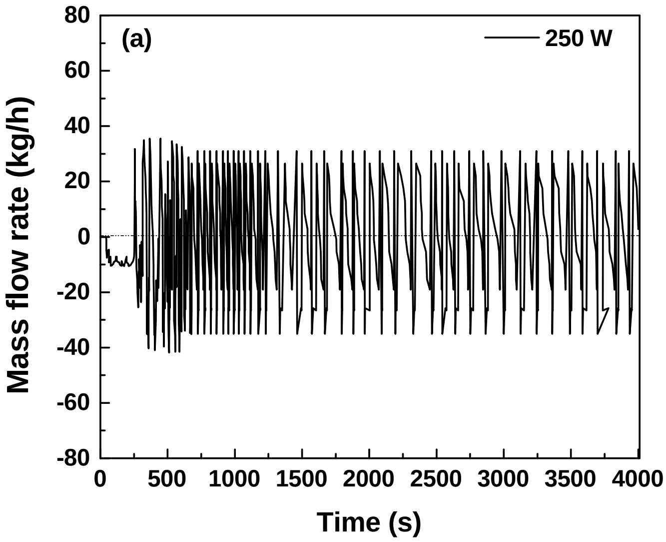

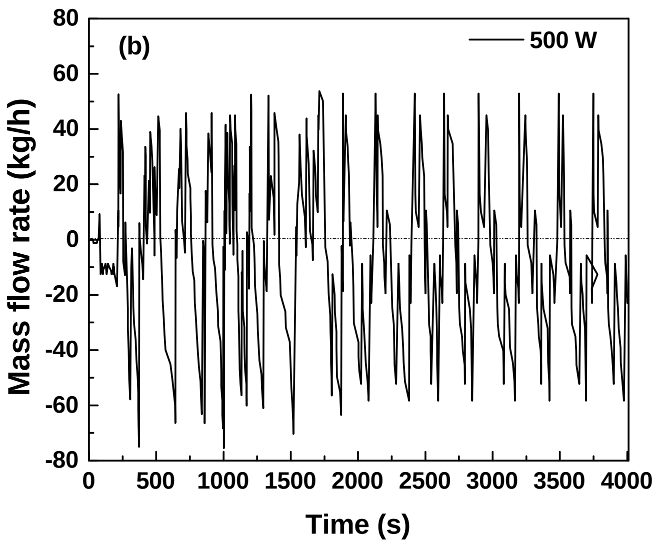

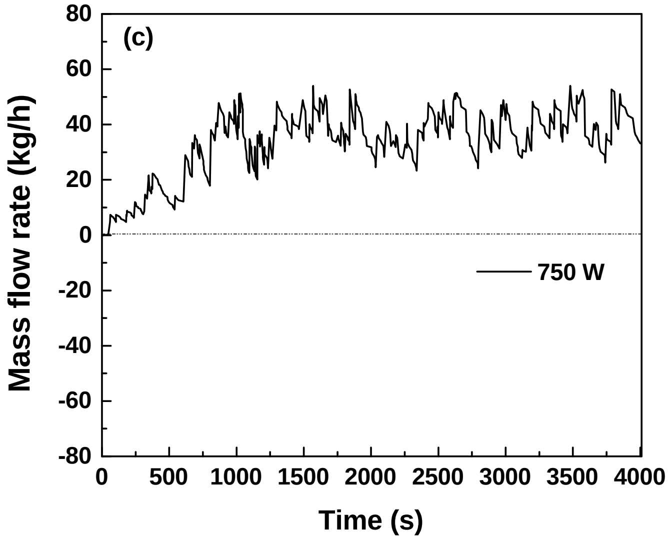

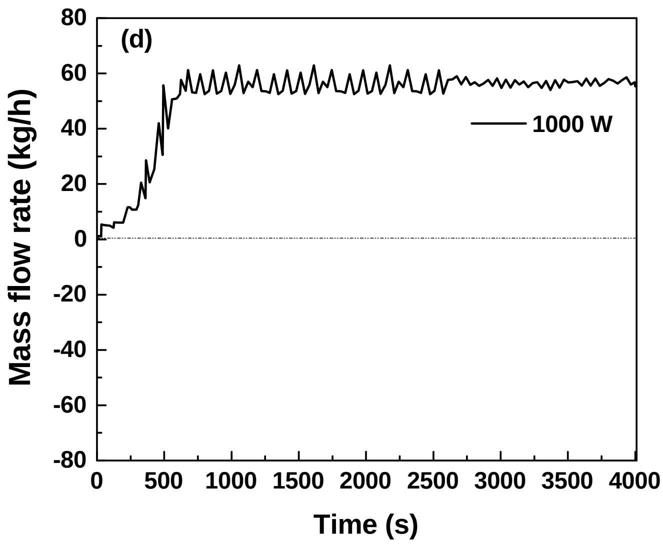

Figure 5.7: Mass flow rate variation at 90 bar with different heat inputs at (a) 250 W, (b) 500 W, (c) 750 W and (d) 1000 W.

At 1000 kW power input at source, it is found that the mass flow fluctuation reduces to very low amplitude. This effect may be due to the driving force dominance over all the resistive forces of the loop.

5.6.2 Temperature variations

Figure 5.8(a-d) shows the transient variation of loop fluid temperature in Heater- CHX loop at various heat input at 80 bar pressure. In the heater section constant heat flux of 250 W, 500 W, 750 W and 1000 W is imposed on the Heater-CHX loop.

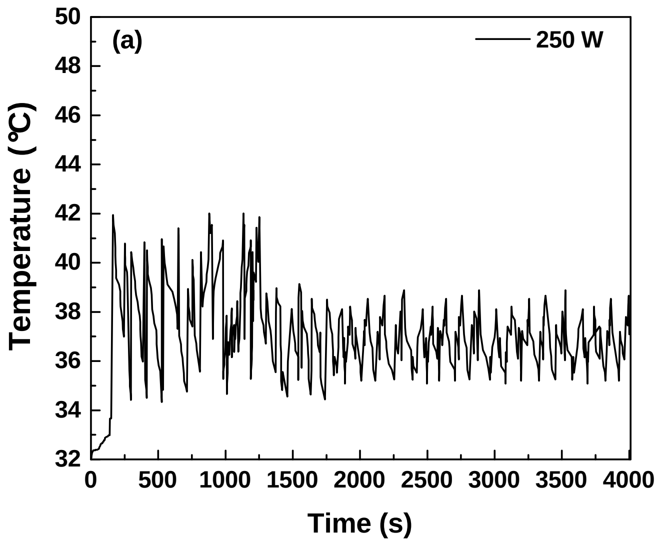

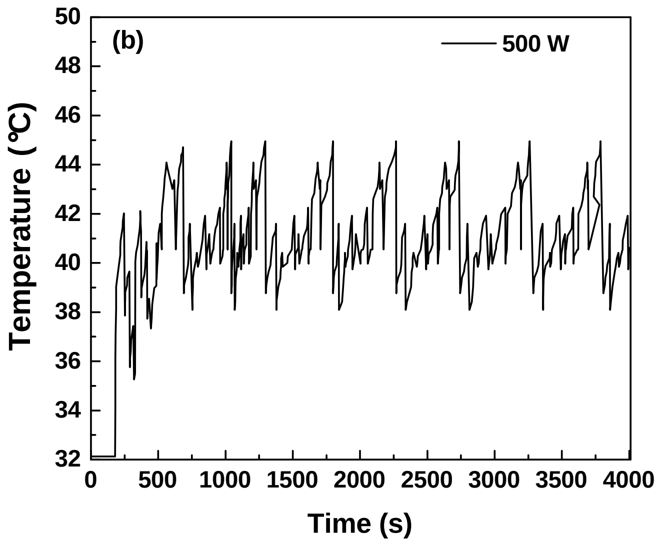

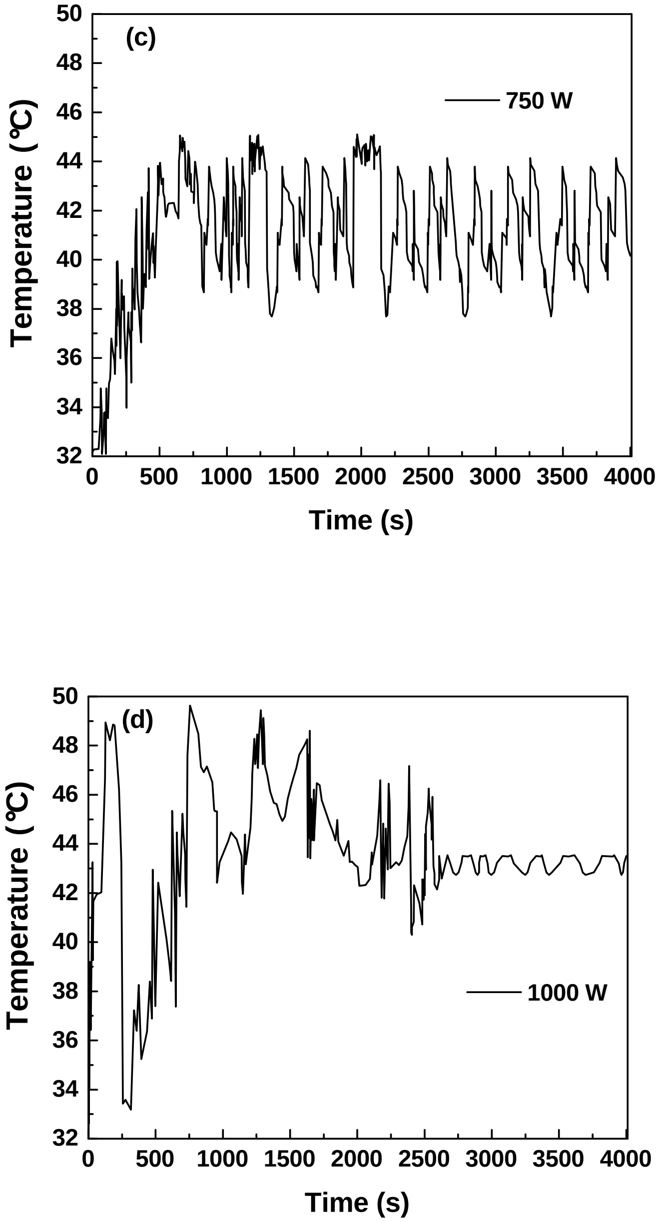

Figure 5.8: Variation of temperature at 80 bar for NCL with different heat inputs at (a) 250 W, (b) 500 W, (c) 750 W and (d) 1000 W.

The experiment have been carried out to analyse the stability behaviour at lower and higher heat input at source by keeping the sink temperature constant at all levels of heat input. That is the stability behaviour studied by widening the differential temperature of working fluid at the out let of source and the sink by heating and cooling respectively. At lower differential temperature the amplitude of temperature fluctuation is very consistent throughout the operation of the loop fluid and it never reaches to a steady state.

However, at higher differential temperature the fluctuation of temperature of the loop fluid is very mild in nature and also reaches to a steady state over a period of time. At intermittent heat input, the fluctuation of temperature is very high in Heater-CHX loop compared to lower and higher temperature. The temperature fluctuation in loop keep on increase with increase in heat input from lower level to intermediate level of heat input and at higher level it starts to decline and eventually reaches to a steady state.

5.6.3 Effect of operating pressure on mass flow rate and flow instability

Figures 5.9(a-d) depict the variation of differential pressure across the heater in the NCL. Influence of operating pressure on the mass flow rate of working fluid of Heater-CHX loop is checked at 250 W and 1000 W of heat input at source. As the loop fluid pressure increases, the mass flow rate increases and it is very much obvious from the results obtained from the experiment. Further, dampening of mass flow oscillation as well as time required to reach a steady state reduces at a faster rate as the loop fluid pressure increases. It is very clear from the obtained experimental results, at higher operating pressure and heat input, the working fluid mass flow rate reaches to steady state at a faster rate compare to lower operating pressure. The Mass flow rate is very high at all level of loop fluid pressure at higher heat input compared to the lower heat input. At lower pressure and lower heat input at source it can be seen that the mass flow follows bidirectional path whereas even at lower pressure and higher heat input the mass flow takes unidirectional path. Immaterial of the pressure level, at both lower and higher level of heat input, the loop fluid mass flow takes anticlockwise direction whereas it takes bidirectional path at lower heat input and pressure and clockwise directional path at higher heat input and pressure. The experimental results indicate that the loop is very stable at higher level of heat input and loop fluid pressure.

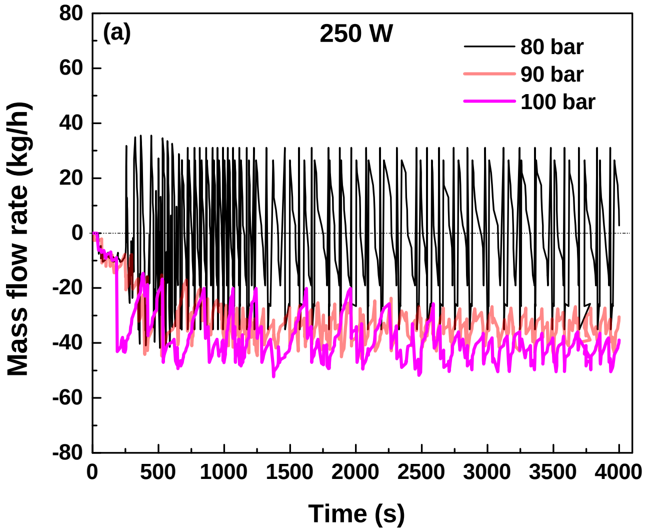

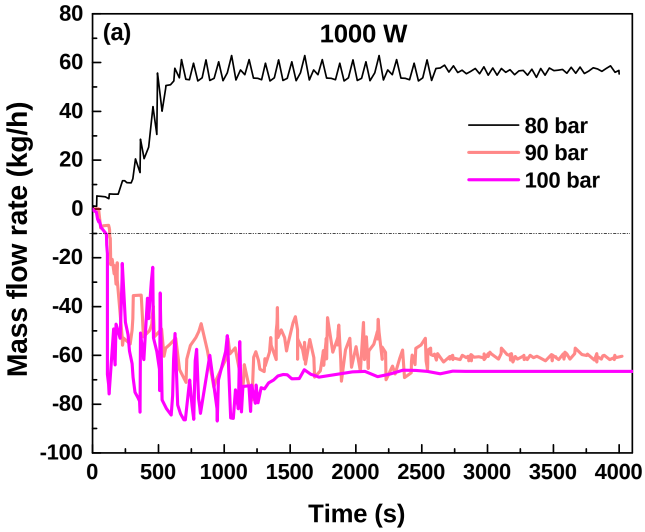

Figure 5.9: Variation of differential pressure across heater at 80 bar, 90 bar and 100 bar for NCL with different heat inputs at (a) 250 W and (b) 1000 W.

5.7 Validation

Figure 5.10 show the mass flow rate comparison between the CFD simulation and experimental results at 80 bar pressure and 500 W heat input at source. Mass flow is bidirectional in both the cases, however the pattern of fluctuation slightly differs, it is mainly due the uneven internal surface of the pipe in case of experiment.

Similarly, temperature graphs has been validated considering the same heat input and pressure, as shown in Fig. 5.11. Reasonably a good match is found.

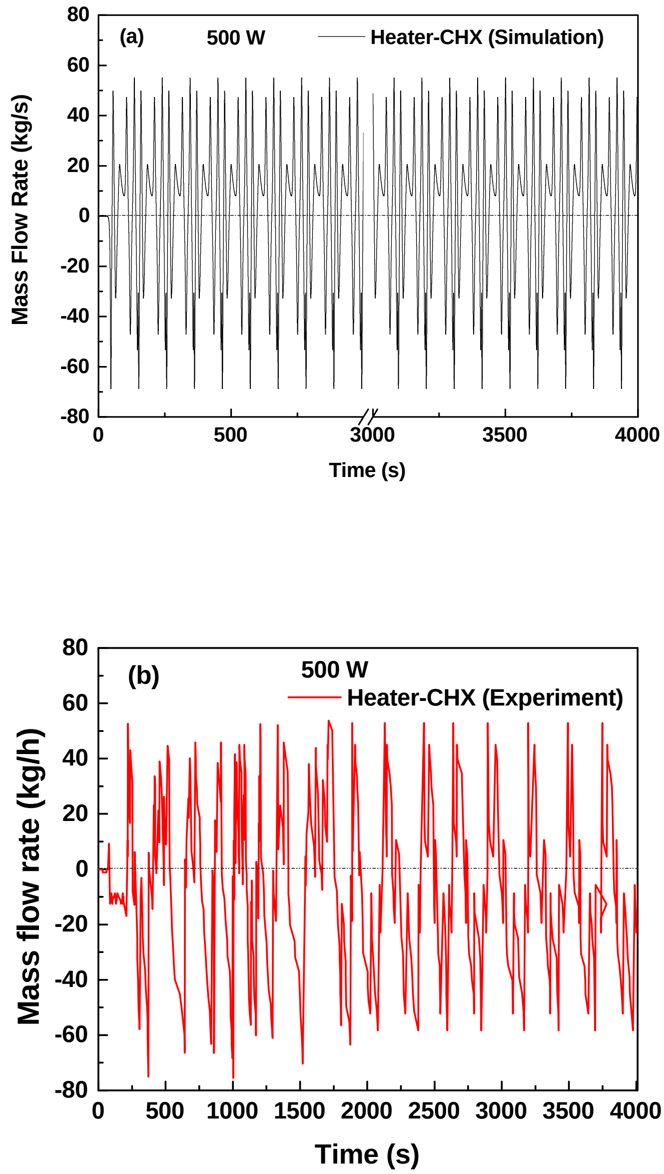

Figure 5.10: Mass flow rate instability for at 500 W heat inputs for (a) Numerical Simulation and (b) Experimental Analysis.

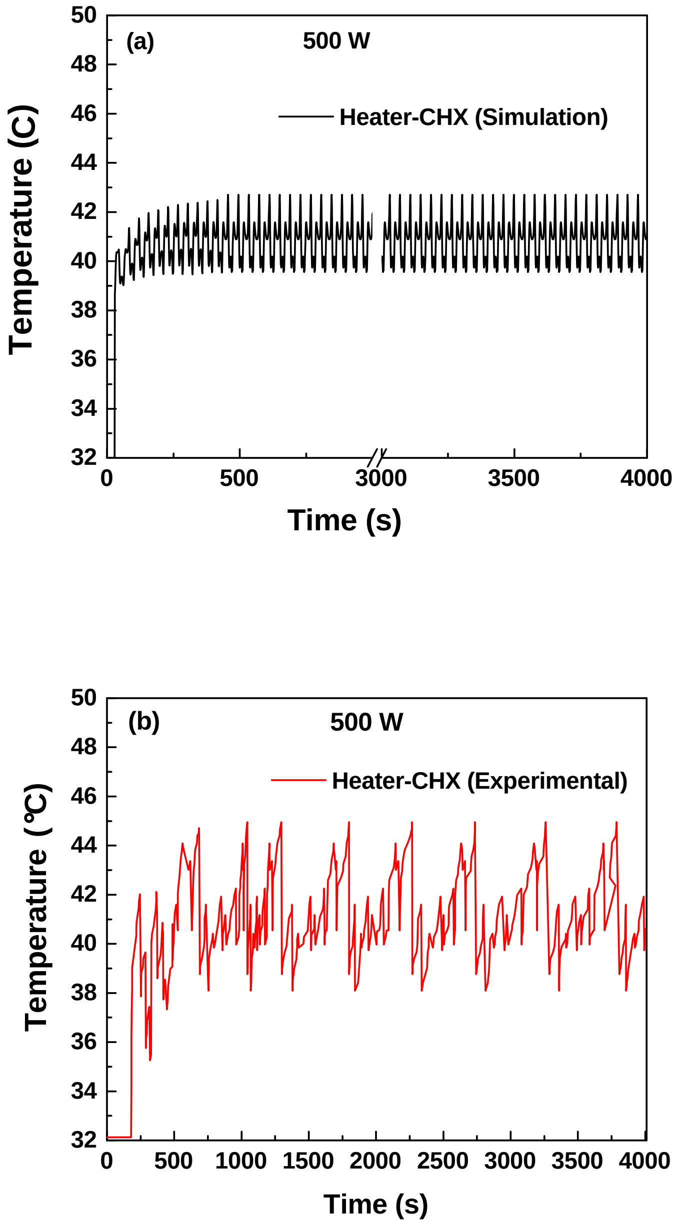

Figure 5.11: Temperature instability for at 500 W heat inputs for (a) Numerical Simulation and (b) Experimental Analysis.

Validation of obtained simulation results are done with the experimental data and available correlation given by Chen and Zhang (2011) in terms of non-dimensional parameters (shown in Fig. 5.12), a good agreement is found between them.

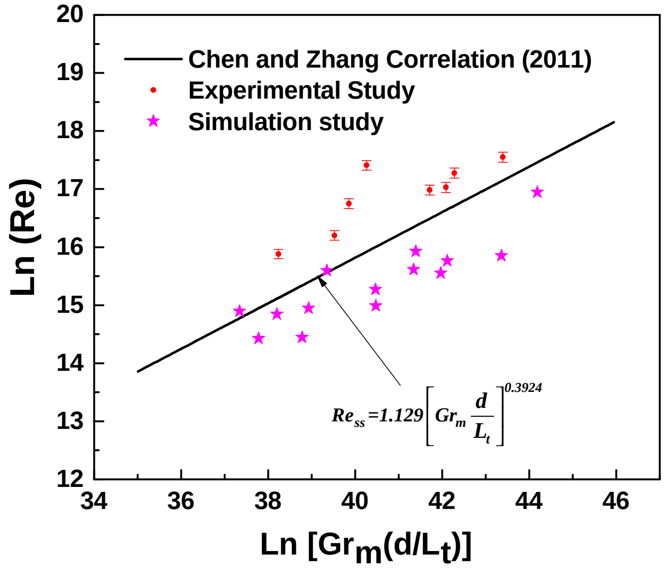

Figure 5.12: Validation of 3D simulation data with experimental results and available correlation.

Reynolds number and Grashof number are calculated on the basis of below formulae:

$$Re = \frac{4m}{\pi d \mu}$$

$$Gr_m = \frac{g\beta d^3 \rho^2 Q H_0}{A \mu^3 C_p}$$

Where, m i.e., mass flow rate is calculated from Coriolis flow meter and thermophysical properties are calculated from NIST (2018) data, based on the loop temperature taken from thermocouple.

The CFD simulation results obtained for 80 bar are also plotted to validate the experimental results. Good agreement was found between the experimental results and existing correlations, as shown in Fig. 5.12. The maximum discrepancies are found to be less than 4% with the correlation. Obtained results are closer to Chen and Zhang (2011) correlation than the simulation result, as in case of simulation activity, the following ideal conditions are assumed:

a. CHX cooling water inlet temperature has been kept constant at 305K.

b. Both the right and left legs are assumed to be adiabatic.

c. Heating at Heater section is considered to be uniform throughout the heating section.

d. The cooling of loop fluid at Cold exchanger is considered to be perfect.

e. The frictional loss in the loop is neglected.

f. The Loop fluid pressure is assumed to be constant throughout the simulation activity.

The maximum difference is found to be 6% between the experimental and the numerical data. The deviations are due to the three-dimensional (experimental) analysis and two-dimensional CFD simulation.

5.8 Summary

Experiment conducted on sCO_2 based square-natural circulation loops to study the influence of change in boundary conditions, at source, on transient and instability behaviour reveals the following:

i. The mass flow rate of loop fluid increases with increase in fluid pressure .

ii. Dampening of mass flow oscillation as well as time required to reach a steady state reduces at a faster rate as the loop fluid pressure increases.

iii. Experimental results indicate that the loop is very stable at higher level of heat input and higher loop fluid pressure.

iv. At a lower heat input the mass flow and temperature fluctuation is found to be bidirectional, whereas it is unidirectional at high heat input and pressure.

v. The geometrical as well as thermal symmetry of the loop makes the flow direction more chaotic and it will be very high at low heat input due very weak driving force in the loop.

vi. As the heat input increases at source the amplitude of temperature fluctuation keep on reduces and time required to reach steady state is also keep on reduces.

CHAPTER 6

Conclusions and Scope of Future Work

6.1 Conclusions

Incorporation of NCL technique in heat transportation turf is evidently the safest bet apart from its economical operation and maintenance privileges. NCL application in nuclear reactor core cooling is highly indispensable due to its secured operational feature, exceptionably low capital cost investment and negligible operational as well as maintenance expenditure compared to forced circulation system. Its wide spread applications in the field of Utility/Power boilers, Solar water heaters, Geothermal heat extraction, Internal combustion engine casing cooling, Electrical transformer core/winding cooling, etc., is well established with proven track record. Its application in electronic devices cooling is emerging as a new technique, however it is still in a nascent stage and substantial development is yet to be achieved.

Meticulous and intensive literature survey indicates that significant efforts have been already rendered by various researchers in exploring the fundamental driving mechanism involved in the system and also on its stable operation. It is also evident from the literature that incredible progress has been achieved except profound understanding of stability behaviour at various operating and boundary conditions. Further, comparison of instability behaviour of NCLs configured with various sources of heat is not available in the literatures and it is vital to understand it before incorporating it in a specific application. To fill this gap, present dissertation analyzes several aspects involved in stability behaviour of supercritical CO_2 based NCLs by exposing its source to various boundary conditions at heat sources. Further, all the computational and experimental investigations are briefly summarized and the prominent interpretations are reiterated in the following sections.

6.1.1 Effect of Heat-Exchanger and Isothermal Wall at source on the sCO_2 based Natural Circulation Loop

Following conclusions can be drawn from the two-dimensional transient computational fluid dynamics study carried out to assess the stability behaviour of two different configurations of sCO_2 based natural circulation loop, i.e., (1) NCL with isothermal heater and a cold heat-exchanger, and (2) NCL with both side heat-exchangers.

i. Stability behaviour of mass flow rate and velocity is very abrupt in case of HHX-CHX loop and it never dampens, whereas it get dampen at a faster rate in case of ISO-CHX loop.

ii. In case of HHX-CHX loop, mass flow rate and velocity instability keeps dampening at a definite rate and eventually it get stabilizes beyond certain threshold temperature. However, HHX-CHX loop stabilizes at a slower pace when comparing the same scenario with the ISO-CHX loop. At given pressure, the mass flow rate is almost same in both the cases, whereas velocity magnitude in case of ISO-CHX loop prevails over HHX-CHX loop.

iii. Nusselt number is very high at all heat input at source in case of ISO-CHX loop compared to HHX-CHX loop, which is mainly due to very high turbulent kinetic energy.

iv. Energy transportation from source to sink is more stable in case of ISO-CHX loop compared to HHX-CHX loop.

6.1.2 Numerical assessment of stability behaviour in Supercritical CO_2 based NCLs configured with Heater, Heat exchanger and Isothermal wall as heat sources.

Three-dimentional CFD simulation were conducted on three different combinations of source and sink in sCO2 based square NCLs to assess the influence of change in boundary condition and operating pressures on transient and instability behaviour of loop reveals the following:

i. Notwithstanding to the nature of the boundary condition chosen and quantum of heat injection at source, the natural circulation loops are prone to experience some initial instabilities, either in the form of oscillation or both oscillation and direction reversals before reaching to a steady state condition. However, the time required for reaching to a steady state condition is obviously governed by the nature of boundary condition employed or quantum of heat added at source.

ii. The Loop fluid mass flow rate, temperature and velocity oscillation in Heater-CHX loop is very high compared to ISO-CHX loop. This difference in the behaviour of loops is inherently due to heat transfer rate is fixed and independent of loop fluid temperature in heater, but in other cases heat transfer rate depends on loop fluid temperature.Stability performance of HHX-CHXloop sets in between these two loops.

iii. In ISO-CHX loop, the mass flow and temperature instabilities stabilized at a faster rate compared to Heater-CHX and HHX-CHX loops, as its response at source is instantaneous due to constant temperature throughout the heating section.

iv. For a given boundary conditions, the operating temperature of the loop fluid is highest in case of Heater-CHX loop and it is lowest in case of HHX-CHX loop.

v. In all configurations of NCLs considered in the present study, the mass flow rate increases with an increase in loop fluid operating pressure, whereas, flow instabilities decrease with an increase in loop fluid operating pressure. Further, it is noted that as the operating pressure of the sCO2 increases, the time duration required to reach steady state of the system decreases, the same results are observed in the experimental study of Yadav et al. (2017).

vi At all levels of heat input at source, the average mass flow rate is lower and the time taken for the velocity oscillations to dampen is very high in case of Heater-CHX loop compared to other two loops. Whereas, the amplitude of flow oscillation is very mild and velocity oscillations convergence at a shorter time duration in case of ISO-CHX loop compared to other two loops.

vii In all configurations of NCL, at lower heat input, the loop fluid flow takes bidirectional path at regular intervals. However, at higher heat input, it follows unidirectional path except for inconsequential initial glitches in case of Heater-CHX loop. Further, the direction of flow is highly inconsistent and extremely unpredictable in all configurations of NCL considered. Further, the direction of mass flow is independent of the type of the boundary conditions and quantum of heat input.

viii Further, the Nusselt number in case of Heater-CHX loop is very high compared to HHX-CHX and ISO-CHX loops because of its high turbulent kinetic energy and it leads to better heat transport property in case of Heater-CHX loop.

6.1.3 Experimental investigation

Experiment conducted on sCO_2 based square-natural circulation loops to study the influence of change in boundary conditions, at source, on transient and instability behaviour reveals the following:

i. The mass flow rate of loop fluid increases with increase in fluid pressure

ii. Dampening of mass flow oscillation as well as time required to reach a steady state reduces at a faster rate as the loop fluid pressure increases.

iii. Experimental results indicate that the loop is very stable at higher level of heat input and higher loop fluid pressure.

iv. At a lower heat input the mass flow and temperature fluctuation is found to be bidirectional, whereas it is unidirectional at high heat input and pressure.

v. The geometrical as well as thermal symmetry of the loop makes the flow direction more chaotic and it will be very high at low heat input due very weak driving force in the loop.

vi. As the heat input increases at source the amplitude of temperature fluctuation keep on reduces and time required to reach steady state is also keep on reduces.

6.2 Scope for future work

In the present dissertation very few various boundary conditions are imposed on the sCO_2 based NCLs to understand the inherent stability behavior of the loops. Further, current CFD study is restricted only to sCO_2 as a working fluid in a simple square loop. In NCLs, future study can be extended by considering the following to understand the stability system to the maximum possible extent.

i. Computation assessment of NCLs exposed to isothermal wall in the sink.

ii. Computation assessment of NCLs exposed to various boundary conditions considering most popular working fluids.

iii. Experimental studies on NCLs exposed to various boundary conditions with sCO_2 as a working fluid.

iv. Experimental study using different geometrical loop shapes such as most complex industrial loops.

v. Numerical and experimental investigation of NCLs Stability behaviour considering all the practical aspects.

References

Acosta, R., Sen, M. and Ramos, E. (1987). "Single-phase natural circulation in a tilted square loop." *Wärme-und Stoffübertragung*, 21(5), 269–275.

Adriansyah, W. (2004). "Combined air conditioning and tap water heating plant using CO_2 as refrigerant." *Energy and Buildings*, 36(7), 690–695.

Archana, V., Vaidya, A. and Vijayan, P. (2015). "Numerical modeling of supercritical CO_2 natural circulation loop." *Nuclear Engineering and Design*, 293, 330–345.

Bau, H. H. and Torrance, K. (1981). "Transient and steady behavior of an open, symmetrically-heated, free convection loop." *International Journal of Heat and Mass Transfer*, 24(4), 597–609.

Bernier, M. and Baliga, B. (1992). "A 1-d/2-d model and experimental results for a closed-loop thermosyphon with vertical heat transfer sections." *International journal of heat and mass transfer*, 35(11), 2969–2982.

Bettini, R., Bertolini, G., Frigo, E., Rossi, A., Casini, I., Pasquali, I. and Giordano, F. (2004). "Interaction of pharmaceutical hydrates with supercritical co 2." *Journal of thermal analysis and calorimetry*, 77, 625–638.

Cammarata, L., Fichera, A., Guglielmino, I. and Pagano, A. (2004). "On the effect of gravity on the bifurcation of rectangular closed-loop thermosyphon." *Heat and mass transfer*, 40(10), 801–808.

Cammarata, L., Fichera, A. and Pagano, A. (2003). "Stability maps for rectangular circulation loops." *Applied thermal engineering*, 23(8), 965–977.

Chato, J. (1963). "Natural convection flows in parallel-channel systems." *Journal of Heat Transfer*, 85, 339–345.

Chatoorgoon, V., Voodi, A. and Fraser, D. (2005). "The stability boundary for supercritical flow in natural convection loops: Part i: H_2O studies." *Nuclear Engineering and Design*, 235(24), 2570–2580.

Chauhan, A. and Kandlikar, S. G. (2019). "Characterization of a dual taper thermosiphon loop for cpu cooling in data centers." *Applied Thermal Engineering*, 146, 450–458.

Chen, K. (1985). "On the oscillatory instability of closed-loop thermosyphons." *Journal of Heat Transfer*, 107, 826–832.

Chen, L. and Zhang, X.-R. (2011). "Simulation of heat transfer and system behavior in a supercritical CO_2 based thermosyphon: effect of pipe diameter." *Journal of Heat Transfer*, 133(12), 122–505.

Chen, L. and Zhang, X.-R. (2014). "Experiments on natural convective solar thermal achieved by supercritical CO_2/dimethyl ether mixture fluid." *Journal of solar energy engineering*, 136(3), 031011.

Chen, L., Zhang, X.-R. and Jiang, B. (2014). "Effects of Heater Orientations on the Natural Circulation and Heat Transfer in a Supercritical CO_2 Rectangular Loop.." *Journal of Heat Transfer*, 136(5). 052501.

Chen, L., Zhang, X.-R., Yamaguchi, H. and Liu, Z.-S. S. (2010). "Effect of heat transfer on the instabilities and transitions of supercritical CO_2 flow in a natural circulation loop." *International journal of heat and mass transfer*, 53(19-20), 4101–4111.

Cheng, H., Lei, H. and Dai, C. (2017). "Heat transfer of a single-phase natural circulation loop with heating and cooling fluids." *Energy Procedia*, 142, 3926–3931.

Cho, S. K., Kim, M., Baik, S., Ahn, Y. and Lee, J. I. (2015). "Investigation of the bottoming cycle for high efficiency combined cycle gas turbine system with supercritical carbon dioxide power cycle." In *turbo expo: Power for land, sea, and air*, volume 56802, American Society of Mechanical Engineers, V009T36A011.

Cohen, H. and Bayley, F. (1955). "Heat-transfer problems of liquid-cooled gas-turbine blades." *Proceedings of the Institution of Mechanical Engineers*, 169(1), 1063–1080.

Conboy, T., Pasch, J. and Fleming, D. (2013). "Control of a supercritical CO_2 recompression brayton cycle demonstration loop." *Journal of engineering for gas turbines and power*, 135(11), 111701.

Creveling, F. H., F. De Paz, J., Y. Baladi, J. and J. Schoenhals, R. (1975). "Stability characteristics of a single-phase free convection loop." *Journal of Fluid Mechanics*, 67.

Deng, B., Chen, L., Zhang, X. and Jin, L. (2019). "The flow transition characteristics of supercritical CO_2 based closed natural circulation loop (ncl) system." *Annals of Nuclear Energy*, 132, 134–148.

Dimmick, G., Chatoorgoon, V., Khartabil, H. and Duffey, R. (2002). "Natural-convection studies for advanced candu reactor concepts." *Nuclear Engineering and Design*, 215(1), 27–38.

Furuya, M., Inada, F. and Yasuo, A. (2001). "Inlet throttling effect on the boiling two-phase flow stability in a natural circulation loop with a chimney." *Heat and mass transfer*, 37(2-3), 111–115.

Gamble, R. E., Hinds, D. H., Hucik, S. A. and Maslak, C. E. (2006). "Esbwr... an evolutionary reactor design." In *Proceedings of the 2006 International Congress on Advances in Nuclear Power Plants-ICAPP'06*.

Greif, R. (1988). "Natural circulation loops." *Journal of Heat Transfer*, 110(1243-1259).

Hagen, V. T. and Stekelenburg, A. (1997). “The low-power low-pressure flow resonance in a natural circulation cooled boiling water reactor.” *Nuclear Engineering and Design*, 177(1-3), 229–238.

Hahne, E. W. (1968). “Natural convection heat transfer through an enclosed horizontal layer of supercritical carbon dioxide.” *Wärme-und Stoffübertragung*, 1(3), 190–196.

Jain, P. K. et al. (2008). “Numerical analysis of supercritical flow instabilities in a natural circulation loop.” *Nuclear Engineering and Design*, 238(8), 1947–1957.

Janardhana Reddy, G., Basha, H. and Venkata Narayanan, N. (2018). “Transient natural convection heat transfer to CO_2 in the supercritical region.” *Journal of Heat Transfer*, 140(9), 092502.

Japikse, D. (1973). “Advances in thermosyphon technology.” 9, 1–111.

Jiang, S., Wu, X., Zhang, Y. and Jia, H. (2001). “Thermal hydraulic modeling of a natural circulation loop.” *Heat and mass transfer*, 37(4-5), 387–395.

Jiang, Y. and Shoji, M. (2003). “Flow stability in a natural circulation loop: influences of wall thermal conductivity.” *Nuclear Engineering and design*, 222(1), 16–28.

Kapitz, M. and Wiesche, S. a. d. (2012). “The effect of the location of nucleation sites on the thermal-hydraulic stability of a short-tube natural circulation loop.” *J. Eng. Gas Turbines Power.*, 134(6), 062901.

Keller, J. B. (1966). “Periodic oscillations in a model of thermal convection.” *Journal of Fluid Mechanics*, 26(3), 599–606.

Kim, Y. M., Sohn, J. L. and Yoon, E. S. (2017). “Supercritical CO_2 rankine cycles for waste heat recovery from gas turbine.” *Energy*, 118, 893–905.

Kreitlow, D., Reistad, G., Miles, C. and Culver, G. (1978). “Thermosyphon models for downhole heat exchanger applications in shallow geothermal systems." *Journal of Heat Transfer*, 100(713-719).

Kumar, A. and Khalid, S. (2019). "CO_2 based natural circulation loops for domestic refrigerators." *Saudi J. Eng. Technol*, 4, 192–200.

Kumar, K. K. and Gopal, M. R. (2009a). "Carbon dioxide as a secondary fluid in natural circulation loops." *Proceedings of the Institution of Mechanical Engineers, Part E: Journal of Process Mechanical Engineering*, 223(3), 189–194.

Kumar, K. K. and Gopal, M. R. (2009b). "Steady-state analysis of CO_2 based natural circulation loops with end heat exchangers." *Applied Thermal Engineering*, 29(10), 1893–1903.

Li, H., Su, W., Cao, L., Chang, F., Xia, W. and Dai, Y. (2018). "Preliminary conceptual design and thermodynamic comparative study on vapor absorption refrigeration cycles integrated with a supercritical CO_2 power cycle." *Energy Conversion and Management*, 161, 162–171.

Lifshitz, S. and Zvirin, Y. (1993). "Transient heat and mass transfer in a natural circulation loop." *Waerme-und Stoffuebertragung;(Germany)*, 28(7).

Lin, J.-F., Chiu, S. and Ho, C.-J. (2008). "Conjugate heat transfer simulation of a rectangular natural circulation loop." *Heat and mass transfer*, 45, 167–175.

Lisboa, P. F., Fernandes, J., Simões, P. C., Mota, J. P. and Saatdjian, E. (2010). "Computational-fluid-dynamics study of a kenics static mixer as a heat exchanger for supercritical carbon dioxide." *The Journal of Supercritical Fluids*, 55(1), 107–115.

Liu, G., Huang, Y., Wang, J. and Leung, L. H. (2016). "Heat transfer of supercritical carbon dioxide flowing in a rectangular circulation loop." *Applied Thermal Engineering*, 98, 39–48.

Manero, E., Sen, M. and Ramos, E. (1987). "Two-phase natural circulation in a toroidal loop." *Waerme-Stoffuebertrag.;(Germany, Federal Republic of)*, 21(1).

Manthey, R., Schuster, C., Lippmann, W. and Hurtado, A. (2020). "Effect of throttling on the two-phase flow stability in an open natural circulation system." *Heat and Mass Transfer*, 56, 37–52.

Mertol, A., Greif, R. and Zvirin, Y. (1982). "Two-Dimensional Study of Heat Transfer and Fluid Flow in a Natural Convection Loop." *Journal of Heat Transfer*, 104(3), 508–514.

Mertol, A., Greif, R. and Zvirin, Y. (1984). "Two dimensional analysis of transient flow and heat transfer in a natural circulation loop." *Waerme und Stoffuebertragung*, 18(2), 89–98.

Misale, M. (2016). "Experimental study on the influence of power steps on the thermohydraulic behavior of a natural circulation loop." *International Journal of Heat and Mass Transfer*, 99, 782–791.

Misale, M., Garibaldi, P., Passos, J. and De Bitencourt, G. G. (2007). "Experiments in a single-phase natural circulation mini-loop." *Experimental Thermal and Fluid Science*, 31(8), 1111–1120.

Misale, M., Ruffino, P. and Frogheri, M. (2000). "The influence of the wall thermal capacity and axial conduction over a single-phase natural circulation loop: 2-d numerical study." *Heat and mass transfer*, 36(6), 533–539.

Mochizuki, H. (1994). "Flow instabilities in boiling channels of pressure-tube-type reactor." *Nuclear Engineering and Design*, 149(1-3), 269–277.

Mousavian, S. K., Misale, M., D'Auria, F. and Salehi, M. A. (2004). "Transient and stability analysis in single-phase natural circulation." *Annals of Nuclear Energy*, 31(10), 1177–1198.

Nayak, A., Vijayan, P., Saha, D. and Raj, V. V. (1995). "Mathematical modelling of the stability characteristics of a natural circulation loop." *Mathematical and computer modelling*, 22(9), 77–87.

Nayak, A., Vijayan, P., Saha, D., Raj, V. V. and Aritomi, M. (2000). "Analytical study of nuclear-coupled density-wave instability in a natural circulation pressure tube type boiling water reactor." *Nuclear Engineering and Design*, 195(1), 27–44.

Nekså, P. (2002). "CO_2 heat pump systems." *International Journal of refrigeration*, 25(4), 421–427.

NIST (2018). "Standard reference database-refprop version 9.1." *National Institute of Standards and Technology*.

Ong, K. (1974). "A finite-difference method to evaluate the thermal performance of a solar water heater." *Solar Energy*, 16(3-4), 137–147.

Rao, N., Maiti, B. and Das, P. (2005). "Dynamic performance of a natural circulation loop with end heat exchangers under different excitations." *International journal of heat and mass transfer*, 48(15), 3185–3196.

Rayleigh, L. (1916). "Lix. on convection currents in a horizontal layer of fluid, when the higher temperature is on the under side." *The London, Edinburgh, and Dublin Philosophical Magazine and Journal of Science*, 32(192), 529–546.

Roache, P. (1994). "Perspective: a method for uniform reporting of grid refinement studies." *Journal of Fluids Engineering*, 116(3), 405–413.

Sadhu, S., Ramgopal, M. and Bhattacharyya, S. (2016). "Effect of loop diameter, height and insulation on a high temperature CO_2 based natural circulation loop." *International Journal of Mechanical and Mechatronics Engineering*, 10(8), 1472–1480.

Sadhu, S., Ramgopal, M. and Bhattacharyya, S. (2018). "Steady-state analysis of a high-temperature natural circulation loop based on water-cooled supercritical CO_2." *Journal of Heat Transfer*, 140(6).

Samba, A., Louahlia-Gualous, H., Le Masson, S. and Nörterhäuser, D. (2013). "Two-phase thermosyphon loop for cooling outdoor telecommunication equipments." *Applied Thermal Engineering*, 50(1), 1351–1360.

Schuster, C., Ellinger, A. and Knorr, J. (2000). "Analysis of flow instabilities at the natural circulation loop danton with regard to non-linear effects." *Heat and mass transfer*, 36(6), 557–565.

Seyyedi, S., Sahebi, N., Dogonchi, A. and Hashemi-Tilehnoee, M. (2019). "Numerical and experimental analysis of a rectangular single-phase natural circulation loop with asymmetric heater position." *International Journal of Heat and Mass Transfer*, 130, 1343–1357.

Sharma, M., Vijayan, P., Pilkhwal, D., Saha, D. and Sinha, R. (2010). "Linear and nonlinear stability analysis of a supercritical natural circulation loop." *J. Eng. Gas Turbines Power.*, 132(10), 102904.

Sinha, R. K. and Kakodkar, A. (2006). "Design and development of the ahwr—the indian thorium fuelled innovative nuclear reactor." *Nuclear Engineering and Design*, 236(7-8), 683–700.

Stern, C. and Greif, R. (1987). "Measurements in a natural convection loop." *Wärme- und Stoffübertragung*, 21(5), 277–282.

Swapnalee, B., Vijayan, P., Sharma, M. and Pilkhwal, D. (2012). "Steady state flow and static instability of supercritical natural circulation loops." *Nuclear Engineering and Design*, 245, 99–112.

Thippeswamy, L. and Yadav, A. K. (2020). “Heat transfer enhancement using CO_2 in a natural circulation loop.” *Scientific Reports*, 10(1), 1–10.

Vijayan, P. (2002). “Experimental observations on the general trends of the steady state and stability behaviour of single-phase natural circulation loops.” *Nuclear Engineering and Design*, 215(1-2), 139–152.

Vijayan, P. and Date, A. (1992). “The limits of conditional stability for single-phase natural circulation with throughflow in a figure-of-eight loop.” *Nuclear Engineering and Design*, 136(3), 361–380.

Vijayan, P. and Nayak, A. (2005). “Introduction to instabilities in natural circulation systems.” *Natural Circulation in Water Cooled Power Plants*, 2152–22.

Vijayan, P. and Nayak, A. (2010). “Natural circulation systems: advantages and challenges.” *Natural Circulation in Water Cooled Power Plants*, 2152–21.

Vijayan, P., Sharma, M., Pilkhwal, D., Saha, D. and Sinha, R. (2010). “A comparative study of single-phase, two-phase, and supercritical natural circulation in a rectangular loop.” *Journal of engineering for gas turbines and power*, 132(10).

Vijayan, P., Sharma, M. and Saha, D. (2007). “Steady state and stability characteristics of single-phase natural circulation in a rectangular loop with different heater and cooler orientations.” *Experimental Thermal and Fluid Science*, 31(8), 925–945.

Wahidi, T., Chandavar, R. A. and Yadav, A. K. (2020). “Stability enhancement of supercritical CO_2 based natural circulation loop using a modified tesla valve.” *The Journal of supercritical fluids*, 166, 105020.

Wahidi, T. and Yadav, A. K. (2021). “Instability mitigation by integrating twin tesla type valves in supercritical carbon dioxide based natural circulation loop.” *Applied Thermal Engineering*, 182, 116087.

Wang, C.-C., Zhu, C.-X. and Tang, Y.-C. (2015). "Performance and flow distribution of the plate heat exchanger with supercritical fluid of carbon dioxide." *Journal of Thermal Engineering*, 1(3), 143–151.

Wang, Z., Wang, F., Ma, Z., Lin, W. and Ren, H. (2019). "Investigation on the feasibility and performance of transcritical CO_2 heat pump integrated with thermal energy storage for space heating." *Renewable Energy*, 134, 496–508.

Welander, P. (1967). "On the oscillatory instability of a differentially heated fluid loop." *Journal of Fluid Mechanics*, 29(1), 17–30.

Yadav, A. K., Gopal, M. R. and Bhattacharyya, S. (2012a). "Cfd analysis of a CO_2 based natural circulation loop with end heat exchangers." *Applied Thermal Engineering*, 36, 288–295.

Yadav, A. K., Gopal, M. R. and Bhattacharyya, S. (2012b). "CO_2 based natural circulation loops: new correlations for friction and heat transfer." *International Journal of Heat and Mass Transfer*, 55(17-18), 4621–4630.

Yadav, A. K., Gopal, M. R. and Bhattacharyya, S. (2014). "Transient analysis of subcritical/supercritical carbon dioxide based natural circulation loops with end heat exchangers: Numerical studies." *International Journal of Heat and Mass Transfer*, 79, 24–33.

Yadav, A. K., Gopal, M. R. and Bhattacharyya, S. (2016). "Effect of tilt angle on subcritical/supercritical carbon dioxide-based natural circulation loop with isothermal source and sink." *Journal of Thermal Science and Engineering Applications*, 8(1).

Yadav, A. K., Ramgopal, M. and Bhattacharyya, S. (2017). "Transient analysis of subcritical/supercritical carbon dioxide based natural circulation loop with end heat exchangers: experimental study." *Heat and Mass Transfer*, 53(9), 2951–2960.

Yamaguchi, H., Sawada, N., Suzuki, H., Ueda, H. and Zhang, X. (2010). "Preliminary study on a solar water heater using supercritical carbon dioxide as working fluid." *Journal of Solar Energy Engineering*, 132(1).

Yamaguchi, H., Zhang, X., Sawada, N., Suzuki, H. and Ueda, H. (2009). "Experimental study on a solar water heater using supercritical carbon dioxide as working fluid." 48906, 753–759.

Yoshikawa, S., Smith Jr, R. L., Inomata, H., Matsumura, Y. and Arai, K. (2005). "Performance of a natural convection circulation system for supercritical fluids." *The Journal of Supercritical Fluids*, 36(1), 70–80.

Zhang, X. and Yamaguchi, H. (2008). "An experimental study on evacuated tube solar collector using supercritical CO_2." *Applied Thermal Engineering*, 28(10), 1225–1233.

Zhang, X.-R., Chen, L. and Yamaguchi, H. (2010). "Natural convective flow and heat transfer of supercritical CO_2 in a rectangular circulation loop." *International Journal of Heat and Mass Transfer*, 53(19-20), 4112–4122.

Zvirin, Y. (1985). "Throughflow effects on the transient and stability characteristics of a thermosyphon." *Wärme-und Stoffübertragung*, 19(2), 113–120.

List of Publications based on PhD Research Work

S. No.	Title of the paper	Authors	Name of the Journal/ Conference, Vol., No., Pages	Month, Year of Publication	Category*
1.	Comparative computational appraisal of supercritical CO_2-based natural circulation loop: effect of heat-exchanger and isothermal wall	**Srivatsa Thimmaiah**, Tabish Wahidi, A. K. Yadav & Arun M.	Journal of Thermal Analysis and Calorimetry, vol. 141, 2219–2229 https://doi.org/10.1007/s10973-020-09854-x (**SCI IF= 4.6**)	14 September 2020	1
2.	Numerical Instability Assessment of Natural Circulation Loop Subjected to Different Heating Conditions	**Srivatsa Thimmaiah,** Tabish Wahidi, A. K. Yadav & Arun M.	Springer Book publication	2021	5
3.	Comparative Computational Appraisal of Supercritical CO_2 based Natural Circulation Loop: Effect of Heat-Exchanger and Isothermal Wall	**Srivatsa Thimmaiah,** Tabish Wahidi, A. K. Yadav & Arun M.	Proceedings of IMEC 2019 International Mechanical Engineering Congress (IMEC-2019), NIT Tiruchirappalli, India.	29th Nov-1st December 2019.	3
4.	Numerical assessment of transient and stability behaviour of Supercritical CO_2 based NCLs configured with Heat exchanger and Isothermal wall as heat sources	**Srivatsa Thimmaiah,** Tabish Wahidi, A. K. Yadav & Arun M.	2nd International Conference on Numerical Heat Transfer and Fluid Flow (NHTFF-2020), NIT Warangal	January 17-19, 2020.	3
5.	Numerical Instability Assessment of Natural Circulation Loop Subjected to Different Heating Conditions.	**Srivatsa Thimmaiah,** Tabish Wahidi, A. K. Yadav & Arun M.	A Recent Trends in Fluid Dynamics Research (RTFDR-21), NIT Rourkela, India	April 2-4, 2021.	3
6.	Numerical assessment of stability behaviour in Supercritical CO_2 based NCLs configured with Heater, Heat exchanger and Isothermal wall as heat sources	**Srivatsa Thimmaiah,** Tabish Wahidi, A. K. Yadav & Arun M	Journal of Thermal Engineering Vol. 9, No. 2, pp. 530–550, DOI:10.18186/thermal.1285268 (**ESCI IF= 1.1**)	March 2023	1

*Category: 1: Journal paper, the full paper reviewed

2: Journal paper, Abstract reviewed

3: Conference/Symposium paper, the full paper reviewed

4: Conference/Symposium paper, abstract reviewed

5: others (Book chapter, NITK Research Bulletins, Short notes, etc.)

Srivatsa Thimmaiah	Dr. Arun M.
Research Scholar	**Research Guide**
Name & Signature, with Date	Name & Signature, with Date